Multicomponent turbulence, the spherical limit, and non-Kolmogorov spectra

Chung-Yu Mou
Department of Physics, University of Virginia, Charlottesville, Virginia 22901

Peter B. Weichman
Department of Physics 114-36, California Institute of Technology, Pasadena, California 91125

(Received 1 September 1994; revised manuscript received 10 July 1995)

A set of models for homogeneous, isotropic turbulence is considered in which the Navier-Stokes equations for incompressible fluid flow are generalized to a set of N coupled equations in N velocity fields. It is argued that in order to be useful these models must embody a new group of symmetries, and a general formalism is laid out for their construction. The work is motivated by similar techniques that have had extraordinary success in improving the theoretical understanding of equilibrium phase transitions in condensed matter systems. We consider two classes of models: a simpler class (model I), which does not contain an exact Galilean symmetry, and a more complicated, extended class (model II), which does. The key result is that these models simplify when N is large. The so-called *spherical limit* $N\to\infty$ can be solved exactly, yielding closed sets of nonlinear integral equations for the response and correlation functions. For model I, these equations, known as Kraichnan's direct interaction approximation equations, are solved fully in the scale-invariant turbulent regime. For model II, these equations are more complicated and their full solution is left for future work. Implications of these results for real turbulence ($N=1$) are discussed. In particular, it is argued that previously applied renormalization group techniques, based on an expansion in the exponent y that characterizes the driving spectrum, are incorrect and that the Kolmogorov exponent ζ has a nontrivial dependence on N, with $\zeta(N\to\infty)=\frac{3}{2}$ for both sets of models. This value is close to the experimental result $\zeta\simeq\frac{5}{3}$, which must therefore result from higher-order corrections in powers of $1/N$. Prospects for calculating these corrections are briefly discussed: though daunting, such calculations might provide a controlled perturbation expansion for the Kolmogorov, and other, exponents. Our techniques may also be applied to other nonequilibrium dynamical problems, such as the Kardar-Parisi-Zhang equation for interface growth, and perhaps to turbulence in nonlinear wave systems.

PACS number(s): 47.27.Gs, 64.60.Ht

I. INTRODUCTION

A. The energy cascade

Perhaps the most basic issue in the theory of homogeneous turbulence is the nature of the so-called *Kolmogorov energy cascade* [1]. To describe the problem in the simplest possible terms, consider a three-dimensional fluid that is being stirred on some length scale l_0 much larger than any dissipative length scale l_ν. The stirring force causes (kinetic) energy to be input into large-scale, long-wavelength hydrodynamic flows. If the fluid equations of motion were linear, the energy would remain in these long-wavelength modes for all time. However, the equations are, in fact, nonlinear and energy will gradually be transferred to shorter- and shorter-wavelength modes via the interactions between them. Eventually this cascade process will input energy into small-scale modes, of size l_ν, which are strongly damped by viscosity. At this point the energy is dissipated irreversibly and finally appears as heat. A steady state is then achieved in which energy is dissipated at the same rate that it is generated and there is a kind of momentum-space flux of energy from small wave vectors $k=O(l_0^{-1})$ to large wave-vectors $k=O(l_\nu^{-1})$. In the intermediate *inertial range* $l_0^{-1}\ll k\ll l_\nu^{-1}$, the equations of motion are essentially scale invariant and one expects power-law behavior of the energy spectrum,

$$E(k)\approx Ak^{-\zeta},\quad l_0^{-1}\ll k\ll l_\nu^{-1}\ . \tag{1.1}$$

The exponent ζ is called the *Kolmogorov exponent* and, crudely, the question of its value is the fundamental issue in the theory of turbulence.

To state the problem in more formal terms, consider the Navier-Stokes equations for a three-dimensional incompressible fluid

$$\frac{\partial\mathbf{v}}{\partial t}+\lambda_0(\mathbf{v}\cdot\nabla)\mathbf{v}=-\frac{1}{\rho_0}\nabla p+\nu_0\nabla^2\mathbf{v}+\mathbf{f},\quad \nabla\cdot\mathbf{v}=0\ , \tag{1.2}$$

where $\mathbf{v}(\mathbf{r},t)$ is the velocity field, $p(\mathbf{r},t)$ is the pressure (determined completely by the incompressibility condition), $\mathbf{f}(\mathbf{r},t)$ is the external driving force (without loss of generality, we take $\nabla\cdot\mathbf{f}=0$), ρ_0 is the mass density, ν_0 is the kinematic viscosity, and the coupling constant λ_0, physically equal to unity, is included for convenience. Since we assume the stirring to be large scale, the Fourier amplitudes $\hat{\mathbf{f}}(\mathbf{k},\omega)$ of the driving force vanish rapidly for

$k \gg m_0 \sim l_0^{-1}$. In the absence of the nonlinear convective term $\lambda_0(\mathbf{v}\cdot\nabla)\mathbf{v}$, we would have

$$\hat{\mathbf{v}}(\mathbf{k},\omega)=\hat{\mathbf{f}}(\mathbf{k},\omega)/(-i\omega+\nu_0 k^2) \tag{1.3}$$

and only those velocity Fourier modes $\hat{\mathbf{v}}(\mathbf{k},\omega)$, for which $k \lesssim m_0$ would be substantially excited and no small-scale motions would result. However, the nonlinearity leads to interactions between modes and energy will gradually be transferred to shorter wavelengths.

We may naively estimate the length scale l_ν at which the viscosity becomes important using dimensional analysis [1]. If energy is input into the system at a rate $\rho_0\bar{\epsilon}$ per unit volume and is more or less conserved in the inertial range, then it must be dissipated at the same rate at the length scale l_ν. The Kolmogorov estimate for the simplest viscosity-dependent quantity (with the correct dimensions of length) intrinsic to the dissipation process is

$$l_\nu \equiv \frac{1}{\Lambda}=(\nu_0^3/\bar{\epsilon})^{1/4} . \tag{1.4}$$

A well defined inertial range clearly requires some combination of small viscosity, large energy input, and large stirring length.

The energy spectrum is obtained from the velocity-velocity correlation function

$$U(\mathbf{r}-\mathbf{r}',t-t')=\frac{1}{d-1}\langle \mathbf{v}(\mathbf{r},t)\cdot\mathbf{v}(\mathbf{r}',t')\rangle , \tag{1.5}$$

with Fourier transform

$$\hat{U}(\mathbf{k},\omega)=\int d^d r \int dt\, e^{i(\mathbf{k}\cdot\mathbf{r}+\omega t)}U(\mathbf{r},t) . \tag{1.6}$$

The meaning of the average $\langle\ \rangle$ will be made clear below. The (angular integrated) energy spectrum is then defined by

$$E(k)=B_d\rho_0 k^{d-1}\int_{-\infty}^{\infty}\frac{d\omega}{2\pi}\hat{U}(\mathbf{k},\omega) , \tag{1.7}$$

where the angular factor $B_d=(d-1)/(2\pi)^{(1/2)d}\Gamma(\frac{1}{2}d)$ is chosen so that $E=\int_0^\infty dk\, E(k)=\frac{1}{2}\rho_0\langle \mathbf{v}^2\rangle$ is the total energy density, and for later convenience we have kept the spatial dimension d as a free parameter. It is useful to define a characteristic velocity v_0 via $(d/2)v_0^2=\langle \mathbf{v}^2\rangle=2E/\rho_0$. In the inertial range, the power-law form (1.1) is expected to hold.

B. The Kolmogorov argument

In 1941, Kolmogorov [1] presented a simple argument for determining the value of ζ. The argument was based on two fundamental assumptions. First, the cascade process was assumed to be local: in a sense, to be made precise in Sec. IV F, the fluid equations lead mainly to exchanges of energy between modes with wave numbers of the same order of magnitude. This allows one to define a momentum-space *energy flux,* which is the rate at which energy is transferred "through" wave vectors of magnitude k. Locality postulates that this flux is independent of k in the inertial range and must therefore be precisely equal to $\rho_0\bar{\epsilon}$. Second, the energy spectrum was assumed to be independent of the length scales l_0 and l_ν. This turns out to be the more questionable assumption. It basically postulates that as the stirring length l_0 diverges, with $\bar{\epsilon}$ fixed, the energy spectrum at any given fixed k in the inertial range remains unchanged. The larger-scale motions therefore do not affect the details of the local cascade process. Through simple dimensional analysis these two assumptions together determine $E(k)$: the unique combination of $\bar{\epsilon}$, ρ_0, and k that yields a quantity with the same dimensions as $E(k)$ is

$$E(k)\approx C_K\rho_0\bar{\epsilon}^{2/3}k^{-5/3}, \quad m_0 \ll k \ll \Lambda , \tag{1.8}$$

with exponents independent of the dimension d. The dimensionless *Kolmogorov constant* C_K is postulated to be a universal number (for given d).

There seem to be two schools of thought on the validity of (1.8). The Kolmogorov prediction, and its derivation, would probably not receive the attention it does today if it did not fit the experimental data so well [2]. One school takes this agreement as strong evidence that $\zeta=\frac{5}{3}$ is *exact,* and this has led to numerous attempts, based, to varying degrees, on the actual fluid equations themselves [3] to put the result (1.7) on a firmer theoretical footing. Unfortunately, all of these derivations contain uncontrolled approximations and the inherent danger (demonstrably present in many cases) is that they may all simply be more complicated rephrasings of Kolmogorov's original argument.

The second school (which includes the present authors) takes the view that turbulence is a strongly interacting, nonlinear problem and that it would be very surprising (if not disappointing) if the answer were indeed so simple. Given the failure of all attempts to date to prove its exactness, the proximity of experimental reality to the $\frac{5}{3}$ law should tentatively be viewed as coincidental [4] and some systematic means sought to *distinguish* ζ from $\frac{5}{3}$.

It is simple enough to parametrize such a distinction. If we relax the condition that $E(k)$ be independent of the outer scale l_0, the energy spectrum may then depend on the dimensionless combination $kl_0=k/m_0$ and Eq. (1.8) may be generalized to

$$E(k)=C_K'\rho_0\bar{\epsilon}^{2/3}k^{-5/3}(k/m_0)^{-\mu/9} \tag{1.9}$$

and thus $\zeta=\frac{5}{3}+\mu/9$. This definition of the exponent μ seems standard in the literature, originating from the Kolmogorov-Oboukhov-Yaglom log-normal theory [2] in which μ is proportional to the variance of $(\partial/\partial k)\ln[\epsilon(k)]$, where $\epsilon(k)$ is the (fluctuating) energy flux at scale k (no longer equal to the constant $\bar{\epsilon}$). Experimentally one finds $\mu\approx 0.2$–0.5. Within the theory, this exponent may also be interpreted in terms of the fractal codimension $d-D_f$ of the dissipation region via $\mu=3(d-D_f)$. Of course, deviations from the Kolmogorov $\frac{5}{3}$ law need not rely on the validity of this theory, nor its interpretation. Our own analysis will, in fact, confirm locality and the constancy of $\bar{\epsilon}$ (see Sec. IV F). Deviations result instead from large-scale sweeping effects.

C. Renormalization group approach

The most modern approach to the theory of turbulence is based on renormalization group ideas [5]. The renormalization group method has proven extraordinarily successful in the treatment of strongly interacting, highly nonlinear problems in equilibrium statistical mechanics. One might hope that the method would be equally successful in treating the problem of turbulence and hence resolve the differences between the two schools of thought. This hope turns out to be unfounded, as we shall detail below. However, the method does yield exact results for related problems, which can then serve as a basis for comparison with appropriate limiting cases of a more general theory. For this reason we summarize the renormalization group results in fair detail.

In applying the renormalization group method to turbulence one begins by modeling the stirring force $\mathbf{f}$ as a stochastic variable, usually taken to be Gaussian with zero mean and Fourier transformed variance

$$\langle \hat{f}_i(\mathbf{k},\omega)\hat{f}_j(\mathbf{k}',\omega')\rangle = \hat{D}(\mathbf{k},\omega)\hat{\tau}_{ij}(\mathbf{k})\delta(\mathbf{k}+\mathbf{k}')\delta(\omega+\omega') , \tag{1.10}$$

where $\hat{\tau}_{ij}(\mathbf{k})=\delta_{ij}-k_ik_j/k^2$ is the transverse projection operator arising from the choice $\nabla\cdot\mathbf{f}=0$. The δ functions reflect the basic assumption that the turbulence is *homogeneous*. Within this model, true turbulence is obtained when the driving spectrum $\hat{D}(\mathbf{k},\omega)$ vanishes rapidly for $k \gg m_0$. One may well question whether this model yields the same Kolmogorov spectrum as one with a more deterministic stirring force, i.e., whether or not they lie in the same "universality class." Clearly for a very weak deterministic force, the flows will also be deterministic. However, as the strength of the forcing grows, the onset of turbulence is expected to occur, first, through various routes to temporal chaos. Eventually, through as yet ill understood means, as the driving strength increases, flows that are both temporally *and* spatially chaotic will be generated [6]. Once the flows are chaotic, the behavior in the inertial range is expected to be insensitive to the detailed structure of the forcing and the stochastic model is probably appropriate. This question will not be addressed any further in this work; from now on we simply work with the model (1.10). The meaning of the average in (1.5) is now clear: the velocity field is to be averaged over all realizations of the stochastic driving force.

In addition to the velocity correlator $\hat{U}(\mathbf{k},\omega)$, there is another crucial two-point correlation function, namely, the *response function* $\hat{G}(\mathbf{k},\omega)$, which measures the average response of the velocity field to an infinitesimal forcing field:

$$\left\langle \frac{\delta\hat{v}_i(\mathbf{k},\omega)}{\delta\hat{f}_j(\mathbf{k}',\omega')}\right\rangle = \hat{G}(\mathbf{k},\omega)\hat{\tau}_{ij}(\mathbf{k})\delta(\mathbf{k}+\mathbf{k}')\delta(\omega+\omega') . \tag{1.11}$$

With the Gaussian stochastic driving (1.10), one has the more explicit relation

$$\langle \hat{v}_i(\mathbf{k},\omega)\hat{f}_j(\mathbf{k}',\omega')\rangle = \hat{G}(\mathbf{k},\omega)\hat{D}(\mathbf{k},\omega)\hat{\tau}_{ij}(\mathbf{k}) \times\delta(\mathbf{k}+\mathbf{k}')\delta(\omega+\omega') . \tag{1.12}$$

The response function is *causal*, so that in the time domain $\hat{G}(\mathbf{k},t)=0$ for $t<0$, while

$$\hat{G}(\mathbf{k},t\to 0+)=1 \quad \text{for all } \mathbf{k} . \tag{1.13}$$

The renormalization group method is based on a form of the driving spectrum that has completely opposite characteristics from that required for turbulence. Specifically, the driving spectrum is assumed to grow *stronger* as k increases:

$$\hat{D}(\mathbf{k},\omega)\equiv D(k)=\frac{D_0k^{4-d}}{(k^2+m_0^2)^{(1/2)y}} , \tag{1.14}$$

where the parameter y is assumed to be either negative or positive but *small*.

When $y=2-d, D(k)\approx D_0k^2$ and the model is that of a *thermally driven* fluid (for this case it is certainly safe to take $m_0\equiv 0$). The fluctuation-dissipation theorem then requires that $D_0=k_BT\nu_0/\rho_0$ and the relation $\hat{U}(\mathbf{k},\omega)=(D_0/\nu_0)\mathrm{Re}\hat{G}(\mathbf{k},\omega)$ holds. The model was originally proposed by Forster, Nelson, and Stephen [5(a)] in order to study the effects of small-scale thermal fluctuations on large-scale hydrodynamics. By using a momentum-shell renormalization group technique, in which short length-scale fluctuations are successively integrated out, these authors were able to derive recursion relations for the length-scale-dependent effective viscosity $\nu(l)$ and nonlinearity coefficient (essentially a scale-dependent Reynolds number) $\bar{\lambda}(l)=\lambda(l)[D(l)/\nu(l)^3]^{1/2}$, where l is the renormalization group flow parameter. For $d>2$ they showed that $\lim_{l\to\infty}\nu(l)=\nu_R$ is finite, while $\lim_{l\to\infty}\lambda(l)=0$, indicating that linear hydrodynamics, with a renormalized (eddy) viscosity ν_R, appropriately describes large-scale flows. Generally, ν_R is larger than ν_0 (and is, in fact, positive even when $\nu_0\equiv 0$), indicating enhanced diffusive transport by small-scale eddies. The energy spectrum obeys the equipartition principle $E(k)\sim k^{d-1}$. In contrast, for $d<2$ nontrivial large-scale behavior results: in an expansion in $y=2-d$, $\bar{\lambda}(l)$ flows to a *finite fixed point value* $\bar{\lambda}_R=O(y)$ and $\nu(l)$ *diverges* as $l\to\infty$. However, the energy spectrum still obeys $E(k)\sim k^{d-1}$, a consequence of the fluctuation-dissipation theorem.

These authors also considered the case $y=4-d$, and hence $D(k)\approx D_0$, in which all wave numbers are driven equally ("uniform" driving). In this case, linear hydrodynamics is valid on large scales only when $d>4$. Once more, when $y=4-d>0$, $\bar{\lambda}(l)$ flows to a nontrivial fixed-point value $\bar{\lambda}_R=O(y)$ and now the energy spectrum exhibits nontrivial power-law behavior $E(k)\sim k^{(1/3)(2d-5)}$. Note that in both cases the borderline between the two different kinds of behavior occurs at $y=0$.

A short time later, DeDominicis and Martin [5(b)] formalized and generalized these results using field-theoretic methods. From Ward identities and the general form (1.14) for the driving spectrum, they showed that for $y<0$ linear hydrodynamics results on large scales, while for $y>0$, $\bar{\lambda}_R=O(y)$ is finite. Furthermore, they showed that under the implicit assumption that the limit $m_0\to 0$ may be taken safely, *to all orders in y*, the energy spectrum takes the power-law form

$$E(k)\sim k^{-\zeta(y)},\quad \zeta(y)=\tfrac{2}{3}y-1\ , \tag{1.15}$$

with no further explicit dimensionality dependence in ζ.

The renormalization group picture implies much more than power-law energy spectra. The existence of fixed points implies *scaling* of the correlation functions. Thus, for example, in the inertial range the correlation and response functions are predicted to take the forms

$$\hat{G}(\mathbf{k},\omega)\approx A_1 k^{-z} g(\omega/\tilde{\nu}k^z)\ , \tag{1.16}$$

$$\hat{U}(\mathbf{k},\omega)\approx A_2 k^{-\Delta} u(\omega/\tilde{\nu}k^z),\quad k,\omega\to 0\ , \tag{1.17}$$

where the exponents Δ and z and the *scaling functions* $g(s)$ and $u(s)$ are universal, while A_1, A_2, and $\tilde{\nu}$ are nonuniversal scale factors. The *dynamical exponent* z provides a connection between length scales and time scales. The fact that it appears also in the prefactor of (1.16) is a consequence of the normalization (1.13). DeDominicis and Martin [5(b)] show that, again to all orders in y, these exponents are given by

$$z=2-\tfrac{1}{3}y,\quad \Delta=d+\tfrac{1}{3}y\quad (y>0)\ . \tag{1.18}$$

Notice that this implies the "hyperscaling" relation

$$\Delta+z=d+2\ , \tag{1.19}$$

which will be significant later on. The relation (1.7) gives $E(k)\approx B_d u_0\rho_0\tilde{\nu}k^{-\zeta(\Delta,z)}$, where

$$\zeta(\Delta,z)=\Delta-z-d+1 \tag{1.20}$$

and $u_0=\int_{-\infty}^{\infty}(ds/2\pi)u(s)$. Together with (1.18) this immediately yields the result (1.15). It should be emphasized that (1.20) is a general scaling relation, whereas (1.18) and (1.19) are valid only within the y expansion.

Now, what connection, if any, do these results have with turbulence? Clearly, what we will call the "short-ranged" driving problem, in which $D(k)$ effectively vanishes for $k\geq m_0$, corresponds, in some sense, to the limit $y\to\infty$ of the "long-ranged" driving problem. If we blindly take this limit in (1.15), ζ diverges to positive infinity, which is clearly nonsensical. This is our first hint that the y expansion must have a finite radius of convergence y_0.

From theories of critical phenomena one knows that "input" exponents, such as y, need not actually be infinite to recover short-range behavior. Rather, for sufficiently large values $y>y_c$, one expects long-range driving (1.14) to become technically *irrelevant* and give rise only to lower-order corrections to the leading short-range (i.e., turbulent) behavior. In the simplest, most optimistic scenario, the value of y at which this happens is precisely the radius of convergence of the expansion around $y=0$, i.e., $y_c=y_0$. In the renormalization group picture, this corresponds to a continuous coalescence of the long-range fixed point with the short-range one and the exponents, correspondingly, merge continuously with their short-range values. We would conclude, in this case, that $\zeta=\frac{2}{3}y_c-1$, $z=2-\frac{1}{3}y_c$, and $\Delta=d=2+\frac{1}{3}y_c$.

Unfortunately, within the y expansion there is no direct way of ascertaining either y_0 or y_c. DeDominicis and Martin [5(b)] have shown that for $y>4$ there is an infinite number of *relevant* Galilean invariant perturbations to the *linear* hydrodynamical fixed point. This, unfortunately, says nothing about the stability of the long-range fixed point and neither establishes that $y_0=4$ nor that $y_0=y_c$, though a great deal of work has been based on precisely these assumptions [7]. What makes them so compelling is that, as first noticed by DeDominicis and Martin [5(b)], these assumptions yield precisely the Kolmogorov result for the energy spectrum $\zeta=\frac{5}{3}$.

D. Analogy to spin models with long-range interactions

In order to place the renormalization group results in a clearer context, the following analogy is useful [8]. Consider the standard ferromagnetic phase transition in an Ising model with *long-range interactions*. The Hamiltonian is

$$H_I=-\tfrac{1}{2}\sum_{i\neq j}J_{ij}s_i s_j\ , \tag{1.21}$$

where $s_i=\pm 1$ is the Ising spin at d-dimensional lattice site i and the exchange constants have the power-law behavior

$$J_{ij}=J_0|\mathbf{R}_{ij}|^{-(d+\sigma)},\quad i\neq j,\ J_0>0\ , \tag{1.22}$$

in contrast to those for the standard Ising model, which vanish when i and j are not nearest neighbors. In Fig. 1

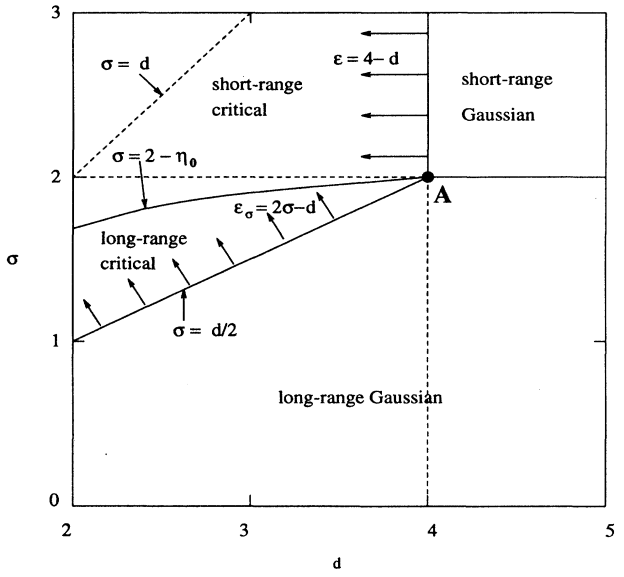

FIG. 1. "Phase diagram" for the Ising model with long-range interactions. Solid lines separate different universality classes of critical behavior. Dashed lines are guides to the eye. As indicated by the arrows, the renormalization group ϵ and ϵ_σ expansions allow one to access perturbatively the behavior near the Gaussian phase boundaries. Of special interest is the nontrivial boundary $\sigma=2-\eta_0$ (where η_0 is the short-range critical correlation decay exponent) between the long-range critical and short-range critical phases.

we show the boundaries between various types of critical behavior in the d-σ plane. For $\sigma < \frac{1}{2}d$ or $d > 4$ a Gaussian model controls the critical behavior. For sufficiently large σ and $d < 4$ the usual short-range critical behavior, characteristic of the nearest-neighbor Ising model, results. For $d < 4$ there is an intermediate range of σ for which *nontrivial* long-range critical behavior results. We make an analogy between Gaussian behavior in the spin model and linear hydrodynamic behavior in the fluid model, between short-range Ising critical behavior and real turbulence, and between nontrivial long-range critical behavior and the long-range driven fluid. Analogous to the y expansion in the fluid problem is the ϵ_σ expansion [9], with $\epsilon_\sigma = 2\sigma - d$, which penetrates upward into the long-range critical region from the line $\sigma = \frac{1}{2}d$. In addition, an analysis equivalent to that of DeDominicis and Martin [5(b)] shows that for $\sigma > d$ there are infinitely many relevant perturbations to the long-range Gaussian fixed point (corresponding to long-range multicritical behavior of all orders). It is clear from Fig. 1 that this line has no significance whatsoever, as long as $d > 2$.

In the spin problem one has the advantage that the short-range critical behavior may be accessed directly through the usual ϵ expansion [10] about $d = 4$. Thus one can check directly the relevance of long-range interactions at the short-range Ising fixed point. This, as well as more general arguments, allows one to fix precisely the boundary between short-range and long-range critical behavior [11], which occurs when $\sigma = 2 - \eta_0$, where $\eta_0(d)$ is the short-range value of the critical decay exponent η. In addition, the long-range value of η is given *exactly* by $\eta_{\mathrm{LR}} = 2 - \sigma$, much like the exact results (1.15) and (1.18) for the fluid problem. Note that this immediately implies continuity of η across the long-range–short-range boundary.

We may now address, by analogy, the question of the position of the equivalent long-range–short-range boundary in the fluid problem. There is no information in the ϵ_σ expansion about the value of η_0 and therefore no hint that the value $\sigma = 2 - \eta_0$ is special. Only by locating *both* fixed points and seeing when they merge, or, equivalently, seeing when the long-range fixed point becomes unstable to the short-range one, can this boundary be located. Naively, one might have expected this boundary to occur at $\sigma = 2$, for this is when the k^2 and k^σ terms in the Fourier transform $\hat{J}(\mathbf{k}) = \hat{J}_0 + \hat{J}_2 k^2 + \hat{J}_\sigma k^\sigma + O(k^4)$ of J_{ij} exchange dominance as $k \to 0$. For subtle reasons, involving the nontrivial rescaling of the k^2 term under renormalization [11], this expectation is false. There is no reason not to have similar doubts about the $y_0 = y_c = 4$ conjecture in the turbulence problem.

It is basically the existence of the point A in Fig. 1, near which all of the four possible fixed points are simultaneously perturbatively accessible (both ϵ and ϵ_σ are small), that allows one to infer the detailed characteristics of the short-range–long-range boundary. The apparent absence of such a point in the d-y plane for fluids is what leads to the failure of the renormalization group method in turbulence. We are therefore forced to seek an alternative approach in order to make progress on this problem.

E. The $1/N$ expansion and the spherical limit: Motivation and results

In the theory of equilibrium phase transitions there are actually *two* analytic techniques that have provided many of the fundamental insights into the nature of critical phenomena: the ϵ expansion [9,10] and the $1/N$ expansion [12]. The first, as we have seen, corresponds most closely to the y expansion and is based on the fact that the critical behavior is simple in sufficiently high dimension $d > d_c$. One can then perform a systematic expansion in $\epsilon = d_c - d$ when $d < d_c$ (here $d_c = 4$ for the short-range Ising model and $d_c = 2\sigma$ for the long-range Ising model when $\sigma < 2$).

The second technique involves analytically continuing the problem to one with a larger number of degrees of freedom N. Thus the Ising Hamiltonian is generalized to the $O(N)$ model $H^{(N)} = -\frac{1}{2}\sum_{i \neq j} J_{ij} \mathbf{s}_i \cdot \mathbf{s}_j$, where $\mathbf{s}_i$ is an N-component unit vector $|\mathbf{s}_i| = 1$. If taken in an appropriate fashion, the so-called *spherical limit* $N \to \infty$ is often analytically tractable and a systematic expansion in $1/N$ may be developed for the exponents [12]. The ϵ expansion has generally proven the more definitive of the two in understanding critical phenomena, mainly because it transpires that the dimensionality of interest, namely, $d = 3$, is usually, in some sense, closer to $d_c = 4$ than are physical values of N, say, $N = 1, 2$, or 3, to $N = \infty$. However, the $1/N$ expansion has the advantage that the dimensionality d is a completely free variable and is therefore useful in the study of physics in lower dimensions where ϵ is not small.

In turbulence, as described, the analog of the ϵ expansion is uncontrolled in the region of interest. We seek, therefore, an approach in which the variable y [or, more generally, the entire driving function $D(\mathbf{k},\omega)$], like the dimensionality d in the spin problem, may be taken as a free parameter. This paper, then, is concerned with the construction of a $1/N$ expansion for turbulence. Our first aim is to appropriately generalize the Navier-Stokes equation to N coupled equations in N (d-component) velocity fields $\mathbf{v}^l(\mathbf{x},t)$, $l = 1, \ldots, N$, in such a way that an analytically tractable spherical limit exists and then to elucidate the dependence of the Kolmogorov spectrum (1.1) on y. In particular, we wish to understand the *analyticity* properties of $\zeta(y)$ and by what mechanism true turbulence is recovered in the limit of large y. By analogy with the $O(N)$ symmetry that lies at the heart of the spherical limit for the spin model, we argue that in order to be useful these equations must be invariant under a new group G of symmetry transformations. This is necessary in order that the diagrammatic perturbation theory have certain desirable invariance properties. We will discuss in detail in Sec. II how such a group of symmetries can be properly incorporated. Our second aim is to understand, as best we are able, the extent to which these generalized equations embody the physics of the usual ($N = 1$) Navier-Stokes equations. The essential results of our study are summarized below and in Figs. 2 and 3.

1. *Models I and II: Integral equations and scaling*

We consider two classes of models, which differ in their treatment of Galilean invariance. Most of our detailed, explicit results are obtained for the simpler class, which we call *model I.* This class has an exact Galilean invariance only when $N=1$ (corresponding to the original Navier-Stokes equations). Partial results are obtained for a more complicated, extended class, which we call *model II.* This class is obtained by coupling one extra velocity field (which we call the *zero mode*) to model I in just such a way that an exact Galilean invariance is preserved for all N. The original Navier-Stokes equations then correspond to the limit in which only the zero mode remains, i.e., to $N=0$.

In the spherical limit, model I yields a pair of coupled, nonlinear integral equations for the functions $\hat{G}(\mathbf{k},\omega)$ and $\hat{U}(\mathbf{k},\omega)$ [see Eqs. (3.17)–(3.20)], which turn out to be precisely Kraichnan's direct interaction approximation (DIA) equations [13]. Although they have been studied for more than 35 years, these equations have never been fully solved. Kraichnan [13], through a series of scaling arguments, concluded that

$$z=1, \quad \Delta=d+\tfrac{3}{2}, \quad \zeta=\tfrac{3}{2} \tag{1.23}$$

for short-range driving. We shall show that these results are, in fact, correct and in Sec. IV we will present *complete solutions* for the scaling functions $g(s)$ and $u(s)$. Note that these exponent values violate the hyperscaling relation (1.19) and therefore *do not correspond to any value of y.* We are also able to compute explicitly the energy flux $\bar{\epsilon}$, which is derived from a three-point correlation function, verifying that it is indeed constant in the inertial range. In addition, we explicitly confirm locality of the energy cascade.

The existence of scaling allows for stringent tests of numerical and experimental data. Dividing the correlation function and frequency by appropriate powers of the wave number should, up to overall nonuniversal scale factors, collapse the data onto a single universal curve. These overall scale factors depend on details of the driving spectrum and therefore vary from system to system. To completely specify such universal curves it is therefore important to know how many independent scale factors there are. Within the Kolmogorov theory there is only one, the energy flux $\bar{\epsilon}$, in terms of which all others may be expressed. For example, $A_2=1/A_1=\bar{\nu}=\bar{\epsilon}^{1/3}$. It is precisely this that leads to the universality of the amplitude C_K in (1.8).

As discussed in detail in Sec. IV G, the DIA equations, on the other hand, predict *two* independent scale factors. Aside from the energy flux $\bar{\epsilon}$, there is a second *velocity* scale v_p [which in the spherical limit is precisely the total root mean square velocity fluctuation v_0 defined below (1.7), but in general might be different], which diverges as $m_0\to 0$ and directly determines the properties of the inertial range. These two parameters are independent and universal amplitudes are now generated by constructing certain ratios in which all dependence on them cancels. The main shortcoming of the Kolmogorov theory is, then, that this second parameter has been left out: intuitively, the velocity scale v_p and the steady state energy flux $\bar{\epsilon}$ scale *independently* with the amplitude and shape of the driving spectrum and both are needed to fully specify the scaling in the inertial range.

From $\bar{\epsilon}$ and v_p one may construct a length scale l_p, which is of the same order as l_0, via $\bar{\epsilon}=\lambda_0^3 v_p^3/l_p$ and thus a time scale $t_p\equiv 1/\omega_p=l_p/v_p$. It is precisely the dimensionless combinations kl_p and ωt_p that appear in the scaling forms and it is then easy to reconstruct all other scale factors once the exponents are known. Motivated by similar results for critical amplitudes at second-order phase transitions [14], we propose that these statements hold also for finite N, in particular $N=1$. We do not have a general theoretical definition of v_p, but for a given experimental or model system it may be inferred from a single well defined inertial range measurement. An important consequence of this is that by using l_p in place of $1/m_0$ in (1.9), the dimensionless constant C_K' is in fact *universal.* For the DIA equations one has $\mu=-\frac{3}{2}$ and $C_K'\simeq 314$ [denoted by c_d in (4.81)].

The spherical limit of model II may also be solved in closed form. It transpires, however, that the fundamental objects are five three-point functions, with five corresponding coupled nonlinear integral equations [see Eqs. (3.37)–(3.39)]. These describe the correlations of the zero mode with each of the other N modes and the two-point functions (1.5) and (1.11) may then be derived from them [see Eq. (3.35) along with (3.17) and (3.18)]. The kernels of these integral equations turn out to involve the solutions to model I, which therefore serve as inputs to model II. We have not yet obtained explicit solutions to these equations; however, we are able to confirm the scaling hypotheses (1.16) and (1.17). We thereby find that the exponents are still given by (1.23). Put another way, the model II solutions represent *finite* renormalizations of the model I solutions.

Since we do not obtain explicit forms for the scaling functions, we have not yet been able to verify within this model the proposed results for the scale factors. In particular, since the energy flux is a significantly more complicated quantity, its connection to the two-point function scale factors remains untested in this model. We are actively continuing to pursue these questions.

More importantly, perhaps, are fundamental questions about the role of Galilean invariance. It has long been proposed that since large-scale sweeping should not affect the breakup dynamics of a small eddy, energy transfer between scales should significantly reflect Galilean invariance. As we shall discuss further in Sec. V, the DIA equations are known to suffer certain deficiencies in their modeling of energy transfer. It would be of great interest, then, to investigate the detailed physics of energy transfer processes within model II. Unfortunately, the present partial results for model II do not permit us to make a detailed study of the effects of generalized Galilean invariance. This will be left as important work for the future.

2. *Long-ranged versus short-ranged driving and the breakdown of the renormalization group y expansion*

The solution of the DIA equations is intimately related to the interplay between long-ranged and short-ranged driving. Although of intrinsic interest due to its role in renormalization group calculations, it transpires that keeping the exponent y as a free parameter also provides a numerical device for solving the DIA equations in the presence of short-range driving. This will be explained in Sec. IV C. Thus, even if our main purpose here is to understand short-ranged driving appropriate to real turbulence in the spherical limit, it turns out that an understanding of long-ranged driving is required first anyway.

If one examines the solutions to the DIA equations in the presence of long-range driving one discovers some amazing things. First, as long as the integrals converge in the scaling limit $m_0 \to 0$, one finds precisely the hyperscaling relation (1.19). If, furthermore, it is assumed that $D(k)$ controls the scaling (i.e., that the driving term is of the same order as the interaction terms in the inertial range), then (1.18) and (1.15) hold and the y-expansion results are reproduced exactly. In fact, it can be shown that the DIA equations are an *exact resummation* of the $O(y)$ renormalization group recursion relations (see Sec. III). The limit $N \to \infty$ therefore reproduces the properties of the original Navier-Stokes equations exactly to $O(y)$. However, the DIA equations also extend these recursion relations to arbitrary driving $D(\mathbf{k},\omega)$ and allow us to see where the y-expansion results *break down.* Specifically, when $y \geq 3$ the DIA integrals no longer converge and the limit $m_0 \to 0$ becomes subtle. The radius of convergence of the y expansion is then $y_0 = 3$ (at least when $N \to \infty$; we shall argue later that this is also correct for general N). By careful asymptotic analysis one can show that the dynamical exponent *sticks* at $z = 1$ and, again, as long as the driving still controls the scaling, one finds

$$\Delta = d + 1 + \frac{y-3}{2}, \quad \zeta = 1 + \frac{y-3}{2} . \tag{1.24}$$

Finally, to connect these with the Kraichnan [13] $\zeta = \frac{3}{2}$ result, one must determine the value of y at which the driving ceases to control the scaling. This occurs at $y = y_c = 4$: for $y > 4$ long-range driving becomes technically irrelevant and except for lower-order corrections to scaling is equivalent to the short-range driving problem. For $y > 4$ all exponents then stick at values determined by (1.24) with $y = 4$, i.e., precisely the values (1.23) predicted by Kraichnan [13].

In Fig. 2 these results for the exponents in the spheri-

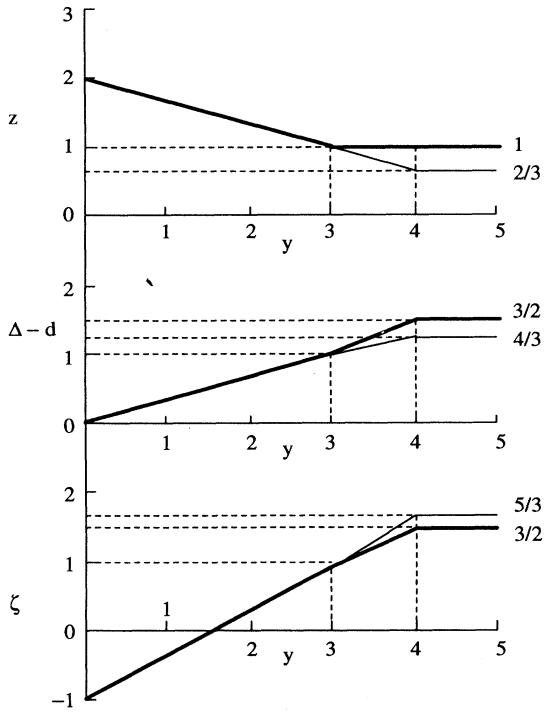

FIG. 2. Turbulent spectral exponents as a function of driving exponent y. Heavy lines denote the behavior in the spherical limit; light lines denote the behavior predicted by the naive extrapolation of the renormalization group results. Dashed lines are guides to the eye.

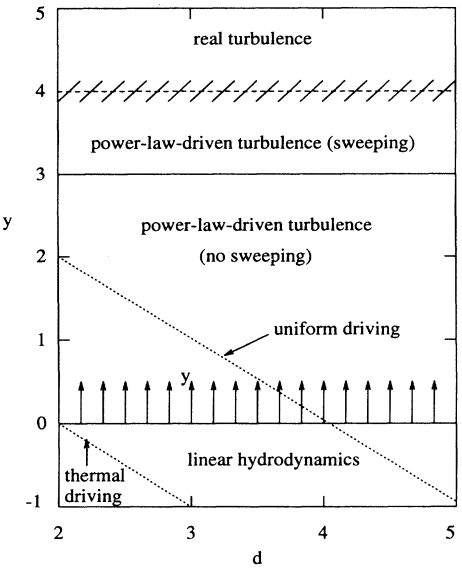

FIG. 3. "Phase diagram" for power-law driven incompressible turbulence. Solid lines separate different universality classes of behavior. The dashed line at $y = 4$ denotes the true turbulent phase boundary in the spherical limit $N \to \infty$. The hatching indicates that this line may be a nontrivial function of N. The boundaries at $y = 0$ and 3 are claimed to be exact. As indicated by the arrows, the renormalization group y expansion allows one to access perturbatively the behavior for small $y > 0$. The dotted lines are physical trajectories in parameter space for particular forms of the driving spectrum. Of special interest is the new universality class, in the interval $3 < y < 4$, that intervenes between the region of validity of the y expansion $0 < y < 3$ and the region of true turbulence $y > 4$. It is the existence of this region that causes the exponents in Fig. 2 to break away from their renormalization group counterparts.

cal limit, which we argue to be valid also for the spherical limit of model II, are contrasted with those obtained from the $y_0=y_c=4$ conjecture. In Fig. 3 we show a "phase diagram" analogous to that for the Ising model, Fig. 1. Our basic prediction is then that a *new* type of long-range driven turbulence intervenes between the boundary of convergence for the y expansion $y_0=3$ (which we believe to be exact for finite N as well; see below) and the onset of effectively short-range driving appropriate to true turbulence, which in the spherical limit occurs at $y_c=4$ (and will likely have corrections for finite N). Thus, although effectively short-range driving indeed occurs for $y>y_c=4$, the different behavior in the intermediate interval $3<y<4$ changes completely the values of the turbulent exponents. In renormalization group language, a *new* stable fixed point bifurcates away from the now unstable long-range driving fixed point and only later coalesces with the short-range driving fixed point. In more physical terms, sweeping effects become important *before* power-law driving becomes effectively short ranged. This scenario is clearly even more involved than that for the Ising model, where the analogs σ_0 and σ_c of y_0 and y_c, though nontrivial, are at least *equal*, $\sigma_0=\sigma_c=2-\eta_0$.

3. Relevance to $N=1$

The physics behind the conjectured $y=3$ borderline is, in fact, well known, corresponding to the oft-quoted effects of sweeping of smaller eddies by larger ones (this will be discussed in more detail in Sec. V). The dynamical exponent value $z=1$ then confirms the Taylor "frozen in" hypothesis: small-scale turbulent structures are swept past a fixed observer at a speed that fluctuates, but remains more or less constant in order of magnitude. This speed basically determines the shortest time scale in the problem and the small-scale structures change very little in the time it takes them to be swept by. Therefore, the measurement of the temporal velocity fluctuations at a single point is nearly equivalent to the measurement of spatial velocity fluctuations along a one-dimensional line at a single time. Inertial range frequency spectra and wave-number spectra should then be the same, up to a rescaling factor that depends on the large-scale velocity v_0. The fact that the spherical model equations are proven to reflect this physics is heartening and leads us to believe that $y_0=3$ and $z=1$ are exact results, independent of N for models I and II. It is not clear to us at this stage whether the subsequent y dependence (1.24) of the exponents is different for general N or whether only the boundary y_c shifts.

Another interesting feature of the $y=3$ borderline is that the Kolmogorov exponent passes through unity at this point. This means that the energy spectrum goes from being ultraviolet dominated to infrared dominated. Thus for $y>3$ most of the energy resides at small wave numbers, which then gives rise to the sweeping effects on the high wave numbers (this then indicates that the fact that $\zeta=1$ and $z=1$ occur simultaneously is not a coincidence). Therefore, in order to obtain a finite total energy for $y<3$, one must regularize the driving spectrum at short distances and look for universal power laws at large distances: this is the usual case in critical phenomena (where a lattice spacing plays the role of the short-distance cutoff) and lies at the basis of the original renormalization group approach to the Navier-Stokes equations [5]. However, for $y>3$ one must regularize the driving spectrum at large distances (this is the role of l_0) and look for universal power laws at short distances, the opposite of the usual case in critical phenomena. From a renormalization group point of view this means that the fixed point is conjectured to go from being infrared stable to ultraviolet stable as y increases through 3 [15].

In a nutshell, it is attempts to *remove* the boundary at $y=3$ that motivates many of the attempts to show that the Kolmogorov $\frac{5}{3}$ law is exact [see especially [3(b)]. At the level of the DIA equations, these efforts focus on producing, in some natural way, extra terms that *cancel* the divergent parts of the integrals when $y\geq 3$ (this will be alluded to at the end of Sec. IV E). One problem with such procedures is that if these same terms are produced when $y<3$, there will be large-k divergences in the region described (presumably correctly, even for the original Navier-Stokes equations) by the y expansion. The theory will then fail to encompass the known exact results.

The second problem is connected with the entire philosophy of the large-N approach. The limit $N\rightarrow\infty$ produces an exactly soluble model. Any alterations in this model can come only from finite-N corrections; the DIA equations, not their subtracted versions, are fundamental. The same realizability problem occurs in more sophisticated *Lagrangian history* versions of the direct interaction approximation [16]. Although the exponents take the Kolmogorov values, there is no known limiting model for which the equations provide an exact solution. On the other hand, in our approach the differences between the value $\zeta=\frac{3}{2}$ we establish at $N\rightarrow\infty$ and the experimental result $\zeta\simeq\frac{5}{3}$ at $N=1$ are now accounted for in a very natural way: we propose that, just as for the $O(N)$ spin model, the exponents Δ and ζ (and most likely the boundary y_c) vary continuously with N, interpolating between $\zeta(\infty)=\frac{3}{2}$ and $\zeta(1)\simeq\frac{5}{3}$. The fact that $\zeta(\infty)\neq\frac{5}{3}$ is strong evidence that $\zeta(1)$ is a nontrivial exponent, not obtainable through any simple argument. A real test of our approach would be to compute the first correction, in powers of $1/N$, to $\zeta(\infty)$. As will be seen in later sections, this is a daunting task, but seems a necessary step in order to confirm our ideas.

4. Turnover times

Finally, we discuss efforts to define internal "Lagrangian" turnover time scales that differ from the sweeping time scale. Although only the latter appears in the scaling of the two-point functions, this leaves open the question of whether other longer time scales, associated in some sense with dynamical time scales of moving inertial range eddies, can be defined and calculated. We do not know the general answer to this question, but in Sec. V B we describe one possible way of defining such a time scale, yielding an associated "internal dynamical exponent" $z_{\rm int}<1$, even in the spherical limit.

The definition involves the scaling of the relative size of the inertial range $l_0/l_\nu=\Lambda/m_0$ with Reynolds number $\mathrm{Re}\equiv\lambda_0 v_p l_p/\nu_0\sim\lambda_0 v_0 l_0/\nu_0$. The idea is that, since the local dissipation rate is a Galilean invariant quantity, at the boundary $k\sim\Lambda$ between the inertial and dissipation ranges, the dissipation time scale $\tau_\Lambda\equiv 1/\omega_\Lambda=\nu_0\Lambda^2$ should also reflect the intrinsic eddy dynamics. We therefore define $z_{\rm int}$ via $\omega_\Lambda t_0\sim(\Lambda l_0)^{z_{\rm int}}$, where $t_0=l_0/v_0$ is the outer sweeping time scale. The Kolmogorov theory yields $z_{\rm int}=\frac{2}{3}$, while the DIA equations yield $z_{\rm int}=\frac{1}{2}$, which are indeed different from $z=1$. We also give a general scaling argument, valid for general N, which implies the scaling relation $z_{\rm int}=\zeta-1$, completely consistent with these two special cases.

The existence of an extra time scale is a feature special to turbulence and arises from the fact that $z\to 1$ as $y\to 3$. Since energy transfer involves a three-point correlation function, this time scale cannot be obtained from the two-point correlation functions alone and there is therefore no contradiction with the previous conclusion that $z=1$. We do not know at this stage whether this argument can be generalized to obtain explicit inertial range scaling functions for more complicated quantities based on a scaling variable $\omega/k^{z_{\rm int}}$.

F. Outline

This completes our survey of the results described in detail in later sections. The remainder of this paper is organized as follows. In Sec. II we generalize the Navier-Stokes equations (1.2) to N equations for N d-dimensional velocity fields. We discuss in detail how the new group G of symmetries can be properly incorporated. We find that incorporation of an exact Galilean symmetry is nontrivial and requires an extension of the simplest, irreducible, representations of the symmetry group to reducible representations that include the zero mode.

In Sec. III we discuss the spherical limit $N\to\infty$. We outline the general methodology for analyzing this limit and then, using a particular choice for the symmetry group G, derive the spherical limit integral equations. For model I, which does not possess an exact Galilean symmetry, the DIA equations result. For model II, which does possess an exact Galilean symmetry, there results a more complicated set of equations, which actually demand the solutions to the DIA equations as input.

In Sec. IV we solve the DIA equations, deriving the key results shown in Figs. 2 and 3. In so doing we exhibit full solutions for the scaling functions $g(s)$ and $u(s)$ and derive the physical scales l_p and v_p. Following Kraichnan [13], we are then able to give a detailed demonstration of locality and derive the various universal amplitudes, generalizing, for example, the Kolmogorov constant C_K in (1.8). Locality has long been proposed as a property of real Navier-Stokes turbulence and we therefore conjecture that similar universal amplitudes exist at $N=1$. In Sec. IV H we outline partial solutions to model II, confirming Figs. 2 and 3 for this model as well, but leave detailed analysis of the inertial range properties for future work.

In Sec. V we conclude by reviewing previous theories of turbulence, and some of their shortcomings, in the light of our own results. In particular, we attempt to reconcile Lagrangian coordinate viewpoints of the local cascade process, eddy turnover times, etc., with our own more Eulerian viewpoint. For example, the common notion of an intrinsic eddy turnover time, different from and much longer than the sweeping time, is at the heart of the Taylor hypothesis, but would seem to require two (or more) different dynamical exponents. We illustrate one way of extracting a second time scale by discussing the scaling of the dissipation length with Reynolds number.

Finally, we discuss open questions and work for the future. For example, it has been known for a long time that the DIA equations possess certain unphysical features that are directly connected to the problem of Galilean invariance (this was alluded to in Sec. I E 1 and is discussed at the end of Sec. V A). A high priority, then, is to examine this same physics in the context of model II. Other work will include the calculation of finite-N corrections and applications of large-N techniques to other nonequilibrium dynamical problems.

The Appendixes are devoted to more technical derivations. In Appendix A we discuss Ward identities and the status of Eqs. (1.15) and (1.18) for general N. In Appendix B we generalize the von Kármán–Howarth result for the third-order velocity moment to general N. In Appendix C we summarize a failed attempt to use the adjoint representation of SU(N) to construct a large-N theory. In Appendix D we give a simpler analysis, parallel to that of the full DIA equations given in Sec. IV, using a set of simplified DIA equations. Finally, in Appendix E we give details of the numerical techniques used in Sec. IV to solve for the scaling function $u(s)$ and related universal amplitudes. A preliminary report of our results has appeared previously [17].

II. GENERALIZATION TO N VELOCITY FIELDS

A. Analogy to spin models

The most straightforward generalization of the Navier-Stokes equations (1.2) to N velocity fields $\mathbf{v}^l$, $l=1,\ldots,N$, is

$$\frac{\partial\mathbf{v}^l}{\partial t}+\lambda_0\sum_{m,n=1}^{N}A_N^{lmn}(\mathbf{v}_m\cdot\nabla)\mathbf{v}_n=-\frac{1}{\rho_0}\nabla p^l+\nu_0\nabla^2\mathbf{v}^l+\mathbf{f}^l\,,$$
$$\nabla\cdot\mathbf{v}^l=0,\ l=1,\ldots,N\,, \qquad (2.1)$$

where $\mathbf{f}^l$ are independent random forces. The only question one must address is that of the choice of the tensor $\mathbf{A}_N$ (for later convenience, a distinction, to be defined below, has been made between upper and lower "isospin" indices l, m, and n).

Here we again appeal to the spin model analogy [8]. The generalization of the Ising Hamiltonian (1.21) to N-component spins $\mathbf{s}_i=(s_{i,1},\ldots,s_{i,N})$ is

$$H^{(N)}=-\tfrac{1}{2}\sum_{i\neq j}J_{ij}\sum_{l,m=1}^{N}C_N^{lm}s_{i,l}s_{j,m},\quad|\mathbf{s}_i|^2=N\,, \qquad (2.2)$$

where one must choose an appropriate $N\times N$ positive

definite matrix $\mathbf{C}_N$ (the normalization $|\mathbf{s}_i|^2=N$ is chosen by convention and yields the correct large- and small-N limits). Since $\mathbf{C}_N$ is symmetric one may perform a rotation in spin space to diagonalize it, obtaining

$$H^{(N)}=-\tfrac{1}{2}\sum_{i\neq j}J_{ij}\sum_{l=1}^{N}\lambda^l s_{i,l}s_{j,l},\quad |\mathbf{s}_i|^2=N\ , \tag{2.3}$$

where λ^l are the eigenvalues of $\mathbf{C}_N$. Clearly, any state with long-range magnetic order will energetically prefer to align along the component of $\mathbf{s}$ with largest eigenvalue, say, λ^1. If λ^1 is unique one can, in fact, show that the critical behavior is completely dominated by this "easy axis" [18] and lies in the same universality class as that of the Ising model (1.21). We have therefore gained nothing by giving $\mathbf{s}_i$ extra components. Only if λ^1 is *not* unique does the critical behavior change. Thus if $\lambda^1=\lambda^2=\cdots=\lambda^M$, $M\leq N$, are the largest eigenvalues, then the model has $O(M)$ symmetry and the critical behavior depends on the value of M. Again, however, the $N-M$ components with smaller eigenvalues are redundant and do not effect the asymptotic critical behavior. Clearly, then, in order to obtain the simplest possible model, one should take $M=N$ (i.e., $C_N^{lm}=\delta_{lm}$) and

$$H^{(N)}=-\tfrac{1}{2}\sum_{i\neq j}J_{ij}\mathbf{s}_i\cdot\mathbf{s}_j\ . \tag{2.4}$$

This is the so-called *N-vector model.* Special cases are $N=1$, Ising; $N=2$, XY; and $N=3$, Heisenberg. The crucial property of $H^{(N)}$ is its invariance under the group of rotations $O(N)$ in spin space and this is what allows the universality class of the transition to vary with N [18].

By analogy, if we seek a generalized model for turbulence in which Kolmogorov-type exponents depend continuously on N, it seems likely that one must build into the equations an extra group of symmetries. Thus, by analogy with the set of rotations

$$s'_{i,l}=\sum_{m=1}^{N}R_N^{lm}(g)s_{i,m},\quad g\in O(N),\ \mathbf{R}_N^T\mathbf{R}_N=\mathbf{I}_N \tag{2.5}$$

(here $\mathbf{I}_N$ is the $N\times N$ identity matrix and the superscript T denotes matrix transpose) that leave $H^{(N)}$ invariant, we seek an N-dimensional irreducible representation of a group (technically, a simple compact Lie group) G of transformations along with an appropriate tensor $\mathbf{A}_N$, such that the transformation

$$\mathbf{v}'^l=\sum_{m=1}^{N}D_N^{lm}(g)\mathbf{v}^m,\quad g\in G\ , \tag{2.6}$$

leaves the equations of motion (2.1) invariant (later we will relax the irreducibility requirement slightly). Since the group is taken to be compact, the representation may always be taken as unitary $\mathbf{D}_N^\dagger\mathbf{D}_N=\mathbf{I}_N$. We assume, of course, that the pressures p^l and the forces $\mathbf{f}^l$ also transform under (2.6). We leave open the possibility that the velocity fields are complex (their real and imaginary parts then being the physical variables). The distinction between upper and lower indices is then made: $\mathbf{v}_l$ transforms via the inverse (or complex conjugate) representation [19]

$$\mathbf{v}'_l=\sum_{m=1}^{N}\mathbf{v}_m D_N^{ml}(g^{-1})=\sum_{m=1}^{N}\mathbf{v}_m[\mathbf{D}_N^{-1}(g)]^{ml}\ . \tag{2.7}$$

If the representation is unitary (which we assume, unless stated otherwise), then $\mathbf{v}_l\equiv\mathbf{v}^{l*}$ and $D_N^{ml}(g^{-1})=D_N^{lm}(g)^*$. If the representation is orthogonal (in which case all quantities are real), there is no distinction between upper and lower indices. If the representation is not unitary, it differs from unitary only by a similarity transformation and $\mathbf{v}_l$ is then an appropriate linear combination of the $\mathbf{v}^{m*}$. Substituting (2.6) and (2.7) into (2.1) we obtain now the condition

$$A_N^{l'm'n'}=\sum_{l,m,n}D_N^{l'l}(g)D_N^{m'm}(g)D_N^{n'n}(g)A_N^{lmn}\quad\forall g\in G\ , \tag{2.8}$$

i.e., that $\mathbf{A}_N$ be invariant under the group of transformations G. The questions to be addressed, then, are, given a group G, which irreducible representation should we choose and, given a representation, how do we construct appropriate cubic invariants $\mathbf{A}_N$.

B. Diagrammatic formalism

Before addressing these questions it is useful to outline the perturbation-theoretic formalism for the Navier-Stokes equations, including its generalization to $N>1$. The formalism was developed by Martin, Siggia, and Rose [20], extending the earlier Wyld [21] diagrammatic theory, and was used by DeDominicis and Martin [5(b)] in their renormalization group calculations.

First we include the incompressibility condition $\nabla\cdot\mathbf{v}=0$ explicitly by realizing that the gradient of the pressure in (1.2) simply cancels the longitudinal part of the nonlinear term. Thus if we define the k-space transverse projection operator

$$\hat{\tau}_{\alpha\beta}(\mathbf{k})=\delta_{\alpha\beta}-\frac{k_\alpha k_\beta}{k^2} \tag{2.9}$$

and let $\tau_{\alpha\beta}(\mathbf{r})$ be its inverse Fourier transform, then the Navier-Stokes equations may be written

$$\frac{\partial\mathbf{v}}{\partial t}+\lambda_0\overleftrightarrow{\tau}\cdot(\mathbf{v}\cdot\nabla)\mathbf{v}=\nu_0\nabla^2\mathbf{v}+\mathbf{f}\ , \tag{2.10}$$

where we have used the shorthand notation $[\overleftrightarrow{\tau}\cdot(\mathbf{v}\cdot\nabla)\mathbf{v}]_\alpha(\mathbf{r})=\sum_\beta\int d^3r'\tau_{\alpha\beta}(\mathbf{r}-\mathbf{r}')\mathbf{v}(\mathbf{r}')\cdot\nabla v_\beta(\mathbf{r}')$. Let us define the "Navier-Stokes operator"

$$\mathbf{N}(\mathbf{r},t)\equiv\frac{\partial\mathbf{v}}{\partial t}+\lambda_0\overleftrightarrow{\tau}\cdot(\mathbf{v}\cdot\nabla)\mathbf{v}-\nu_0\nabla^2\mathbf{v}\ ; \tag{2.11}$$

then we may formally compute the statistical average of any functional $F[\mathbf{v}]$ of the velocity field via

$$\langle F[\mathbf{v}]\rangle=\int D\mathbf{v}\,F[\mathbf{v}]J[\mathbf{v}]\langle\delta(\mathbf{N}[\mathbf{v}]-\mathbf{f})\rangle\ , \tag{2.12}$$

where $\int D\mathbf{v}$ is a functional integral over all incompressible velocity fields, and is defined by an appropriate continuum limit

$$\int D\mathbf{v} \equiv \lim_{M\to\infty} \prod_{i=1}^{M} \int d^d v(\mathbf{r}_i,t_i)\delta[\nabla\cdot\mathbf{v}(\mathbf{r}_i,t_i)] , \tag{2.13}$$

where $\{\mathbf{r}_i,t_i\}_{i=1}^{M}$ runs over a discrete space-time grid and $\nabla\cdot\mathbf{v}(\mathbf{r}_i,t_i)$ is the obvious discretized divergence at lattice point $(\mathbf{r}_i,t_i)$. Similarly,

$$\delta(\mathbf{N}[\mathbf{v}]-\mathbf{f}) = \lim_{M\to\infty} \prod_{i=1}^{M} \delta(\mathbf{N}(\mathbf{r}_i,t_i)-\mathbf{f}(\mathbf{r}_i,t_i)) \tag{2.14}$$

enforces the Navier-Stokes equations at all space-time points. The Jacobian $J[\mathbf{v}]$ is given by

$$J[\mathbf{v}] = \det\left[\frac{\delta\mathbf{N}(\mathbf{r},t)}{\delta\mathbf{v}(\mathbf{r}',t')}\right] , \tag{2.15}$$

with the operator

$$\frac{\delta N_\alpha(\mathbf{r},t)}{\delta v_\beta(\mathbf{r}',t')} = \delta_{\alpha\beta}(\partial_t-\nu_0\nabla^2)\delta(\mathbf{r}-\mathbf{r}')\delta(t-t') + \lambda_0\delta(t-t')\{[\mathbf{v}(\mathbf{r}',t)\cdot\nabla]\tau_{\alpha\beta}(\mathbf{r}-\mathbf{r}') + \sum_\gamma \tau_{\alpha\gamma}(\mathbf{r}-\mathbf{r}')\partial_\beta v_\gamma(\mathbf{r}',t)\} \tag{2.16}$$

inside the determinant, and is precisely what is needed to convert $\delta(\mathbf{v}-\mathbf{N}^{-1}[\mathbf{f}])$ to $\delta(\mathbf{N}[\mathbf{v}]-\mathbf{f})$.

We now represent the δ function using the identity $\delta(x)=\int_{-\infty}^{\infty}(dw/2\pi)e^{-iwx}$ for each space-time point, so that

$$\langle F[\mathbf{v}]\rangle = \int D\mathbf{v}\int D\mathbf{w}\, F[\mathbf{v}]\exp\left[-i\int d^dr\int dt\,\mathbf{w}(\mathbf{r},t)\cdot\mathbf{N}(\mathbf{r},t)+\ln J[\mathbf{v}]\right]\left\langle\exp\left[-i\int d^dr\int dt\,\mathbf{w}(\mathbf{r},t)\cdot\mathbf{f}(\mathbf{r},t)\right]\right\rangle , \tag{2.17}$$

where $\mathbf{w}(\mathbf{r},t)$ is also incompressible, i.e., $\nabla\cdot\mathbf{w}=0$. It can be shown that causality (i.e., the fact that $\delta\mathbf{N}(\mathbf{r},t)/\delta\mathbf{v}(\mathbf{r}',t')$ vanishes when $t'>t$) implies that the Jacobian term reduces to [22]

$$\ln J[\mathbf{v}] = C_1 + \int d^dr\int dt\sum_\alpha \frac{\delta N_\alpha(\mathbf{r},t)}{\delta v_\alpha(\mathbf{r},t)} = C_1 + \mathbf{C}_2\cdot\int d^dr\int dt\,\mathbf{v}(\mathbf{r},t) . \tag{2.18}$$

Rotation invariance implies that $\mathbf{C}_2$ must vanish and the Jacobian term is therefore a constant, independent of the velocity field.

Performing the average over the Gaussian random field $\mathbf{f}(\mathbf{r},t)$ we finally arrive at

$$\langle F[\mathbf{v}]\rangle = \frac{1}{Z}\int D\mathbf{v}\int D\mathbf{w}\, F[\mathbf{v}]e^{\mathcal{L}[\mathbf{v},\mathbf{w}]} , \tag{2.19}$$

where the Lagrangian is

$$\mathcal{L}[\mathbf{v},\mathbf{w}] = -i\sum_{\alpha,\beta}\int d^dr\int dt\,[w_\alpha(\partial_t-\nu_0\nabla^2)v_\beta\delta_{\alpha\beta}+\lambda_0 w_\alpha\tau_{\alpha\beta}(\mathbf{v}\cdot\nabla)v_\beta] - \tfrac{1}{2}\sum_{\alpha,\beta}\int d^dr\int dt\int d^dr'\int dt' w_\alpha(\mathbf{r},t)D_{\alpha\beta}(\mathbf{r}-\mathbf{r}',t-t')w_\beta(\mathbf{r}',t') , \tag{2.20}$$

with $D_{\alpha\beta}(\mathbf{r}-\mathbf{r}',t-t')=\langle f_\alpha(\mathbf{r},t)f_\beta(\mathbf{r}',t')\rangle$ [see (1.10)], and $Z=\int D\mathbf{v}\int D\mathbf{w}\,e^{\mathcal{L}[\mathbf{v},\mathbf{w}]}$ ensures correct normalization by canceling out the (formally divergent) constant C_1. One may now extend, in the obvious way, the quantities being averaged to functionals of both $\mathbf{w}$ and $\mathbf{v}$:

$$\langle F[\mathbf{v},\mathbf{w}]\rangle = \frac{1}{Z}\int D\mathbf{v}\int D\mathbf{w}\, F[\mathbf{v},\mathbf{w}]e^{\mathcal{L}[\mathbf{v},\mathbf{w}]} . \tag{2.21}$$

This is important as it turns out that *response* functions may be generated in this way [20]. In particular, for homogeneous driving (1.10), we have

$$\langle i\hat{w}_\alpha(\mathbf{k},\omega)\hat{v}_\beta(\mathbf{k}',\omega')\rangle = \hat{G}(\mathbf{k},\omega)\hat{\tau}_{\alpha\beta}(\mathbf{k})\delta(\mathbf{k}+\mathbf{k}')\delta(\omega+\omega') \tag{2.22}$$

[compare (1.11) and (1.12)] while, as before,

$$\langle\hat{v}_\alpha(\mathbf{k},\omega)\hat{v}_\beta(\mathbf{k}',\omega')\rangle = \hat{U}(\mathbf{k},\omega)\hat{\tau}_{\alpha\beta}(\mathbf{k})\delta(\mathbf{k}+\mathbf{k}')\delta(\omega+\omega') , \tag{2.23}$$

where (1.5) is obtained by realizing that $\mathrm{tr}[\hat{\tau}(\mathbf{k})]=d-1$. In Fourier space the Lagrangian may be written $\mathcal{L}=\mathcal{L}_0+\lambda_0\mathcal{L}_1$, with

$$\mathcal{L}_0[\mathbf{v},\mathbf{w}] = \int_{\mathbf{k}}\int_{\omega}[-i(-i\omega+\nu_0k^2)\hat{\mathbf{w}}(-\mathbf{k},-\omega)\cdot\hat{\mathbf{v}}(\mathbf{k},\omega) - \tfrac{1}{2}|\hat{\mathbf{w}}(\mathbf{k},\omega)|^2D(\mathbf{k},\omega)] , \tag{2.24}$$

$$\mathcal{L}_1[\mathbf{v},\mathbf{w}] = -i\int_{\mathbf{k}}\int_{\omega}\int_{\mathbf{q}}\int_{\Omega}\sum_{\alpha,\beta,\gamma}\frac{i}{2}P_{\alpha\beta\gamma}(\mathbf{k})\hat{w}_\alpha(-\mathbf{k},-\omega) \times\hat{v}_\beta(\mathbf{k}-\mathbf{q},\omega-\Omega) \times\hat{v}_\gamma(\mathbf{q},\Omega) , \tag{2.25}$$

where $P_{\alpha\beta\gamma}(\mathbf{k})=\tau_{\alpha\beta}(\mathbf{k})k_\gamma+\tau_{\alpha\gamma}(\mathbf{k})k_\beta$ and we have

used the shorthand notation $\int_{\mathbf{k}} \equiv \int d^d k/(2\pi)^d$, $\int_\omega \equiv \int d\omega/2\pi$, etc. Recalling that $\mathbf{k}\cdot\hat{\mathbf{v}}(\mathbf{k},\omega) = \mathbf{k}\cdot\hat{\mathbf{w}}(\mathbf{k},\omega)=0$, we easily compute the zeroth-order ($\lambda_0=0$) forms

$$\hat{G}_0(\mathbf{k},\omega)=\frac{1}{-i\omega+\nu_0 k^2}\ , \tag{2.26}$$

$$\hat{U}_0(\mathbf{k},\omega)=\hat{D}(\mathbf{k},\omega)|\hat{G}_0(\mathbf{k},\omega)|^2\ . \tag{2.27}$$

The usual diagrammatic perturbation theory [20] in λ_0 results by expanding $e^{\lambda_0\mathcal{L}_1}$ in a Taylor series and performing the averages term by term. Representing the resulting integrals by Feynman diagrams, the zeroth-order correlation function $\hat{U}_0$ becomes a straight line and the zeroth-order response function $\hat{G}_0$ becomes a combination straight-wavy line. Vertices have three legs (one wavy one and two straight ones) and a momentum-conserving δ function, along with a factor $(i/2)\lambda_0 P_{\alpha\beta\gamma}(\mathbf{k})$ (where $\mathbf{k}$ is the incoming momentum on the wavy leg) that accompanies each one (see Fig. 4).

Generalizing the formalism to N velocity fields is straightforward. Introducing incompressible fields $\mathbf{w}^l$ and $\mathbf{w}_l$, $l=1,\ldots,N$, which bear the same relationship to each other as does $\mathbf{v}^l$ to $\mathbf{v}_l$, and assuming $\langle f^l_\alpha(\mathbf{k},\omega) f_{\beta,m}(\mathbf{k}',\omega')\rangle = \hat{D}(\mathbf{k},\omega)\hat{\tau}_{\alpha\beta}(\mathbf{k})\delta(\mathbf{k}+\mathbf{k}')\delta(\omega+\omega')\delta^l_m$, one finds a Lagrangian $\mathcal{L}^{(N)}=\mathcal{L}_0^{(N)}+\lambda_0\mathcal{L}_1^{(N)}$, with

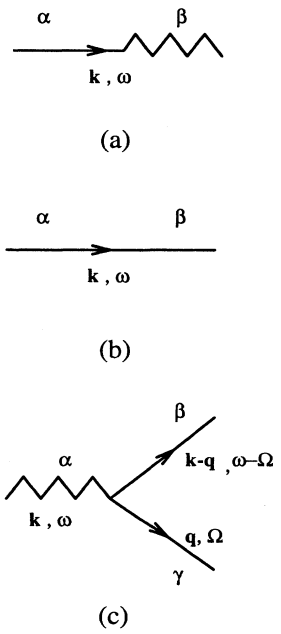

FIG. 4. Building blocks for Navier-Stokes diagrammatic perturbation theory. (a) The zeroth-order response function $\hat{G}_0(\mathbf{k},\omega)\hat{\tau}_{\alpha\beta}(\mathbf{k})$; v_α is represented by the straight part of the line and $\hat{w}_\beta$ by the wavy part of the line. (b) The zeroth-order correlation function $\hat{U}_0(\mathbf{k},\omega)\tau_{\alpha\beta}$. (c) The vertex $(i/2)\lambda_0 P_{\alpha\beta\gamma}(\mathbf{k})$.

$$\mathcal{L}_0^{(N)}=\sum_{l=1}^{N}\int_{\mathbf{k}}\int_\omega\left\{-\frac{i}{2}[(-i\omega+\nu_0 k^2)\hat{\mathbf{w}}_l(-\mathbf{k},-\omega)\cdot\hat{\mathbf{v}}^l(\mathbf{k},\omega)+\text{c.c}]-\tfrac{1}{2}D(\mathbf{k},\omega)\hat{\mathbf{w}}^l(-\mathbf{k},-\omega)\cdot\hat{\mathbf{w}}_l(\mathbf{k},\omega)\right\}, \tag{2.28}$$

$$\mathcal{L}_1^{(N)}=-\frac{i}{2}\sum_{l,m,n}\sum_{\alpha,\beta,\gamma}\int_{\mathbf{k}}\int_\omega\int_{\mathbf{q}}\int_\Omega\left[A_N^{lmn}\frac{i}{2}P_{\alpha\beta\gamma}(\mathbf{k})\hat{\mathbf{w}}_{\alpha,l}(-\mathbf{k},-\omega)\hat{\mathbf{v}}_{\beta,m}(\mathbf{k}-\mathbf{q},\omega-\Omega)\hat{\mathbf{v}}_{\gamma,n}(\mathbf{q},\Omega)+\text{c.c.}\right] \tag{2.29}$$

(here c.c. stands for complex conjugate). The fields $\mathbf{w}^l$ are assumed to transform in precisely the same way (2.6) as the fields $\mathbf{v}^l$. The properties (2.7) and (2.8) then immediately imply that both $\mathcal{L}_0^{(N)}$ and $\mathcal{L}_1^{(N)}$ are invariant under the group G of transformations. When $\lambda_0=0$ we have

$$\langle i\hat{w}^l_\alpha(\mathbf{k},\omega)\hat{v}_{\beta,m}(\mathbf{k}',\omega')\rangle = \hat{G}_0(\mathbf{k},\omega)\hat{\tau}_{\alpha\beta}(\mathbf{k})\delta^l_m\delta(\mathbf{k}+\mathbf{k}')\delta(\omega+\omega')\ , \tag{2.30}$$

$$\langle \hat{v}^l_\alpha(\mathbf{k},\omega)\hat{v}_{\beta,m}(\mathbf{k}',\omega')\rangle = \hat{U}_0(\mathbf{k},\omega)\hat{\tau}_{\alpha\beta}(\mathbf{k})\delta^l_m\delta(\mathbf{k}+\mathbf{k}')\delta(\omega+\omega')\ , \tag{2.31}$$

with $\hat{G}_0$ and $\hat{U}_0$ given by (2.26) and (2.27).

Perturbation theory in $\lambda_0\mathcal{L}_1^{(N)}$ is also straightforward. The only changes are that it is now convenient to define for each graph a "shadow" diagram containing the isospin dependence (see Fig. 5). Since $\hat{G}_0$ and $\hat{U}_0$ are independent of l, this dependence factors out of each diagram and can be treated separately from the momentum and frequency dependence. This will be discussed further in Sec. III A. The extra index l is associated with each line in the shadow isospin diagram, the vertices are A_N^{lmn} and $A_{N,lmn}$, where $A_{N,lmn}\equiv A_N^{lmn*}$, and lines joining two vertex legs imply a contraction between the corresponding indices. We adopt the convention that an arrow coming into a vertex carries an *upper* index, while an arrow going out of a vertex carries a *lower* index.

C. Symmetries of $\mathbf{A}_N$

In order to limit our search for appropriate cubic invariants, we now discuss symmetry requirements on the coefficients A_N^{lmn}. First, since the projection-type operator $P_{\alpha\beta\gamma}(\mathbf{k})$ is symmetric under interchange of β and γ, it is natural to choose A_N^{lmn} symmetric in m and n. It is easy to check that the equations of motion (2.1) are still nontrivial even if A_N^{lmn} is *antisymmetric* in m and n (the nonlinear term does *not* vanish identically, as long as $N>1$), but this does not give a sensible $N=1$ limit. In particular the diagonal terms $n=m$, which are the only

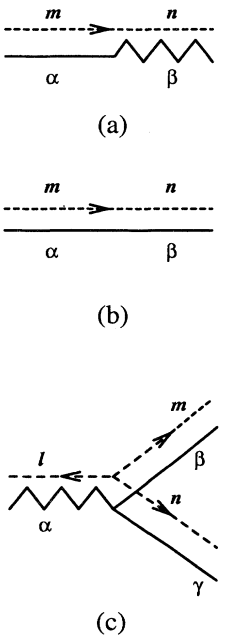

FIG. 5. Generalization of Fig. 4 to $N>1$. The directed dashed lines connect up to form a "shadow diagram" carrying the isospin dependence. (a) The zeroth-order response function $\hat{G}_0\hat{\tau}_{\alpha\beta}\delta^n_m$. (b) The zeroth-order correlation function $\hat{U}_0\hat{\tau}_{\alpha\beta}\delta^n_m$. (c) The vertex $(i/2)\lambda_0 P_{\alpha\beta\gamma}A_{N,lmn}$.

ones that survive when $N=1$, are canceled. We therefore assume $A_N^{lmn}=A_N^{lnm}$.

Second, we impose the constraint that the total energy be conserved in the absence of viscosity and forcing. The total energy is defined as

$$E=\int d^dr\,\varepsilon(\mathbf{r},t)\ ,$$
$$\varepsilon(\mathbf{r},t)\equiv\tfrac{1}{2}\rho_0\sum_{l=1}^{N}\mathbf{v}^l(\mathbf{r},t)\cdot\mathbf{v}_l(\mathbf{r},t)\ , \tag{2.32}$$

whose integrand reduces to $\frac{1}{2}\rho_0\sum_l|\mathbf{v}^l|^2$ when the representation is unitary, but is in any case real and positive. Using the incompressibility conditions and appropriate integrations by parts, one finds

$$\frac{dE}{dt}=-\frac{1}{2}\rho_0\lambda_0\mathrm{Re}\sum_{l,m,n}(A_N^{lmn}-A_N^{nml})\int d^dr\,\mathbf{v}_l\cdot(\mathbf{v}_m\cdot\nabla)\mathbf{v}_n\ , \tag{2.33}$$

which therefore vanishes automatically if $A_N^{lmn}=A_N^{nml}$ (more complicated assumptions that allow for an antisymmetric part may be possible, but we again appeal to a sensible $N=1$ limit). Associated with this conservation law is the conserved energy current $\mathbf{j}_\varepsilon(\mathbf{r},t)=\lambda_0\rho_0\mathrm{Re}\sum_{l,m,n}A_N^{lmn}(\mathbf{v}_l\cdot\mathbf{v}_n)\mathbf{v}_m+\mathrm{Re}\sum_l p^l\mathbf{v}_l$, which obeys $\partial\varepsilon/\partial t+\nabla\cdot\mathbf{j}_\varepsilon=0$. Together with the symmetry in m and n, this implies that we require full symmetry under all permutations of the three indices

$$A_N^{lmn}=A_N^{lmn}=A_N^{nml}=A_N^{mln}\ . \tag{2.34}$$

D. Group-theoretical considerations

We now treat more technical issues involving the relation between $\mathbf{A}_N$ and the group G. We shall discuss two approaches to the construction of group invariants: trace invariants and Wigner symbols. The first is actually a special case of the second, but is easier to motivate and hence worth introducing separately.

1. Trace invariants

Perhaps the simplest way to generate invariants is to associate the indices l, m, and n with the *generators* of the group G. Thus we let $\mathbf{J}^l$, $l=1,\ldots,N$ be a set of finite-dimensional Hermitian matrices (the so-called Lie algebra of the representation) such that the unitary matrix $\mathbf{U}(g)$ representing any group element $g\in G$ may be expressed as

$$\mathbf{U}(g)=\exp\left[i\sum_{l=1}^{N}a_l(g)\mathbf{J}^l\right],\quad g\in G\ , \tag{2.35}$$

where the a_l are real numbers. The group structure is completely specified by the structure constants f^{lmn}, which are real and defined by the commutation relations

$$[\mathbf{J}^l,\mathbf{J}^m]=i\sum_{n=1}^{N}f^{lmn}\mathbf{J}^n\ . \tag{2.36}$$

We will always take $\mathrm{tr}[\mathbf{J}^l]=0$ [since an overall phase factor in (2.35) has no effect]. By choosing suitable linear combinations if necessary, we may also take $\mathrm{tr}[\mathbf{J}^l\mathbf{J}^m]=\lambda\delta_{lm}$, where the real number $\lambda>0$ is chosen for convenience. In this case $f^{lmn}=(1/i\lambda)\mathrm{tr}\{[\mathbf{J}^l,\mathbf{J}^m]\mathbf{J}^n\}$ is completely antisymmetric in all three indices. For example, if $G=\mathrm{SU}(2)$ and $\mathbf{J}^l=\sigma^l$, $l=1,2,3$, are the Pauli matrices, then $\lambda=2$ and $f^{lmn}=2\epsilon_{lmn}$, where ϵ_{lmn} is the fully antisymmetric tensor with $\epsilon_{123}=1$.

Suppose we now define matrix dynamical variables $\Omega_\alpha[\mathbf{x}]$ by

$$\Omega_\alpha[\mathbf{x}]=\sum_{l=1}^{N}x_{\alpha,l}\mathbf{J}^l,\quad \alpha=1,\ldots,d\ , \tag{2.37}$$

where $\mathbf{x}^l(\mathbf{r},t)=\mathbf{x}_l(\mathbf{r},t)$ are *real* vector field dynamical variables. The unitary transformation (2.35) induces a transformation on the $\mathbf{x}^l$ via

$$\Omega_\alpha[\mathbf{x}']\equiv\mathbf{U}^\dagger(g)\Omega_\alpha[\mathbf{x}]\mathbf{U}(g)=\sum_{l=1}^{N}x'_{\alpha,l}\mathbf{J}^l\ , \tag{2.38}$$

which defines an $N\times N$ real orthogonal matrix $D_N^{ll'}(g)$ via

$$\mathbf{U}^\dagger(g)\mathbf{J}^l\mathbf{U}(g)=\sum_{l'=1}^{N}D_N^{ll'}(g)\mathbf{J}^{l'}\ , \tag{2.39}$$

$$x'^l_\alpha=\sum_{l'=1}^{N}D_N^{ll'}(g)x^{l'}_\alpha,\quad \mathbf{D}_N^T(g)\mathbf{D}_N(g)=\mathbf{I}_N \tag{2.40}$$

[compare (2.6)] and there is no distinction between upper

and lower indices in this case. We now ask what equations of motion for the $\mathbf{x}_\alpha^l$ can one write down that are invariant under this group of transformations. To see the answer, note that, due to the cyclic property of the trace, any quantity of the form

$$\mathrm{tr}\{\Omega_\alpha[\mathbf{x}]\Omega_\beta[\mathbf{y}]\cdots\Omega_\gamma[\mathbf{z}]\} \equiv \sum_{l_1,l_2,\ldots,l_m} A_N^{l_1 l_2\cdots l_m} x_{\alpha,l_1} y_{\beta,l_2}\cdots z_{\gamma,l_m} , \quad (2.41)$$

where

$$A_N^{l_1 l_2\cdots l_m} \equiv \mathrm{tr}\{\mathbf{J}^{l_1}\mathbf{J}^{l_2}\cdots\mathbf{J}^{l_m}\} , \quad (2.42)$$

is an invariant of order m. Other invariants, in addition to those defined by (2.42), can also be constructed: simply contract the indices on products of lower-order $\mathbf{A}_N$'s. For example, both $\delta_{l_1 l_2}\delta_{l_3 l_4}$ and $\sum_n A_N^{l_1 l_2 n} A_N^{n l_3 l_4}$ are fourth-order invariants (which may or may not differ significantly from $A_N^{l_1 l_2 l_3 l_4}$).

Consider, then, any set of equations of motion of the form

$$\dot{x}_\alpha^l = \mathcal{F}_\alpha^l[\mathbf{x}], \quad l=1,\ldots,N, \quad \alpha=1,\ldots,d , \quad (2.43)$$

where $\mathcal{F}_\alpha^l[\mathbf{x}]$ is a sum over all possible m and for each m, all possible mth-order invariants (which we will still denote generically by $A_N^{l_1\cdots l_m}$) of terms of the form

$$\mathcal{F}_\alpha^{l;m}[\mathbf{x}] \equiv \sum_{l_2,\ldots,l_m} A_N^{l l_2\cdots l_m} \times \sum_{\alpha_2,\ldots,\alpha_m} O_{\alpha\alpha_2\cdots\alpha_m} x_{\alpha_2,l_2}\cdots x_{\alpha_m,l_m} , \quad (2.44)$$

where $O_{\alpha\alpha_2\cdots\alpha_m}$ could be any spatial-rotation invariant integrodifferential operator acting on the $\mathbf{r}$ dependences of the $x_\alpha^l(\mathbf{r},t)$. In particular, the form

$$O_{\alpha\alpha_2\alpha_3} = \delta_{\alpha\alpha_3}\int d^d r_2 \int d^d r_3 \delta(\mathbf{r}-\mathbf{r}_2)\frac{\partial}{\partial r_{\alpha_2}}\delta(\mathbf{r}-\mathbf{r}_3) \quad (2.45)$$

yields the nonlinear term in (2.1) with $\mathbf{x}^l \equiv \mathbf{v}^l$. These equations must transform covariantly since multiplication by $x_{\alpha,l}$ followed by summation over l yields a scalar on both sides of the equation.

Given a group G, there are many possible choices for the generators $\mathbf{J}^l$. However, within a given representation, any choice may be obtained from any other by taking appropriate linear combinations. The resulting invariants are then corresponding linear combinations of each other. The number N of generators is determined by the dimension of the group. Thus, if N is to vary (in particular, to become large) the group G must vary with N. The dimension of the matrices $\mathbf{J}^l$ (i.e., the dimension of the representation) is of no consequence here. Though the details of the representation may enter [more than just the structure constants (2.36) are relevant in computing (2.42)], the matrices $\mathbf{D}_N$ are representation independent and a single maximal set of independent invariants must exist. It is simplest to assume that the $\mathbf{J}^l$ generate the *fundamental* representation, i.e., have minimal dimension. For SU(2) these are the Pauli matrices; for SU(M) they are any orthogonal set of $N=M^2-1$, $M\times M$ traceless matrices. Below we will discuss invariants that depend more significantly on the representation.

In the example of SU(2) represented by the Pauli matrices, the first few invariants are

$$\begin{aligned} A_3^l &= \mathrm{tr}(\sigma^l) = 0 , \\ A_3^{l_1 l_2} &= \mathrm{tr}(\sigma^{l_1}\sigma^{l_2}) = 2\delta_{l_1 l_2} , \\ A_3^{l_1 l_2 l_3} &= \mathrm{tr}(\sigma^{l_1}\sigma^{l_2}\sigma^{l_3}) = 2i\epsilon_{l_1 l_2 l_3} , \\ A_3^{l_1 l_2 l_3 l_4} &= \mathrm{tr}(\sigma^{l_1}\sigma^{l_2}\sigma^{l_3}\sigma^{l_4}) \\ &= 2[-\delta_{l_1 l_3}\delta_{l_2 l_4} + \delta_{l_1 l_4}\delta_{l_2 l_3} + \delta_{l_1 l_2}\delta_{l_3 l_4}] . \end{aligned} \quad (2.46)$$

Note that $A_3^{lmn} = if^{lmn}$ is completely *antisymmetric* in this case and therefore violates the requirements in Sec. II C. It will always be the case that $A_N^{lmn} - A_N^{mln} = i\lambda f^{lmn}$. The only question is whether or not there is a nontrivial symmetric part [clearly not, for SU(2)]. Note also that the fourth-order invariant can be constructed trivially from sums of products of the second-order one. In fact, in this case, all higher-order invariants may be constructed from products of Kronecker δ's functions and ϵ tensors. This implies the well-known result that all rotation invariant combinations of vectors in three dimensions may be constructed from dot products and cross products.

2. *Wigner coefficients*

In the second approach to constructing invariants we associate the index l with the basis vectors (or states) on which the $\mathbf{J}^l$ operate. Thus N is now the dimension of the matrices rather than their number and may vary even when the group G is taken to be fixed, independent of N. Using a quantum-mechanical bra-ket notation, if $\{|1\rangle,\ldots,|N\rangle\}$ is an orthonormal basis for the vector space (with corresponding Hermitian conjugates $\{\langle 1|,\ldots,\langle N|\}$), then we define dynamical states

$$|x_\alpha\rangle = \sum_{l=1}^N x_\alpha^l |l\rangle, \quad \langle x_\alpha| = \sum_{l=1}^N x_{\alpha,l}\langle l|, \quad l=1,\ldots,d . \quad (2.47)$$

The operation

$$|x'_\alpha\rangle = \mathbf{U}(g)|x_\alpha\rangle, \quad \langle x'_\alpha| = \langle x_\alpha|\mathbf{U}^\dagger(g) \quad (2.48)$$

then defines the group of transformations on the x_α^l via

$$x'^l_\alpha = \sum_{l'=1}^N D_N^{ll'}(g)x_\alpha^{l'}, \quad x'_{\alpha,l} = \sum_{l'=1}^N D_N^{l'l}(g^{-1})x_{\alpha,l'} , \quad \mathbf{D}_N^\dagger\mathbf{D}_N = \mathbf{I}_N , \quad (2.49)$$

where

$$D_N^{ll'}(g)=\langle l|\mathbf{U}(g)|l'\rangle \ . \tag{2.50}$$

For the group SU(2), the representations are labeled by the total spin $j=0,\frac{1}{2},1,\frac{3}{2},2,\ldots$, and have dimension $N=2j+1$. A convenient basis is formed by the eigenstates of angular momentum component J_z:

$$|l\rangle\equiv|j,m\rangle, \quad -j\le m=l-j-1\le j \ . \tag{2.51}$$

For integer j these are most familiar in the form of the spherical harmonics $Y_{jm}(\theta,\phi)$. The transformation matrices (2.49) are the famous quantum-mechanical D matrices [23,24].

We now wish to construct quantities of the form

$$\mathcal{J}_{\alpha_1\cdots\alpha_m}=\sum_{l_1,\ldots,l_m} A_N^{l_1\cdots l_m}x_{\alpha_1,l_1}\cdots x_{\alpha_m,l_m} \ , \tag{2.52}$$

where $\mathbf{A}_N$ is chosen to make $\mathcal{J}$ invariant under (2.49). Since, by (2.50),

$$\mathbf{U}(g)|l\rangle=\sum_{l'=1}^{N} D_N^{l'l}(g)|l'\rangle \ , \tag{2.53}$$

the kets transform under group element g in the same way that the $x_{\alpha,l}$ do under group element g^{-1}. We may therefore state the problem alternatively: we seek a tensor $\mathbf{A}_N$ such that the linear combination of product states

$$|\mathcal{J}^{(m)}\rangle=\sum_{l_1,\ldots,l_m} A_N^{l_1\cdots l_m}|l_1\rangle\otimes\cdots\otimes|l_m\rangle \tag{2.54}$$

is a *scalar* (normalized in some fashion) under the transformation (2.53). For the group SU(2) this means that we wish to add m angular momenta together to obtain a state with zero total angular momentum. This is a well-known problem in group theory and quantum mechanics, closely related to the problem of decomposing the direct product of $m-1$ irreducible representations of a group into a direct sum of irreducible representations. The solutions $A_N^{l_1\cdots l_m}$ are called *Wigner coefficients.* For SU(2), with basis states given by (2.51) and with $m=3$, one uses the notation

$$A_N^{l_1l_2l_3}\equiv\begin{bmatrix} j & j & j \\ m_1 & m_2 & m_3\end{bmatrix}, \qquad m_i=-j,-j+1,\ldots,j \ . \tag{2.55}$$

These are special cases of the Wigner $3j$ symbols [24]. In general, the states in the direct product (2.53) can belong to different representations $N_1,\ldots,N_m$ and we would seek coefficients $A_{N_1\cdots N_m}^{l_1\cdots l_m}$ that make the result a scalar. The general SU(2) Wigner $3j$ symbol is then $\begin{pmatrix} j_1 & j_2 & j_3 \\ m_1 & m_2 & m_3\end{pmatrix}\equiv A_{N_1N_2N_3}^{l_1l_2l_3}$, with $N_i=2j_i+1$ and $m_i=l_i-j_i-1$. We are clearly interested only in the case in which all representations are the same.

Appropriate equations of motion may now be written down precisely as before. Equations (2.44) and (2.45) are valid with the new tensors $\mathbf{A}_N$ defined above.

As an aside, the relation to the Clebsch-Gordan coefficients is made clear by constructing the state

$$|\mathcal{J}_l^{(m)}\rangle=\sum_{l_2,\ldots,l_m} A_N^{ll_2\cdots l_m}|l_2\rangle\otimes|l_3\rangle\otimes\cdots\otimes|l_m\rangle \ . \tag{2.56}$$

From (2.54) we have the obvious relation

$$|\mathcal{J}^{(m)}\rangle=\sum_{l=1}^{N}|l\rangle\otimes|\mathcal{J}_l^{(m)}\rangle \ . \tag{2.57}$$

Since $|\mathcal{J}^{(m)}\rangle$ is a scalar it is clear that $|\mathcal{J}_l^{(m)}\rangle$ must transform in the same way that $\langle l|$ does, i.e., with the complex conjugate representation. More generally, if the states in the product come from different representations $N_2,\ldots,N_m$, the resulting states transform via the complex conjugate of the representation N. Thus, by letting N vary over all permitted values, the Wigner symbols allow one to decompose the transformation of the given direct product into a direct sum of irreducible representations (this is known as the *Clebsch-Gordan decomposition* of the direct product). This does not quite define the usual Clebsch-Gordan coefficients. These are defined in such a way that the resulting product state transforms via the representation N, not its complex conjugate. In the case where the representation is real (i.e., where the complex conjugate representation is the same as the representation itself), there is a matrix $g_N^{ll'}$ such that

$$|l\rangle=\sum_{l'=1}^{N} g_N^{ll'}\langle l'| \tag{2.58}$$

translates the bras into kets. This matrix is really a special case of the invariant tensors $\mathbf{A}_N$ in which there are only two indices since $|\mathcal{J}^{(2)}\rangle=\sum_{l,l'}g_N^{ll'}|l\rangle\otimes|l'\rangle$ is clearly a scalar. If we then define the Clebsch-Gordan coefficients

$$C_{N;N_2\cdots N_m}^{l;l_2\cdots l_m}=c(N,N_1,\ldots,N_m)\sum_{l'=1}^{N} g_N^{ll'}A_{NN_2\cdots N_m}^{l'l_2\cdots l_m} \ , \tag{2.59}$$

where the prefactor is an appropriate normalization, it is clear that

$$|\bar{\mathcal{J}}_l^{(m)}\rangle=\sum_{l_2,\ldots,l_m} C_{N;N_2\cdots N_m}^{l;l_1\cdots l_m}|l_2\rangle\otimes\cdots\otimes|l_m\rangle \tag{2.60}$$

transforms just as $|l\rangle$ does. For $m\ge4$ these coefficients are no more unique than the Wigner coefficients are [see the discussion below (2.42)]. For the group SU(2) the representations are all real and one more commonly denotes

$$\begin{aligned} C_{N;N_2N_3}^{l;l_2l_3}&\equiv\langle jm|j_2m_2j_3m_3\rangle \\ &=(-1)^{j_2-j_3+m}\sqrt{2j+1} \\ &\quad\times\begin{bmatrix} j & j_2 & j_3 \\ -m & m_2 & m_3\end{bmatrix} . \end{aligned} \tag{2.61}$$

The corresponding translation matrix is

$g_N^{ll'}=(-1)^{l'}\delta_{l',N-l}$ and the conventional normalization is $c(N,N_1,N_2)=-(-1)^{(1/2)(N_2-N_3)-N}\sqrt{N}$ [24].

Finally, we mentioned at the beginning of this subsection that the trace invariants are really special cases of the Wigner coefficients. They are constructed, in effect, by using the group generators as states. This, in fact, corresponds to a special representation, known as *the adjoint representation* [25], and it can be shown that in this representation the Wigner coefficients as defined above are precisely the traces of products of generators (2.42). The demonstration of this fact is a special case of the use of tensor methods in the theory of group representations [24,25] where invariants are constructed as traces of products of more general tensor quantities. In the case of the adjoint representation these tensors have only two indices [one transforming under the fundamental representation, the other under its complex conjugate, exactly as in (2.38)] and are traceless and hence may always be written as linear combinations of the generators, precisely as in (2.37).

E. Graphical considerations

A crucial property of the group-theoretical formulation is the preservation of the coefficients $A_N^{l_1\cdots l_m}$ under vertex renormalization. Stated more simply, different order diagrams, with the same structure of m external legs, will have the same dependence on the indices $l_1,\ldots,l_m$ and must therefore be proportional to some linear combination of $\mathbf{A}_N$'s with the same m. For small m ($m=2$ or 3, say) there will be only a *single* type of $\mathbf{A}_N$ and the dependence on the indices $l_1,\ldots,l_m$ will be uniquely specified.

The reason for this is that $\mathcal{L}_1^{(N)}$ is a scalar and therefore the average of an operator $\mathcal{O}^{l_1,\ldots,l_m}$, which transforms in the same way that $x^{l_1}y^{l_2}\cdots z^{l_m}$ does, is given by the sum over p of

$$O_p^{l_1\cdots l_m}\equiv\lambda_0^p\langle\mathcal{O}^{l_1\cdots l_m}(\mathcal{L}_1^{(N)})^p\rangle_{0,c} \tag{2.62}$$

(the subscript c denotes the usual connected part), which therefore must also transform in the same way. Now $O_p^{l_1\cdots l_m}$ is independent of the $\mathbf{v}$ and $\mathbf{w}$ fields and a contraction of the form

$$O_p=\sum_{l_1\cdots l_m}O_p^{l_1\cdots l_m}x_{l_1}y_{l_2}\cdots z_{l_m} \tag{2.63}$$

is, by construction, a scalar. However, the $A_N^{l_1\cdots l_m}$ comprise all invariants, therefore $O_p^{l_1\cdots l_m}$ must be some linear combination of them.

At the level of graphical technology, it is precisely this property that is responsible for the variation of the universality class with N in the spin models. Without the group symmetry, diagrams with the same external leg structure would have essentially random dependence on the indices and would therefore not add up in any coherent fashion. Without the O(N) symmetry, this is precisely what leads to Ising-like behavior for all finite N. We expect similar behavior to occur in the turbulence problem. In Sec. III we will use these group properties and the associated properties of the diagrams to analyze the large-N limit.

F. Galilean invariance

In Sec. I we alluded to the importance of Galilean invariance in the establishment of the exact renormalization group results (1.15) and (1.18) for the exponents. We would like to be able to establish similar results for all N. It turns out that this can be done only if we generalize the model somewhat.

For $N=1$ the Galilean transformation

$$\mathbf{v}'(\mathbf{r},t)=\mathbf{v}(\mathbf{r}+\lambda_0\mathbf{u}_0t,t)-\mathbf{u}_0\ , \tag{2.64}$$

where $\mathbf{u}_0$ is an arbitrary fixed (real) velocity, leaves the Navier-Stokes equations invariant since

$$\frac{\partial\mathbf{v}'}{\partial t}+\lambda_0(\mathbf{v}'\cdot\nabla)\mathbf{v}'=\frac{\partial\mathbf{v}}{\partial t}+\lambda_0(\mathbf{v}\cdot\nabla)\mathbf{v}\ . \tag{2.65}$$

If, in addition, we assume that $\mathbf{w}'(\mathbf{r},t)=\mathbf{w}(\mathbf{r}+\lambda_0\mathbf{v}_0t,t)$ transforms without an additive term (as do $\mathbf{f}$ and p), then the Lagrangian (2.20) is Galilean invariant $\mathcal{L}[\mathbf{v}',\mathbf{w}']=\mathcal{L}[\mathbf{v},\mathbf{w}]$. It is precisely this invariance that was exploited by DeDominicis and Martin [5(b)] to prove (1.15) and (1.18) to all orders in y.

For $N>1$, consider the generalization of (2.64)

$$\begin{aligned}\mathbf{v}'^l(\mathbf{r},t)&=\mathbf{v}^l(\mathbf{r}+\lambda_0\mathbf{u}_0t,t)-\frac{1}{\mu}h^l\mathbf{u}_0\ ,\\ \mathbf{v}'_l(\mathbf{r},t)&=\mathbf{v}_l(\mathbf{r}+\lambda_0\mathbf{u}_0t,t)-\frac{1}{\mu^*}h_l\mathbf{u}_0\ ,\end{aligned} \tag{2.66}$$

where $h^l=h_l^*$ is any set of complex numbers, normalized so that $\sum_{l=1}^N h_lh^l=1$, and μ is yet to be determined. We then have

$$\begin{aligned}&\frac{\partial\mathbf{v}'^l}{\partial t}+\lambda_0\sum_{m,n}A_N^{lmn}(\mathbf{v}'_m\cdot\nabla)\mathbf{v}'_n\\ &\quad=\frac{\partial\mathbf{v}^l}{\partial t}+\lambda_0\sum_{m,n}A_N^{lmn}(\mathbf{v}_m\cdot\nabla)\mathbf{v}_n\\ &\qquad+\lambda_0(\mathbf{u}_0\cdot\nabla)\left[\mathbf{v}^l-\frac{1}{\mu}\sum_n A_N^{ln}(h)\mathbf{v}_n\right]\ ,\end{aligned} \tag{2.67}$$

where $A_N^{ln}(h)=\sum_m A_N^{lmn}h_m$. The last term on the right-hand side cannot generally be made to vanish simultaneously for all l, unless further assumptions are made (see below). Thus, full invariance of the equations of motion under (2.66) is not generally possible. One may try focusing instead on equations of motion for scalar combinations

$$\mathbf{v}_q(\mathbf{r},t)=\tfrac{1}{2}\sum_{l=1}^N[q_l\mathbf{v}^l(\mathbf{r},t)+q^l\mathbf{v}_l(\mathbf{r},t)]\ , \tag{2.68}$$

where $q^l=q_l^*$ is another set of complex numbers with $\sum_l q^lq_l=1$. From (2.67), the equation of motion for $\mathbf{v}_q$ is invariant under the transformation (2.66) only if

$$\mu q^n=\sum_{l=1}^N A_N^{ln}(h)q_l=\sum_{l,m}A_N^{lmn}h_mq_l\ . \tag{2.69}$$

This is a kind of eigenvalue problem for the q^n, with eigenvalue μ. The matrix $A_N^{ln}(h)$ is symmetric, but not necessarily real.

Associated, then, with each Galilean transformation (2.66) is a set of N invariant velocity fields $\mathbf{v}_q(\mathbf{r},t)$, one for each eigenvector q^l of $A_N^{ln}(h)$, transforming with the associated eigenvalue μ. Since μ is generally different for each eigenvector, a different transformation is associated with each one. This invariance property clearly respects the group symmetry: if $\mathbf{v}^l$ is transformed according to (2.6), transforming h^l and q^l in exactly the same way yields the same scalar $\mathbf{v}_q$ in (2.71) and the same eigenvalue equation (2.72). Clearly, when $N=1$ the standard Galilean invariance (2.64) and (2.65) is recovered with the eigenvalue $\mu=1$.

These invariance properties, though compelling, are insufficient to imply the result we seek, namely, that the renormalization group results for the exponents generalize to any $N>1$. As shown in Appendix A, a true symmetry of the Lagrangian is required and this exists only if the last term in (2.67) can be made to vanish for all l for some choice of h_m, i.e., only if

$$\frac{1}{\mu}\sum_n A_N^{ln}(h)\mathbf{v}_n=\mathbf{v}^l \quad \text{for all } l \ . \tag{2.70}$$

Comparing (2.58), this means that

$$\frac{1}{\mu}A_N^{ln}(h)=g_N^{ln} \tag{2.71}$$

is just the quadratic invariant. If the group representation is irreducible, (2.71) can never hold because it requires that h^m be an invariant: $\sum_{m=1}^N D_N^{lm}(g)h^m=h^l$ for all g. This requires that the transformation act like the identity on some subspace, immediately implying reducibility.

Suppose, then, that we relax the irreducibility assumption. We introduce a single real velocity field $\mathbf{v}^0=\mathbf{v}_0$ (the "zero mode"), which, by definition, is a *scalar* under the group of transformations. Quantities referring to the extended system of $N+1$ velocity fields that includes $\mathbf{v}^0$ will be written with an overbar. We define, then, the transformation matrices

$$\bar{D}_N^{lm}(g)=D_N^{lm}(g)+\delta_{l0}\delta_{m0} \ ,$$
$$l,m=0,1,2,\ldots,N \text{ for all } g \ , \tag{2.72}$$

where unbarred quantities are taken to vanish when any index vanishes. The quadratic invariants are now of the general form

$$\bar{g}_N^{lm}=g_N^{lm}+c_0\delta_{l0}\delta_{m0} \tag{2.73}$$

and the cubic invariants are [maintaining the symmetry condition (2.34)]

$$\bar{A}_N^{lmn}=A_N^{lmn}+c_1[\delta_{l0}g_N^{mn}+\delta_{m0}g_N^{ln}+\delta_{n0}g_N^{lm}]$$
$$+c_2\delta_{l0}\delta_{m0}\delta_{n0} \ , \tag{2.74}$$

where c_0, c_1, and c_2 are, for now, arbitrary constants. The zero mode therefore introduces two new invariant isospin vertices [Fig. 5(d)], which then must be summed over to produce the full isospin symmetry factor [and are produced from (2.62) when any index vanishes].

Returning now to Galilean invariance, it is clear that in order to satisfy (2.71) (which should now be written with overbars) we should choose $h_m=\delta_{m0}$ and $c_1=c_2=\mu$. From (2.66), this means that only the zero mode $\mathbf{v}^0$ transforms with an additive term

$$\mathbf{v}'^l(\mathbf{r},t)=\mathbf{v}^l(\mathbf{r}+\lambda_0\mathbf{u}_0t,t)-\frac{1}{\mu}\mathbf{u}_0\delta_{l0} \ . \tag{2.75}$$

The value of μ appropriate to a well defined $N\to\infty$ limit will be determined in Sec. III E. The introduction of the zero mode is especially compelling in the adjoint representation: $\mathbf{v}^0$ is just the coefficient of the *identity* matrix. It is then trivial to see that (2.42) produces (2.74). In effect, one is now using a representation of U(N) rather than of SU(N).

In Appendix A we use this invariance property of model II to derive the Ward identities used by DeDominicis and Martin [5(b)] to establish (1.15) and (1.18). The validity of these results lends further credence to our proposition that the general N equations really do represent a logical generalization of the original Navier-Stokes equations and do not violate any fundamental symmetries present in the original equations. We therefore might hope that all properties (of the correlation functions, for example) will then vary smoothly with N, just as do those of the N-vector models of magnetism. In particular, any "discontinuity" in behavior between the Navier-Stokes equations and their general N extensions would be surprising. In Appendix B, as further evidence in support of these hopes, we show that the von Kármán–Howarth result [1(b)] for the third radial velocity moment generalizes naturally to arbitrary N.

In the following sections we shall treat the extended and unextended models separately. Hereafter we will call them *model II* and *model I*, respectively. It transpires that their large-N limits are closely related and model II requires the model I results as inputs.

III. THE SPHERICAL LIMIT

A. Further graphical considerations

In this section we shall consider finally the limit $N\to\infty$. We begin by making a few general observations, reiterating in a little more detail some of the necessary properties of the graphical perturbation theory. We will discuss first the simpler case of model I in which the zero mode is absent and then make the necessary generalizations to model II at the end.

Of primary importance are the N-dependent symmetry factors that accompany each graph. Since the zeroth-order response and correlation functions are independent of the "isospin" index l, the temporal and spatial integrations over products of these functions, which represent a given graph, are completely independent of this extra index and yield precisely the same analytic expression as when $N=1$. As shown in Fig. 5, we may then think of each graph as a product of two distinct expressions, one carrying all of the isospin dependence, the other carrying

all of the space and time dependence. Since we assume that A_N^{lmn} is fully symmetric [Eq. (2.38)], there is no distinction between straight and straight-wavy lines as far as the isospin parts are concerned, which may then be represented as graphs composed purely of directed, dashed lines.

Having worked hard in Sec. II to establish the group-theoretical properties of the A_N^{lmn}, we shall now see these properties bear fruit. In Fig. 6 we represent diagrammatically some important graph decomposition rules that follow from these properties [26] and which we shall now discuss. As noted in Sec. II E, the fact that the Lagrangian is a scalar implies that the group covariance properties of the statistical average of some operator must be identical to those of the operator itself. Thus, for example, the Mth-order term in the perturbation expansion of the response function

$$\mathcal{G}^{l}_{M,l'} = \langle i\mathbf{w}^{l}\cdot\mathbf{v}_{l'}[\lambda_0\mathcal{L}_1^{(N)}]^M\rangle_{0,c} \tag{3.1}$$

(the subscript c denoting the connected part) transforms exactly as does $\mathbf{w}^l\cdot\mathbf{v}_{l'}$. Now, assuming that $\mathbf{w}^l$ and $\mathbf{v}_{l'}$ transform according to the *irreducible* representations of the group G, then, by Schur's lemma [27], $\delta^l_{l'}$ is the only second-rank tensor invariant under the group of transformations. This implies immediately that $\mathcal{G}^{l}_{M,l'}\equiv\mathcal{G}_M\delta^l_{l'}$. Similarly, as long as A_N^{lmn} is the only invariant third-rank tensor, any three-point correlation function must be proportional to it. In model II, which includes the zero mode, care must be taken when indices vanish. This will be discussed in Sec. III E.

We now use these observations to derive the identities, which we shall call rules (a), (b), (c), and (d), shown in Fig. 6. Rule (a) simply generalizes the observation contained in the preceding paragraph: for any second-rank tensor operator $B^l_{l'}$ whose average is represented in Fig. 6(a) by the bubble with two external legs, we have

$$b^l_{l'}\equiv\langle B^l_{l'}\rangle=\frac{1}{N}\delta^l_{l'}\sum_l b^l_l\ . \tag{3.2}$$

The contraction $\sum_l b^l_l$ is represented by the closed diagram on the right-hand side of Fig. 6(a) (a closed diagram being one without any external legs).

Rule (b) states that if an isospin diagram is composed of two subgraphs $b^l_{l'}$ and $c^l_{l'}$ contracted together as shown in Fig. 6(b), then, since each must be proportional to $\delta^l_{l'}$, we must have

$$\begin{aligned}\sum_{l,l'} b^l_{l'}c^{l'}_l &= \left[\frac{1}{N}\sum_l b^l_l\right]\left[\frac{1}{N}\sum_l c^l_l\right]\sum_{l,l'}\delta^l_{l'}\delta^{l'}_l \\ &= \frac{1}{N}\sum_l b^l_l\sum_l c^l_l\ .\end{aligned} \tag{3.3}$$

Rule (c) states that the average of any rank-three operator Γ^{lmn} must be proportional to A_N^{lmn} and hence

$$\gamma^{lmn}\equiv\langle\Gamma^{lmn}\rangle=\frac{1}{I_2}A_N^{lmn}\sum_{l',m',n'}\gamma^{l'm'n'}A_{N,l'm'n'}\ , \tag{3.4}$$

where

$$I_2=\sum_{l,m,n}A_N^{lmn}A_{N,lmn}\ . \tag{3.5}$$

The contraction $\sum_{l'm'n'}\gamma^{l'm'n'}A_{N,l'm'n'}$ is represented by the closed diagram on the right-hand side of Fig. 6(c).

Rule (d) states that if an isospin graph is composed of two subgraphs β^{lmn} and γ_{lmn} contracted together as shown in Fig. 6(c), then, since each must be proportional to A_N^{lmn}, we must have

$$\begin{aligned}&\sum_{l,m,n}\beta^{lmn}\gamma_{lmn} \\ &\quad=\left[\frac{1}{I_2}\sum_{l,m,n}\beta^{lmn}A_{N,lmn}\right] \\ &\qquad\times\left[\frac{1}{I_2}\sum_{l,m,n}\gamma_{lmn}A_N^{lmn}\right]\sum_{l,m,n}A_N^{lmn}A_{N,lmn} \\ &\quad=\frac{1}{I_2}\left[\sum_{l,m,n}\beta^{lmn}A_{N,lmn}\right]\left[\sum_{l,m,n}\gamma_{lmn}A_N^{lmn}\right]\ .\end{aligned} \tag{3.6}$$

Clearly, if invariants of fourth or higher order were *unique* we could continue to derive analogous identities with more external legs and internal lines. However, generally, there is more than one invariant when the order is four or larger, and one would have to consider linear combinations of them. We shall not find it necessary to pursue such complications.

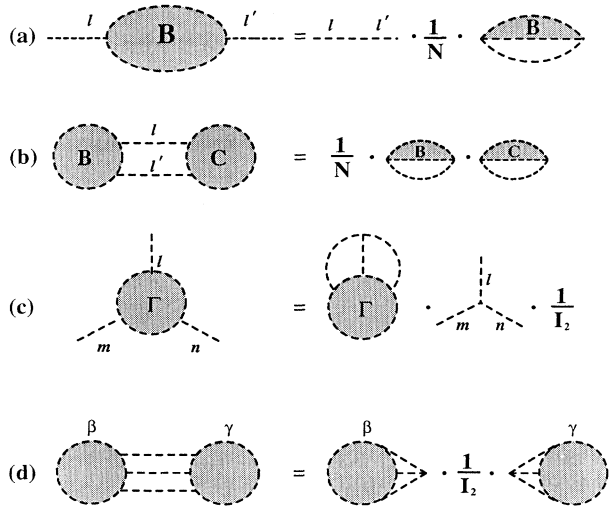

FIG. 6. Reduction rules (a)–(d) for the isospin shadow diagrams. See the text for details.

B. The large-N limit

We can now use rules (a) and (b) to formalize our investigation of the limit $N\to\infty$. Consider the two-point correlation functions. We first use rule (a) to close the diagrams and then ask whether or not the resulting closed diagram takes the form shown in Fig. 6(b), i.e., whether

or not it can be cut into two pieces by severing two internal lines. Such diagrams are called two-particle reducible (2PR). If so, then rule (b) allows us to decompose the diagram into two lower-order ones. If these lower-order diagrams are in turn 2PR, we may reduce them further, continuing the process until only two-particle *irreducible* (2PI) graphs remain. In Fig. 7 we show a few of the lowest-order 2PI graphs. If, after this reduction, only θ graphs [see Fig. 7(a)—note that this is just I_2] remain, the original diagram is called *fully* 2PR.

Since, in our problem, diagrams are composed of vertices with three legs each, it is clear that any closed diagram must contain an even number of vertices. Let us denote the closed 2PI diagrams by $I_{2k}^{(i)}$, where $i=1,\ldots,n_k$ runs over the number of topologically distinct graphs with $2k$ vertices. For example, $n_1=n_2=1, n_3=2$, etc. [26]. As mentioned, $I_2^{(1)}\equiv I_2$ was used already in rules (c) and (d). For the group SU(2) the "tetrahedron graph" Fig. 7(b) is a special case of the Wigner $6j$ symbols and, in general, $I_{2k}^{(i)}$ is a special case of the type-(i) Wigner $3kj$ symbols [28]. In general, the representation could be different for each index sum (i.e., internal line) and the diagrams would then be functions of the $3k$ representation labels—hence the name [see the discussion following (2.60)].

According to rule (b), each time a 2PR graph is reduced, a factor $1/N$ results. Suppose that a given isospin diagram D reduces to a product of $m_{2k}^{(i)}$ diagrams each of type $I_{2k}^{(i)}$. If we define $m_D=\sum_{k=1}^{\infty}\sum_{i=1}^{n_k} m_{2k}^{(i)}$, then the original diagram was severed m_D-1 times. Including the factor $1/N$ arising from the original use of rule (a), we obtain

$$D=\delta_I^{I'}\prod_{k=1}^{\infty}\prod_{i=1}^{n_k}\left[\frac{I_{2k}^{(i)}}{N}\right]^{m_{2k}^{(i)}} . \tag{3.7}$$

For example, if D is fully 2PR then $m_{2k}^{(i)}=0$ for $k\geq 2$ and $D=\delta_I^{I'}(I_2/N)^{m_2}$, where $m_2\equiv m_2^{(1)}$. It is clear, then, that in order to obtain the large-N limit of any diagram, it suffices to understand the large-N behavior of the 2PI graphs.

Recall that we are still free to choose the normalization of A_N^{lmn}. Let us choose it in such a way that

$$I_2\equiv\sum_{l,m,n} A_N^{lmn}A_{N,lmn}=N . \tag{3.8}$$

The fully 2PR diagrams then all have unit weight. Let us then parametrize the large-N behavior of $I_{2k}^{(i)}$ via

$$I_{2k}^{(i)}\approx J_{2k}^{(i)}N^{1-\alpha_{2k}^{(i)}},\quad N\to\infty , \tag{3.9}$$

where $J_{2k}^{(i)}$ are bounded functions of N (in the simplest case, $J_{2k}^{(i)}$ is a constant, but in general it can oscillate with N [24,26]). Equation (3.7) then reduces to

$$\begin{aligned} D&\approx\delta_I^{I'}N^{-\alpha_D}\prod_{k=1}^{\infty}\prod_{i=1}^{n_k}(J_{2k}^{(i)})^{m_{2k}^{(i)}} ,\\ \alpha_D&\equiv\sum_{k=1}^{\infty}\sum_{i=1}^{n_k}\alpha_{2k}^{(i)} . \end{aligned} \tag{3.10}$$

By construction, $\alpha_2\equiv\alpha_2^{(1)}=0$ and $J_2\equiv J_2^{(1)}=1$. If all $\alpha_{2k}^{(i)}$, for $k\geq 2$, are positive, then all higher-order terms vanish when $N\to\infty$. Only the fully 2PR diagrams survive in the spherical limit. Conversely, if some $\alpha_{2k}^{(i)}$ is negative, diagrams that reduce to powers only of $I_{2k}^{(i)}$ become more important than the fully 2PR diagrams and (3.8) is an inappropriate normalization. Let $\alpha_{2k_0}^{(i_0)}$ be the most negative exponent. The appropriate normalization would then be

$$I_{2k_0}^{(i_0)}=N , \tag{3.11}$$

which, in turn, would translate into a new normalization for A_N^{lmn}. In this case, only 2PR diagrams that reduce to powers of $I_{2k_0}^{(i_0)}$ survive in the spherical limit and all others may be dropped. The generalization of this analysis to the case of model II will be discussed in Sec. III E.

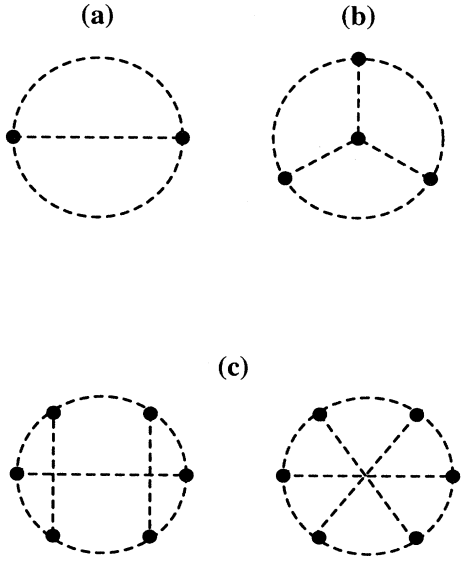

FIG. 7. A few of the lowest-order two-particle irreducible (2PI) isospin graphs: (a) the two-vertex "theta graph," (b) the four-vertex "tetrahedron graph," and (c) the two possible six-vertex graphs.

C. Results for SU(2)

Although the above procedure for determining the nature of the spherical limit is quite general, without considering specific choices of the A_N^{lmn} we are not able to make any general statements about the large-N behavior of the graphs $I_{2k}^{(i)}$. In this paper we will concentrate on the group SU(2), for which the essential results exist already in the literature [26]. In Appendix C we outline similar but, as it turns out, fruitless efforts using the adjoint representation of SU(M) (for which $N=M^2-1$).

As mentioned in Sec. II, the cubic invariants for SU(2) are the Wigner $3j$ symbols

$$A_N^{lmn} \equiv f(N) \begin{bmatrix} j & j & j \\ l & m & n \end{bmatrix},$$

$$l,m,n = -j, -j+1, \ldots, j \ , \quad (3.12)$$

where $N=2j+1$, $f(N)$ is a normalization factor (see below), and it is convenient to allow the indices to range from $-j$ to j rather than from 1 to N (though $m=0$ here should not be confused with the zero mode defined in Sec. II F and treated below in Sec. III E). Under interchange of any two columns the $3j$ symbol acquires a factor $(-1)^{3j}$ [$(-1)^{j_1+j_2+j_3}$ in general] [24] and is therefore symmetric [see (2.34)] only if j is an even integer. The allowed values of N are therefore $N=1,5,9,13,\ldots$. Also, as mentioned, the transformation matrices $\mathbf{D}_N$ are the quantum-mechanical D matrices that determine the behavior of the spherical harmonics under rotation. Thus $\mathbf{v}^m$ transforms in the same way that $Y_{jm}(\theta,\phi)$ does. The identity $Y^*_{jm}(\theta,\phi)=(-1)^m Y_{j,-m}(\theta,\phi)$ implies that

$$\mathbf{v}_m \equiv \mathbf{v}^{m\,*} = (-1)^m \mathbf{v}^{-m} \quad (3.13)$$

and hence that $g^{ll'}=(-1)^l \delta_{-l'l}$ in Eq. (2.58). This may be used to raise and lower indices on any tensor. For example,

$$A_{N,lmn} = (-1)^{l+m+n} A_N^{-l,-m,-n} = A_N^{lmn} \quad (3.14)$$

since the $(3j)$ symbols vanish unless $l+m+n=0$ and since $A_N^{-l,-m,-n}=(-1)^{3j}A_N^{lmn}$ [the factor is again $(-1)^{j_1+j_2+j_3}$ in general] [24]. The $3j$ symbols are therefore all real. The fact that A_N^{lmn} is proportional to $\delta_{l+m+n,0}$ means that indices are "conserved" at each vertex in a diagram and immediately implies rule (a), without resorting to any general principles.

The $3j$ symbols obey the orthogonality condition [24]

$$\sum_{l,m} \begin{bmatrix} j & j & j \\ l & m & n \end{bmatrix} \begin{bmatrix} j & j & j \\ l & m & n' \end{bmatrix} = \frac{1}{2j+1} \delta_{nn'} \ . \quad (3.15)$$

Therefore $\sum_{l,m,n} \left(\begin{smallmatrix} j & j & j \\ l & m & n \end{smallmatrix}\right)^2 = 1$ and the normalization condition (3.8) then requires

$$f(N) = \sqrt{N} \quad (3.16)$$

and the conventional $3kj$ symbols are then multiplied by N^k. Amit and Roginsky [26] have considered N-component generalizations of the Potts model, which also requires cubic invariants. They investigated in great detail the behaviors of the SU(2) graphs $I_{2k}^{(i)}$ for large N. Using a combination of analytic and numerical estimates, they concluded that, indeed, all exponents $\alpha_{2k}^{(i)}$ are strictly positive for $k \geq 2$ and bounded below by $\frac{1}{2}$. Unfortunately, they were unable to provide a complete proof and we have nothing to add in this regard. In addition, there seem to be several different graphs $I_{2k}^{(i)}$ with $\alpha_{2k}^{(i)} \simeq \frac{1}{2}$, all of which would then have to be included in any evaluation of the *leading finite-N corrections* to the spherical limit. In more conventional $1/N$ expansions (that for the s^4 model, for example) the α's increase rapidly with the number of vertices in the graph and it is relatively easy to order the corrections in integer powers of $1/N$. Here a similar procedure seems very difficult and calculating corrections to the spherical limit perhaps unfeasible [see, however, the discussion at the end of Sec. V C]. We are presently looking into groups other than SU(2) [see Appendix C for an example] in hope of simplifying the analysis.

D. Integral equations in the spherical limit

In order to obtain the full solution in the spherical limit, we must characterize the fully 2PR graphs. Fortunately, this is very easy to do: they are simply the bubble diagrams shown in Fig. 8(a). The reduction process consists of cutting out the bubbles one by one, each of which then closes to yield a θ graph Fig. 7(a). It is easy to see that graphs containing lines that connect different bubbles or different sides of the same bubble necessarily give rise to higher order $I_{2k}^{(i)}$ with $k \geq 2$. Since we have chosen $I_2=N$, from (3.7), each bubble diagram carries precisely unit weight. Therefore, summing the bubble diagrams when $N \to \infty$ is no different than summing them when $N=1$. The latter is a very standard approximation in turbulence, known as the *direct interaction approximation* [13]. In the spherical limit these really are the only graphs that survive and the DIA provides an exact solution.

The bubble diagrams can be generated by iterating the diagrammatic equation shown in Fig. 8(b). Here thick lines correspond to the sum of all bubble graphs and thin lines to their zeroth-order counterparts $\delta^I_{l'}$. Including

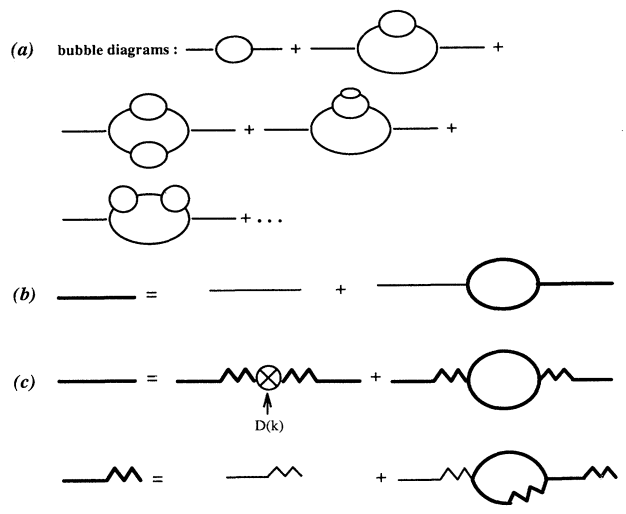

FIG. 8. Surviving diagrams in the spherical limit. (a) The bubble graphs. (b) The diagrammatic equation that, when iterated, generates all isospin bubble graphs. The thick lines denote the full set of bubble graphs, the thin lines the zeroth-order result δ^n_m. (c) The diagrammatic equation that generates the direct interaction approximation (DIA). Thick lines denote the full two-point functions, thin lines their zeroth-order counterparts. This approximation becomes exact in the spherical limit.

once again the space- and time-dependent parts of the graphs, the DIA may be expressed in the form of two coupled integral equations. These are shown diagrammatically in Fig. 8(c). Thick lines now correspond to the full two-point functions $\hat{G}$ and $\hat{U}$ and thin lines to their zeroth-order counterparts [note that only $\hat{G}_0$ is actually needed; see (2.27)]. The derivation of these equations is standard [13] and we shall not repeat it here. In analytic form they read

$$\frac{1}{\hat{G}(\mathbf{k},\omega)} = -i\omega + \nu_0 k^2 - \hat{\Sigma}_{vw}(\mathbf{k},\omega) , \tag{3.17}$$

$$\hat{U}(\mathbf{k},\omega) = |\hat{G}(\mathbf{k},\omega)|^2 [\hat{D}(\mathbf{k},\omega) + \hat{\Sigma}_{ww}(\mathbf{k},\omega)] , \tag{3.18}$$

where the self-energies are

$$\hat{\Sigma}_{vw}(\mathbf{k},\omega) = -\lambda_0^2 k^2 \int_{\mathbf{q}} \int_{\Omega} b(\mathbf{k},\mathbf{q}) \hat{U}(\mathbf{k}-\mathbf{q},\omega-\Omega) \hat{G}(\mathbf{q},\Omega) , \tag{3.19}$$

$$\hat{\Sigma}_{ww}(\mathbf{k},\omega) = \lambda_0^2 k^2 \int_{\mathbf{q}} \int_{\Omega} a(\mathbf{k},\mathbf{q}) \hat{U}(\mathbf{k}-\mathbf{q},\omega-\Omega) \hat{U}(\mathbf{q},\Omega) , \tag{3.20}$$

in which, using $\mathbf{p} \equiv \mathbf{k}-\mathbf{q}$,

$$\begin{aligned} a(\mathbf{k},\mathbf{q}) &= \frac{1}{2k^2} \frac{1}{d-1} \sum_{\alpha,\beta,\gamma,\mu,\nu} P_{\alpha\beta\gamma}(\mathbf{k}) \hat{\tau}_{\beta\mu}(\mathbf{p}) \hat{\tau}_{\gamma\nu}(\mathbf{q}) P_{\alpha\mu\nu}(\mathbf{k}) \\ &= \frac{1}{d-1} \left[d-2-2\frac{(\mathbf{k}\cdot\mathbf{p})^2(\mathbf{k}\cdot\mathbf{q})^2}{k^4 q^2 p^2} + \frac{(\mathbf{k}\cdot\mathbf{q})(\mathbf{k}\cdot\mathbf{p})(\mathbf{q}\cdot\mathbf{p})}{k^2 q^2 p^2} \right. \\ &\quad \left. + \frac{3-d}{2} \frac{(\mathbf{k}\cdot\mathbf{q})^2}{k^2 q^2} + \frac{3-d}{2} \frac{(\mathbf{k}\cdot\mathbf{p})^2}{k^2 p^2} \right] , \end{aligned} \tag{3.21}$$

$$\begin{aligned} b(\mathbf{k},\mathbf{q}) &= \frac{1}{k^2} \frac{1}{d-1} \sum_{\alpha,\beta,\gamma,\mu} P_{\alpha\beta\gamma}(\mathbf{k}) \hat{\tau}_{\beta\mu}(\mathbf{p}) P_{\gamma\mu\alpha}(\mathbf{q}) \\ &= \frac{1}{d-1} \frac{q}{k} \left[-\frac{d-1}{2} \frac{(\mathbf{q}\cdot\mathbf{p})(\mathbf{k}\cdot\mathbf{p})}{kqp^2} \right. \\ &\quad \left. + \frac{(\mathbf{k}\cdot\mathbf{q})^3}{k^3 q^3} + \frac{d-3}{2} \frac{(\mathbf{k}\cdot\mathbf{q})}{kq} \right] . \end{aligned} \tag{3.22}$$

These coefficients are scale invariant

$$a(\mathbf{k},\mathbf{q}) = a\left[\hat{\mathbf{k}}, \frac{\mathbf{q}}{k}\right], \quad b(\mathbf{k},\mathbf{q}) = b\left[\hat{\mathbf{k}}, \frac{\mathbf{q}}{k}\right] \tag{3.23}$$

(here $\hat{\mathbf{k}} \equiv \mathbf{k}/k$) and are related via

$$a(\mathbf{k},\mathbf{q}) = \tfrac{1}{2}[b(\mathbf{k},\mathbf{q}) + b(\mathbf{k},\mathbf{p})] = a(\mathbf{k},\mathbf{p}) . \tag{3.24}$$

As promised, the driving function $\hat{D}(\mathbf{k},\omega)$ is completely arbitrary, appearing as an inhomogeneous term on the right-hand side of (3.18).

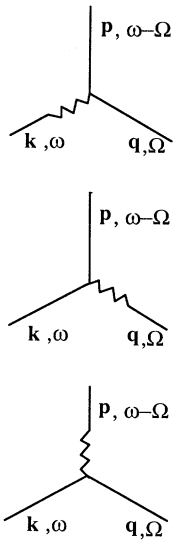

FIG. 9. Three-point velocity correlator $\langle \hat{v}_\alpha(\mathbf{k},\omega) \hat{v}_\beta(\mathbf{p},\omega') \hat{v}_\gamma(\mathbf{q},\omega'') \rangle$ in the spherical limit. The thick lines denote the full two-point functions.

The DIA integral equations are *nonlinear* and include the energy cascade phenomenon. Thus, even if $\hat{D}(\mathbf{k},\omega)$ vanishes outside a small range $k \le m_0$, the nonlinear term on the right-hand side of (3.18) still permits $\hat{U}(\mathbf{k},\omega)$ to be nonzero in the inertial range. One can see this explicitly by considering the bubble diagram series that makes up the perturbation expansion for $\hat{U}$: the diagram with one bubble vanishes only for $k > 2m_0$, diagrams with two nested bubbles vanish only for $k > 3m_0$, and so on. The inertial range $k \gg m_0$ is therefore dominated by high-order diagrams with many nested bubbles. It is then clear why simple perturbation theory in λ_0 fails to describe turbulence.

So far we have discussed only the two-point functions. The third-order correlation functions are also easy to describe. We may close the diagrams using rule (c). The discussion above implies that only bubble graphs may survive this closure. It is easy to see that this means that only "bubble renormalization" of the external legs is permitted in the original diagram. Lines that cross connect different legs lead to nonbubble diagrams after the closure. This implies that the third-order *vertex* functions are unrenormalized: the only nonzero three-point vertex is given by the usual undressed three-point interaction $(i/2)\lambda_0 P_{\alpha\beta\gamma}(\mathbf{k}) A_N^{lmn}$. For example, the triple velocity correlator is given by (see Fig. 9)

$$\begin{aligned} \langle \hat{v}_\alpha^l(\mathbf{k},\omega) \hat{v}_\beta^m(\mathbf{p},\omega') \hat{v}_\gamma^n(\mathbf{q},\omega'') \rangle &= \sum_{\alpha',\beta',\gamma'} [\hat{G}(\mathbf{k},\omega) \hat{U}(\mathbf{p},\omega') \hat{U}(\mathbf{q},\omega'') P_{\alpha'\beta'\gamma'}(\mathbf{k}) + (2 \text{ permutations})] \\ &\quad \times \lambda_0 \hat{\tau}_{\alpha\alpha'}(\mathbf{k}) \hat{\tau}_{\beta\beta'}(\mathbf{p}) \hat{\tau}_{\gamma\gamma'}(\mathbf{q}) A_N^{lmn} \delta(\mathbf{k}+\mathbf{p}+\mathbf{q}) \delta(\omega+\omega'+\omega'') . \end{aligned} \tag{3.25}$$

The general theory [20] implies that yet higher-order vertex functions may always be built up out of third-order vertex functions connected together by the exact, fully dressed two-point functions (the so-called skeleton diagrams). It is tempting to conjecture that in the spherical limit only *tree graphs* (skeleton graphs with no internal sums) survive. To prove this, however, one would have to generalize the closure relations, rules (a) and (c), to graphs with arbitrary numbers of external legs. This in turn would require the characterization of all higher-order invariants (2.42) or (2.54). If, to leading order, for example, all higher-order invariants could be reduced to sums of products of cubic invariants and Kronecker δ's functions, the result would follow. However, this is not obviously the case and we have not pursued this question any further. For our purposes, only the result for the three-point vertices will be needed.

E. Analysis of model II

Let us now address the necessary generalizations of the theory to the model that includes a zero mode. Consider first the extended rules $(\bar{a})$–$(\bar{d})$ (we remind the reader that overbars distinguish model II quantities). From (2.73) it is easy to see that rule $(\bar{a})$ must take the form

$$\bar{b}^l_{l'} \equiv \langle \bar{B}^l_{l'} \rangle = \left[\frac{1}{N}(1-\delta_{l0}) \sum_{l=1}^{N} \bar{b}^l_l + \bar{b}^0_0 \delta_{l0} \right] \delta^l_{l'} , \tag{3.26}$$

which, though still diagonal, generally yields a different result when $l=l'=0$ than when $l=l'\neq 0$. From this it is trivial to see that rule $(\bar{b})$ is

$$\sum_{l,l'=0}^{N} \bar{b}^l_{l'} \bar{c}^{l'}_l = \frac{1}{N} \left[\sum_{l=1}^{N} \bar{b}^l_l \right] \left[\sum_{l=1}^{N} \bar{c}^l_l \right] + \bar{b}^0_0 \bar{c}^{\,0}_0 . \tag{3.27}$$

Similarly, rule $(\bar{c})$ must now take into account the general form (2.74) of the cubic invariants. Thus (3.4) becomes

$$\begin{aligned} \bar{\gamma}^{lmn} \equiv \langle \bar{\Gamma}^{lmn} \rangle = \frac{1}{I_2} A_N^{lmn} \sum_{l',m',n'=1}^{N} \bar{\gamma}^{l'm'n'} A_{N,l'm'n'} \\ + \frac{1}{N}(\delta_{l0} g_N^{mn} + \delta_{m0} g_N^{ln} + \delta_{n0} g_N^{lm}) \\ \times \sum_{l'm'=1}^{N} \bar{\gamma}^{0l'm'} g_{N,l'm'} + \bar{\gamma}^{000} \delta_{l0} \delta_{m0} \delta_{n0} , \end{aligned} \tag{3.28}$$

where I_2 is still given by (3.5) and we reiterate that the unbarred tensors $\mathbf{A}_N$ and $\mathbf{g}_N$ are taken to vanish whenever any index vanishes. It is now easy to substitute this form into (3.6) to obtain rule $(\bar{d})$:

$$\sum_{l,m,n=0}^{N} \bar{\beta}^{lmn} \bar{\gamma}_{lmn} = \frac{1}{I_2} \left[\sum_{l,m,n=1}^{N} \bar{\beta}^{lmn} A_{N,lmn} \right] \left[\sum_{l,m,n=1}^{N} \bar{\gamma}_{lmn} A_{N,lmn} \right] + \frac{3}{N} \left[\sum_{l,m=1}^{N} \bar{\beta}^{0lm} g_{N,lm} \right] \left[\sum_{l,m=1}^{N} \bar{\gamma}_{0lm} g_N^{lm} \right] + \bar{\beta}^{000} \bar{\gamma}_{000} . \tag{3.29}$$

Next consider the diagrammatic reduction process. Rule $(\bar{b})$ implies that reductions proceed as before, except that the zero mode must be considered separately. Each time a graph is reduced, two terms now result [see (3.26)]. Graphically, it is better to rewrite the result in the form

$$\begin{aligned} \sum_{l,l'=0}^{N} \bar{b}^l_{l'} \bar{c}^{l'}_l = \frac{1}{N} \left[\sum_{l=0}^{N} \bar{b}^l_l \right] \left[\sum_{l=0}^{N} \bar{c}^l_l \right] - \frac{1}{N} \bar{b}^0_0 \sum_{l=0}^{N} \bar{c}^l_l \\ - \frac{1}{N} \bar{c}^0_0 \sum_{l=0}^{N} \bar{b}^l_l + \left[1 + \frac{1}{N} \right] \bar{b}^0_0 \bar{c}^0_0 , \end{aligned} \tag{3.30}$$

where the full sums over l clearly yield the usual closure rule Fig. 6(b). How, then, do we graphically interpret $\bar{b}^0_0$ and $\bar{c}^0_0$? Since $\sum_{n,n'=1}^{N} A_N^{lmn} g_{N,nn'} A_{N,l'm'}^{n'} = \sum_{n=1}^{N} A_N^{lmn} A_{N,l'm'n}$, it is clear that, except for an overall prefactor, an external zero mode leg has no effect whatsoever on the graph's internal isospin sums (this is crucial also in the Galilean invariance analysis in Appendix A). The quantity $\bar{b}^0_0$ therefore may be calculated from the *closed* graph, which is obtained simply by *removing* these external legs, along with the vertices to which they connect (we shall call this process *excision*). The overall prefactor is just μ^2, the square of the coefficient of g_N^{lm} in (2.74). We will now fix the value of μ by demanding a well defined $N\to\infty$ limit, as well as recovery of the original Navier-Stokes equations at $N=0$ (*not* $N=1$, as the zero mode still remains). It seems clear that in order to obtain a proper spherical limit, we should ensure that the couplings to the zero mode are as similar as possible to those between the other N modes.

To this end, consider the basic bubble graph

$$\begin{aligned} \sum_{l,m=0}^{N} \bar{A}_N^{lmn} \bar{A}_{N,lmn'} \\ = [(1+\mu^2)(1-\delta_{n0}) + (N-1)\mu^2 \delta_{n0}] \delta^n_{n'} , \end{aligned} \tag{3.31}$$

where we have maintained the normalization (3.12) and $\sum_{l,m} g_N^{lm} g_{N,lm} = N$. If we choose

$$\mu = \frac{1}{\sqrt{N+1}} , \tag{3.32}$$

then, as $N\to\infty$, the distinction between the two terms in square brackets disappears. Furthermore, when $N=0$ the result is $\mu=1$, as required. With this choice, $\bar{b}^0_0$ and

$\bar{c}_0^0$ are $1/(N+1)$ times the closed graphs obtained by excising the externally connected vertices.

Consider now the large-N limit. It is very easy to see that the leading dependence on N of any *closed* graph is *unchanged* from (3.9). The point is that the index 0 contributes negligibly to the internal sums in the limit $N \to \infty$. Each time a vertex contains one or more zeros, a factor $1/\sqrt{N+1}$ results. Such vertices always occur in pairs, so corrections to (3.9) are at most of relative order $1/N$.

Let us now understand which graphs for the two-point correlation functions survive in the spherical limit. We write these functions in the form

$$\hat{G}^l_{l'} = [\hat{\mathcal{G}}\delta_{l0} + \hat{G}(1-\delta_{l0})]\delta^l_{l'} ,$$

$$\hat{U}^l_{l'} = [\hat{\mathcal{U}}\delta_{l0} + \hat{U}(1-\delta_{l0})]\delta^l_{l'} . \tag{3.33}$$

We may alternatively write

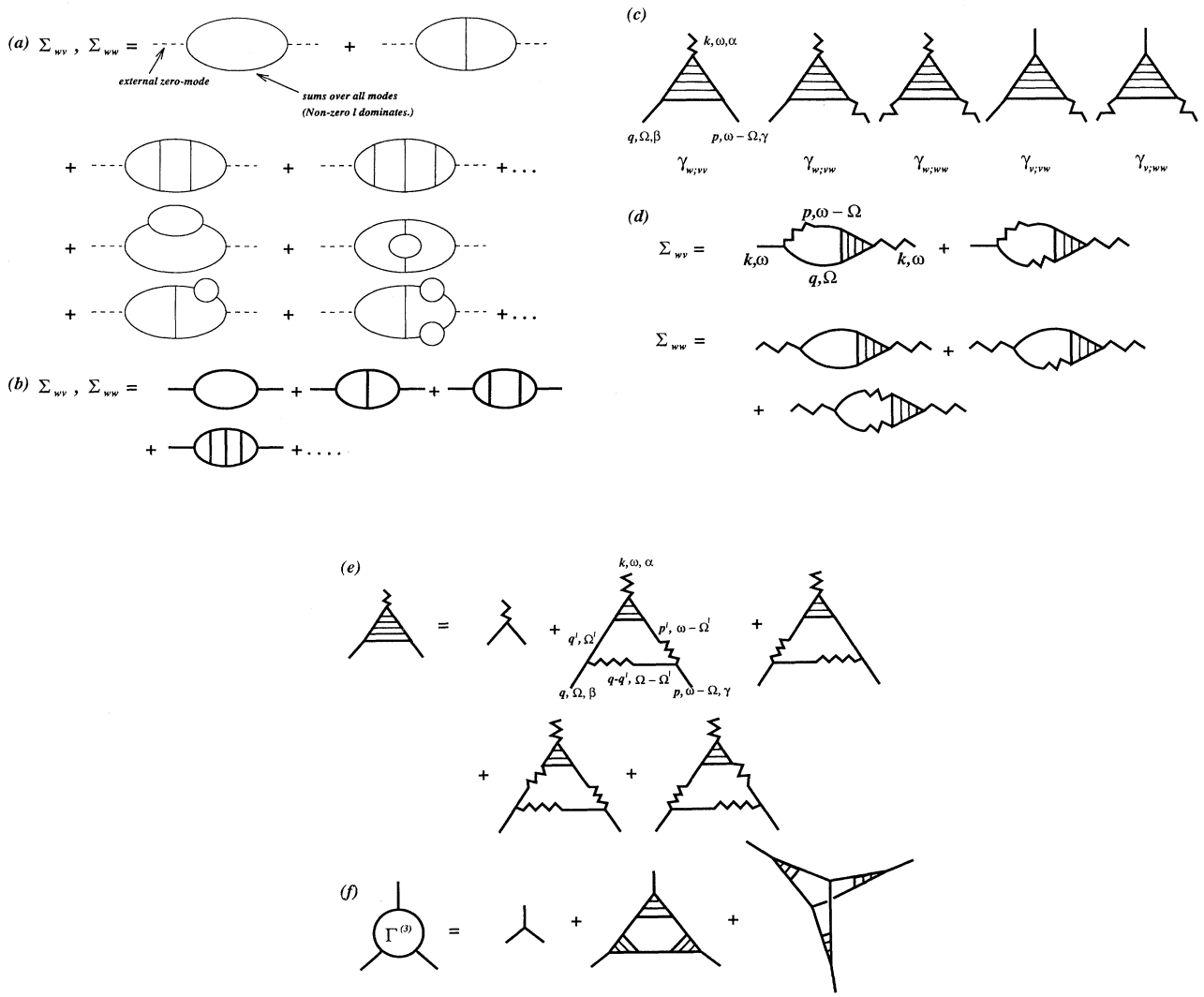

FIG. 10. Surviving diagrams for the zero mode in the spherical limit of the extended model. (a) Schematic diagrams for the self-energies. (b) Schematic representation for the self-energy ladder diagrams for the zero mode. Here, and below, each thick line is "fully bubble renormalized" and corresponds to a full DIA response or correlation function. (c) The five three-point functions needed to resum the ladder diagrams. (d) The diagrammatic representation of the self-energies in terms of these three point functions. (e) The diagrammatic representation of the self-consistent integral equation satisfied by the three-point function $\gamma_{w;vv}$. The other four satisfy similar equations. (f) Schematic representation of the two topological types of diagram entering the full three-point function for the zero mode in the spherical limit. Each three-point vertex is one of the five three-point functions in (c) and the full set of diagrams is constructed by connecting them together in all possible ways.

$$\hat{G}=\frac{1}{N}\sum_{l=0}^{N}\hat{G}_l^l-\frac{1}{N}\hat{\mathcal{G}}=\frac{1}{N}\sum_{l=0}^{N}\hat{G}_l^l+O\left[\frac{1}{N}\right] \tag{3.34}$$

and similarly for $\hat{U}$. Thus, to leading order for large N, we may still obtain the isospin symmetry factors in the diagrammatic expansions of $\hat{G}$ and $\hat{U}$ via the closure rule (a). As we have argued that (3.9) is unchanged, we conclude that $\hat{G}$ and $\hat{U}$ are also completely unchanged by the presence of the zero mode: in the limit $N\to\infty$ this mode becomes an infinitesimal perturbation on the others. In particular, the results for the group SU(2) are, as before, precisely the DIA equations (3.17)–(3.20). In contrast, the finite-N corrections will be more complicated, but this does not concern us here.

The zero-mode correlations themselves are, however, more complicated. Though it is clear that the reduction process is unchanged—only the 2PI graph with largest exponent α_D survives—the starting point is now a closed isospin graph with two fewer vertices. In particular, because the graphs are no longer connected through the joining of the external legs, more complicated *internal* connections survive the reduction process. In Fig. 10(a) we show the new class of *ladder* diagrams that now contributes, in addition to the bubble graphs in Fig. 8(a). All possible bubble insertions on the internal lines are permitted as well, as also shown in Fig. 10(a). Since we have seen that the zero mode contributes negligibly to the internal bonds of a graph when $N\to\infty$, we may now completely neglect the zero mode in resuming these diagrams. In particular, we shall now see that $\hat{\mathcal{G}}$ and $\hat{\mathcal{U}}$ *may be expressed completely in terms of* $\hat{G}$ *and* $\hat{U}$. The point is that the summation over all bubble insertions in a given ladder-type diagram simply renormalizes each $\hat{G}_0$ to $\hat{G}$ and each $\hat{U}_0$ to $\hat{U}$ in the undecorated ladder. Thus an independent series of the form shown in Fig. 8(b) [or, more precisely, Fig. 8(c)] replaces each bond. This is shown in Fig. 10(b). Note that the real distinction between the ladder diagrams and the bubble diagrams is that closure at the top and bottom of the ladder involves a product of *two* two-point functions instead of just one. Thus the excision that occurs in the isospin part of the diagram is *not* mirrored in the space-time part.

In order to obtain $\hat{\mathcal{G}}$ and $\hat{\mathcal{U}}$ we must resume the ladder series. To this end, we introduce five three-point functions $\gamma_{w^{\alpha};v^{\beta}v^{\gamma}}$, $\gamma_{w^{\alpha};v^{\beta}w^{\gamma}}$, $\gamma_{w^{\alpha};w^{\beta}w^{\gamma}}$, $\gamma_{v^{\alpha};v^{\beta}w^{\gamma}}$, and $\gamma_{v^{\alpha};w^{\beta}w^{\gamma}}$, which are obtained by excising one of the external vertices on the ladder diagrams [see Fig. 10(c)]. For the purposes of calculating $\hat{\mathcal{G}}$ and $\hat{\mathcal{U}}$ we require only the first three, in terms of which we have

$$\begin{aligned}
\hat{\Sigma}_{vw}(\mathbf{k},\omega)&=\int_{\mathbf{q}}\int_{\Omega}[2\gamma^{(1)}_{w;vv}(\mathbf{k},\omega;\mathbf{q},\Omega)\hat{G}(\mathbf{p},\omega-\Omega)\hat{U}(\mathbf{q},\Omega)+\gamma^{(1)}_{w;wv}(\mathbf{k},\omega;\mathbf{q},\Omega)\hat{G}(\mathbf{p},\omega-\Omega)\hat{G}(-\mathbf{q},-\Omega)]\ ,\\
\hat{\Sigma}_{ww}(\mathbf{k},\omega)&=\int_{\mathbf{q}}\int_{\Omega}[\gamma^{(2)}_{w;vv}(\mathbf{k},\omega;\mathbf{q},\Omega)\hat{U}(\mathbf{p},\omega-\Omega)\hat{U}(\mathbf{q},\Omega)+\gamma^{(2)}_{w;vw}(\mathbf{k},\omega;\mathbf{q},\Omega)\hat{G}(-\mathbf{p},\Omega-\omega)\hat{U}(\mathbf{q},\Omega)\\
&\quad+\gamma^{(2)}_{w;ww}(\mathbf{k},\omega;\mathbf{q},\Omega)\hat{G}(-\mathbf{p},\Omega-\omega)\hat{G}(-\mathbf{q},-\Omega)]\ ,
\end{aligned} \tag{3.35}$$

where, for an arbitrary three point function, we have defined the contractions

$$\begin{aligned}
\gamma^{(1)}(\mathbf{k},\mathbf{q})&=-\frac{i\lambda_0}{d-1}\sum_{\alpha,\beta,\beta',\gamma}\gamma_{\alpha\beta\gamma}(\mathbf{k},\mathbf{q})\hat{\tau}_{\beta\beta'}(\mathbf{q})P_{\gamma\beta'\alpha}(-\mathbf{p})\ ,\\
\gamma^{(2)}(\mathbf{k},\mathbf{q})&=-\frac{i\lambda_0}{d-1}\sum_{\alpha,\beta,\beta',\gamma,\gamma'}\gamma_{\alpha\beta\gamma}(\mathbf{k},\mathbf{q})\hat{\tau}_{\beta\beta'}(\mathbf{q})\hat{\tau}_{\gamma\gamma'}(\mathbf{p})P_{\alpha\beta'\gamma'}(\mathbf{k})\ .
\end{aligned} \tag{3.36}$$

The DIA equations result if $\gamma_{w^{\alpha};v^{\beta}v^{\gamma}}(\mathbf{k},\omega;\mathbf{q},\Omega)$ is replaced by the zeroth-order vertex $-(i/2)\lambda_0 P_{\alpha\beta\gamma}(-\mathbf{k})$ and the remaining ones are set to zero. The functions $\gamma^{(1)}$ and $\gamma^{(2)}$ then reduce to the coefficients $\lambda_0^2k^2b(\mathbf{k},\mathbf{q})$ and $\lambda_0^2k^2a(\mathbf{k},\mathbf{q})$, respectively.

Finally, we must determine these three-point functions. This is done self-consistently, as shown for $\gamma_{w;vv}$ in Fig. 10(e). Explicitly, we have

$$\begin{aligned}
\gamma_{w^{\alpha};v^{\beta}v^{\gamma}}(\mathbf{k},\omega;\mathbf{q},\Omega)&=-\frac{i}{2}\lambda_0P_{\alpha\beta\gamma}(-\mathbf{k})\\
&\quad-\lambda_0^2\sum_{\mu,\nu,\lambda,\sigma}\int_{\mathbf{q}'}\int_{\Omega'}\{[2\gamma_{w^{\alpha};v^{\mu}v^{\nu}}(\mathbf{k},\omega;\mathbf{q}',\Omega')\hat{U}(\mathbf{q}',\Omega')+\gamma_{w^{\alpha};w^{\mu}v^{\nu}}(\mathbf{k},\omega;\mathbf{q}',\Omega')\hat{G}(-\mathbf{q}',-\Omega')]\\
&\qquad\times\hat{G}(\mathbf{p}',\omega-\Omega')\hat{G}(\mathbf{q}-\mathbf{q}',\Omega-\Omega')\hat{\tau}_{\mu\lambda}(\mathbf{q}')P_{\nu\sigma\gamma}(-\mathbf{p}')P_{\sigma\lambda\beta}(\mathbf{q}'-\mathbf{q})+[\mathbf{q},\beta\leftrightarrow\mathbf{p},\gamma]\\
&\qquad+2\gamma_{w^{\alpha};v^{\mu}v^{\nu}}(\mathbf{k},\omega;\mathbf{q}',\Omega')\hat{G}(\mathbf{q}',\Omega')\hat{G}(\mathbf{p}',\omega-\Omega')\\
&\qquad\times\hat{U}(\mathbf{q}-\mathbf{q}',\Omega-\Omega')P_{\mu\lambda\beta}(-\mathbf{q}')P_{\nu\sigma\gamma}(-\mathbf{p}')\hat{\tau}_{\lambda\sigma}(\mathbf{q}-\mathbf{q}')\}\\
&=\gamma_{w^{\alpha};v^{\gamma}v^{\beta}}(\mathbf{k},\omega;\mathbf{p},\omega-\Omega)\ .
\end{aligned} \tag{3.37}$$

Similarly,

$$\gamma_{w^{\alpha};v^{\beta}w^{\gamma}}(\mathbf{k},\omega;\mathbf{q},\Omega)$$

$$\begin{aligned}
=&-\lambda_0^2\sum_{\mu,\nu,\lambda,\sigma,\tau}\int_{\mathbf{q}'}\int_{\Omega'}\{[2\gamma_{w^{\alpha};v^{\mu}v^{\nu}}(\mathbf{k},\omega;\mathbf{q}',\Omega')\hat{U}(\mathbf{q}',\Omega')\hat{U}(\mathbf{p}',\omega-\Omega')+\gamma_{w^{\alpha};w^{\mu}v^{\nu}}(\mathbf{k},\omega;\mathbf{q}',\Omega')\hat{G}(-\mathbf{q}',-\Omega')\hat{U}(\mathbf{p}',\omega-\Omega')\\
&+\gamma_{w^{\alpha};v^{\mu}w^{\nu}}(\mathbf{k},\omega;\mathbf{q}',\Omega')\hat{U}(\mathbf{q}',\Omega')\hat{G}(-\mathbf{p}',\Omega'-\omega)\\
&+2\gamma_{w^{\alpha};w^{\mu}w^{\nu}}(\mathbf{k},\omega;\mathbf{q}',\Omega')\hat{G}(-\mathbf{q}',-\Omega')\hat{G}(-\mathbf{p}',\Omega'-\omega)]\\
&\times\hat{G}(\mathbf{q}-\mathbf{q}',\Omega-\Omega')\hat{\tau}_{\mu\lambda}(\mathbf{q}')\hat{\tau}_{\nu\sigma}(\mathbf{p}')P_{\tau\lambda\beta}(\mathbf{q}'-\mathbf{q})P_{\gamma\sigma\tau}(\mathbf{p})\\
&+[2\gamma_{w^{\alpha};v^{\mu}v^{\nu}}(\mathbf{k},\omega;\mathbf{q}',\Omega')\hat{U}(\mathbf{p}',\omega-\Omega')+\gamma_{w^{\alpha};v^{\mu}w^{\nu}}(\mathbf{k},\omega;\mathbf{q}',\Omega')\hat{G}(-\mathbf{p}',\Omega'-\omega)]\\
&\times\hat{G}(\mathbf{q}',\Omega')\hat{U}(\mathbf{q}-\mathbf{q}',\Omega-\Omega')\hat{\tau}_{\lambda\tau}(\mathbf{q}-\mathbf{q}')\hat{\tau}_{\nu\sigma}(\mathbf{p}')P_{\mu\tau\beta}(-\mathbf{q}')P_{\gamma\lambda\sigma}(\mathbf{p})\}\\
=&\gamma_{w^{\alpha};w^{\gamma}v^{\beta}}(\mathbf{k},\omega;\mathbf{p},\omega-\Omega)
\end{aligned}\tag{3.38}$$

and

$$\gamma_{w^{\alpha};w^{\beta}w^{\gamma}}(\mathbf{k},\omega;\mathbf{q},\Omega)$$

$$\begin{aligned}
=&-\lambda_0^2\sum_{\mu,\nu,\lambda,\sigma,\eta,\tau}\int_{\mathbf{q}'}\int_{\Omega'}\{[\gamma_{w^{\alpha};v^{\mu}v^{\nu}}(\mathbf{k},\omega;\mathbf{q}',\Omega')\hat{U}(\mathbf{q}',\Omega')\hat{U}(\mathbf{p}',\omega-\Omega')\\
&+\gamma_{w^{\alpha};w^{\mu}w^{\nu}}(\mathbf{k},\omega;\mathbf{q}',\Omega')\hat{G}(-\mathbf{q}',-\Omega')\hat{G}(-\mathbf{p}',\Omega'-\omega)\\
&+\gamma_{w^{\alpha};w^{\mu}v^{\nu}}(\mathbf{k},\omega;\mathbf{q}',\Omega')\hat{G}(-\mathbf{q}',-\Omega')\hat{U}(\mathbf{p}',\omega-\Omega')\\
&+\gamma_{w^{\alpha};v^{\mu}w^{\nu}}(\mathbf{k},\omega;\mathbf{q}',\Omega')\hat{U}(\mathbf{q}',\Omega')\hat{G}(-\mathbf{p}',\Omega'-\omega)]\\
&\times\hat{U}(\mathbf{q}-\mathbf{q}',\Omega-\Omega')\hat{\tau}_{\mu\lambda}(\mathbf{q}')\hat{\tau}_{\nu\sigma}(\mathbf{p}')\hat{\tau}_{\eta\tau}(\mathbf{q}-\mathbf{q}')P_{\beta\lambda\tau}(\mathbf{q})P_{\gamma\sigma\eta}(\mathbf{p})\}\\
=&\gamma_{w^{\alpha};w^{\gamma}w^{\beta}}(\mathbf{k},\omega;\mathbf{p},\omega-\Omega)\ .
\end{aligned}\tag{3.39}$$

These three equations must be solved simultaneously for the γ's and then used as inputs to (3.35). One then finally obtains the two-point functions via (3.17) and (3.18) with $\hat{\mathcal{U}}$ and $\hat{\mathcal{G}}$ replacing $\hat{U}$ and $\hat{G}$ and using the new forms (3.35) for the self-energies. Similar equations may be written down for the two functions $\gamma_{v;wv}$ and $\gamma_{v;wv}$, which will be needed below.

Finally, we turn to the three-point functions $\Gamma^{(3)}$. In the case that all three isospin indices are nonzero, these functions are unrenormalized, as in (3.25). In the case that a single isospin index vanishes it is easy to see that one obtains precisely the γ's defined above, in which the variable in front of the semicolon corresponds to the vanishing index. We discuss now the case in which all three isospin indices vanish. Once again, the surviving isospin graphs are determined by excising the three externally connected vertices, yielding closed graphs with three fewer vertices. The large-N limit is then determined in the usual way. As before, we may classify these graphs explicitly for the group SU(2). The idea is to take a closed bubble graph and attach the external legs in all possible ways. Alternatively, we must attach one more leg to a two-point graph (i.e., a ladder-type diagram) in all possible ways. A little thought will convince one that Fig. 10(f) shows schematically the correct result. Thus, if the third leg is attached to a *rung* of the ladder, the third, "propeller," diagram results in which the "blades" of the propeller are γ's. On the other hand, if the third leg is attached to a ladder edge, the second, "triangle," diagram results. The corners are once again γ's. In obtaining this result, the key observation is that the rungs and edges are bubble renormalized in all possible ways and the third leg may be attached to any one of these bubbles which in turn may be nested arbitrarily deeply. The depth of the nesting determines the number of rungs on the new ladder that then extends out of the original one and has the newly attached leg at its apex. A little topological remolding yields the results shown in Fig. 10(f). In order to turn this schematic picture into an analytic expression, we must now distinguish between straight and wavy legs and bonds. For example, for the full vertex $\Gamma^{(3)}_{w^{\alpha}v^{\beta}v^{\gamma}}(\mathbf{k},\omega;\mathbf{q},\Omega)$, Fig. 10(f) translates into 7 distinct triangle graphs and 21 distinct propeller graphs. Furthermore, the last two γ's in Fig. 10(c) are now required. One finds then

$$
\begin{aligned}
&\Gamma^{(3)}_{w^{\alpha}v^{\beta}v^{\gamma}}(\mathbf{k},\omega;\mathbf{q},\Omega) \\
&\quad = -\frac{i}{2}\lambda_0 P_{\alpha\beta\gamma}(\mathbf{k}) \\
&\qquad + \sum_{\mu,\nu,\lambda,\sigma} \int_{\mathbf{q}'}\int_{\Omega'} \{ 2\gamma_{w^{\alpha};v^{\mu}v^{\nu}}(-\mathbf{k},-\omega;-\mathbf{q}',-\Omega')\gamma_{v^{\beta};w^{\mu}v^{\lambda}}(\mathbf{q},\Omega;\mathbf{q}',\Omega')\gamma_{v^{\gamma};w^{\nu}v^{\sigma}}(\mathbf{p},\omega-\Omega;\mathbf{k}-\mathbf{q}',\omega'-\Omega) \\
&\qquad\qquad \times \hat{G}(-\mathbf{q}',-\Omega')\hat{G}(\mathbf{q}'-\mathbf{k},\Omega'-\omega)\hat{U}(\mathbf{q}-\mathbf{q}',\Omega-\Omega')\hat{\tau}_{\lambda\sigma}(\mathbf{q}-\mathbf{q}') + (\text{6 more triangle terms}) \} \\
&\qquad - \lambda_0^2 \sum_{\mu,\nu,\lambda,\sigma,\eta,\tau} \int_{\mathbf{q}'}\int_{\Omega'}\int_{\mathbf{q}''}\int_{\Omega''} \{ 8\gamma_{w^{\alpha};v^{\mu}v^{\nu}}(-\mathbf{k},-\omega;-\mathbf{q}'-\mathbf{q}'',-\Omega'-\Omega'') \\
&\qquad\qquad \times \gamma_{v^{\beta};w^{\lambda}w^{\sigma}}(\mathbf{q},\Omega;\mathbf{q}',\Omega')\gamma_{v^{\gamma};w^{\tau}w^{\eta}}(\mathbf{p},\omega-\Omega;\mathbf{q}'',\Omega'') \\
&\qquad\qquad \times \hat{G}(\mathbf{q}'+\mathbf{q}''-\mathbf{k},\Omega'+\Omega''-\omega)\hat{G}(-\mathbf{q}'-\mathbf{q}'',-\Omega'-\Omega'') \\
&\qquad\qquad \times \hat{G}(-\mathbf{q}',-\Omega')\hat{G}(\mathbf{q}'-\mathbf{q},\Omega'-\Omega)\hat{G}(-\mathbf{q}'',-\Omega'')\hat{G}(\mathbf{q}''-\mathbf{p},\Omega''+\Omega-\omega) \\
&\qquad\qquad \times P_{\mu\lambda\tau}(\mathbf{q}'+\mathbf{q}'')P_{\nu\sigma\eta}(\mathbf{k}-\mathbf{q}'-\mathbf{q}'') + (\text{20 more propeller terms}) \} \ , \qquad (3.40)
\end{aligned}
$$

in which $\mathbf{k},\omega$ are taken to be incoming, while $\mathbf{q},\Omega$ and $\mathbf{p},\omega-\Omega$ are taken to be outgoing.

We end this section by noting that the DIA equations have been obtained previously as a large-N limit. Thus Kraichnan [29,30] has considered generalizations of the Navier-Stokes equations of the form (2.1) in which A_N^{lmn} is *randomly* $\pm 1/\sqrt{N}$, subject only to the symmetry conditions (2.38). In the limit $N\to\infty$ the law of large numbers produces precisely the results we obtain: the DIA equations become exact. In the same work, Kraichnan [29] also realized the significance of Galilean invariance and considered also extended random coupling models analogous to (2.74) in which a zero mode is included. He concluded, as we have, that the nonzero modes still obey the DIA equations in the spherical limit, but did not analyze the zero mode itself. The excision rule is implicit in his model as well, so a similar analysis would certainly produce the same results that we obtain. However, if one contemplates calculating finite-N corrections, only when the generalized fluid equations include the higher-order group symmetry do the identities shown in Fig. 6 hold and can one therefore carry out the reduction process discussed in Sec. III C and in this section. Furthermore, only then may one hope that the universal exponents will vary continuously with N [reducing to the usual Navier-Stokes equations at $N=1$ (or $N=0$ in model II)] and thereby allow a systematic expansion. A finite set of randomly coupled velocity fields do not possess sufficient group structure for these results to follow (see the corresponding discussion for the spin models in Sec. II A).

The fact that Kraichnan also obtained the DIA equations in the limit $N\to\infty$ leads one to expect that this limit will be rather insensitive to the detailed procedure for obtaining it. We have demonstrated this explicitly in Secs. III C and III E: it is necessary and sufficient, both with and without a zero mode, only that the θ graph I_2 dominate at large N. Since this is the simplest graph, it does not require a great deal of optimism to expect that the DIA equations will often result in the spherical limit (see, however, Appendix C for a counter example). Finite-N corrections will, of course, depend on precisely how the limit is taken [but should all coincide, once again, at $N=1$ (or $N=0$)].

IV. EXACT SOLUTION IN THE SPHERICAL LIMIT

In this section we provide exact solutions to the DIA equations in the inertial range, exhibiting the full scaling functions $g(s)$ and $u(s)$ and the exponent behaviors shown in Fig. 2. We use these solutions to compute the energy flux in the inertial range and various associated universal amplitude ratios, such as the generalization of the Kolmogorov constant. We outline the solutions to model II, confirming that although the scaling functions are strongly modified from their DIA counterparts, the exponent behaviors are the same. We leave detailed analysis of energy flux and universal amplitudes for future work, but we will, however, in Sec. V C comment on various questions one might hope to answer that the DIA equations fail to address. The analysis becomes rather involved in some places, so in Appendix D we illustrate all aspects of the calculations using a simplified, time-independent set of model DIA equations. The advantage of this simplification is that all computations may be performed analytically. It may be useful for the reader to study this section and Appendix D in parallel. We begin our analysis by understanding the renormalization group results in the context of the DIA equations.

A. Power-law driving

Let us use the power-law form (1.14) for the driving spectrum. Consider first the case $y<0$. We have stated that a renormalized linear hydrodynamics should then result. To see that the DIA equations reproduce this behavior, suppose that the integrals on the right-hand side of (3.17)–(3.20) are finite when $\mathbf{k},\omega\to 0$. Thus if

$$\nu_1(k)=\lambda_0^2\int_{q<\Lambda}\int_{\Omega} b(\mathbf{0},\mathbf{q})\hat{U}(\mathbf{k}-\mathbf{q},-\Omega)\hat{G}(\mathbf{q},\Omega)\ , \tag{4.1}$$

then we assume that $\nu_1(0)<\infty$. It transpires that the theory is well defined only when an upper cutoff Λ is included [5(a)]. The viscosity correction is therefore nonuniversal and crucially dependent upon detailed microphysics that is beyond the resolution of the hydrodynamic Navier-Stokes equations. Given that $\nu_1(0)$ is finite, for small k and ω we then have

$$\hat{G}(\mathbf{k},\omega)\approx\frac{1}{-i\omega+\nu_R k^2},\quad \nu_R\equiv\nu_0+\nu_1(0)\ . \tag{4.2}$$

The renormalized viscosity ν_R is positive even if ν_0 vanishes: the high-k modes provide an energy sink that mimics viscous damping of the low-k modes. The solution for $\hat{U}(\mathbf{k},\omega)$ is then

$$\hat{U}(\mathbf{k},\omega)\approx\frac{D_R(k)}{\omega^2+\nu_R^2 k^4},\quad D_R(k)\equiv D(k)+D_1(k)\ , \tag{4.3}$$

where

$$D_1(k)=\lambda_0^2 k^2\int_{q<\Lambda}\int_{\Omega} a(\mathbf{0},\mathbf{q})\hat{U}(\mathbf{k}-\mathbf{q},-\Omega)\hat{U}(\mathbf{q},\Omega)\ . \tag{4.4}$$

It is easy to check that if $y<0$ we have, self-consistently,

$$D_1(k)\approx\begin{cases}\bar{D}_1 k^{4-d-2y}, & \dfrac{2-d}{2}\le y<0\\ \bar{D}_0 k^2, & y<\dfrac{2-d}{2}\end{cases} \tag{4.5}$$

when $k\to 0$ (we assume $d>2$ throughout). Thus $D(k)$ dominates $D_1(k)$ for $2-d<y<0$ and

$$D_R(k)\approx\begin{cases}D_0 k^{4-d-y}, & 2-d<y<0\\ \bar{D}_0 k^2, & y<2-d\end{cases} \tag{4.6}$$

when $k\to 0$. Substituting (4.2), (4.3), and (4.6) into (4.1) we find that $\nu_1(k)=\nu_1(0)+O(k^{\min\{-y,d-2\}})$, which confirms our original assumptions. Furthermore, any driving that is weaker than thermal at small k becomes renormalized to thermal by the nonlinearity. Precisely at $y=2-d$ [i.e., $D(k)=D_0k^2$] the fluctuation-dissipation relation must hold and it is easy to check that $\hat{U}(\mathbf{k},\omega)=(D_0/\nu_0)\mathrm{Re}\hat{G}(\mathbf{k},\omega)$ renders (3.3) and (3.4) identical. Note that the actual calculation of the coefficients $\nu_1(0),\bar{D}_0,\bar{D}_1$, etc., requires knowledge of the full functions $\hat{U}$ and $\hat{G}$ for all wave vectors and frequencies and therefore cannot be inferred by simple arguments. Forster, Nelson, and Stephen [5(a)] calculate them using the one-loop order renormalization group recursion relations at small Reynolds number $D_0\lambda_0^3/\nu_0\ll 1$, where the nonlinear terms can be treated perturbatively. As mentioned in Sec. I E, this one loop calculation is, in fact, identical to solving the DIA equations by an iterative scheme. It is actually easy to see why this must be so: the order y recursion relations are obtained precisely by renormalizing the same bubble diagrams that survive at $N\to\infty$ [5(a)]. The renormalization group recursion relations therefore result essentially by applying the method of characteristics to the DIA equations [31].

Consider now $y>0$, but not too large. The correction $\nu_1(k)$ now diverges at small k: the nonlinearity dominates. To understand the resulting behavior we now substitute the general scaling forms (1.16) and (1.17) into the DIA equations, treating them as exact. We must check the consistency of this assumption in the end. In particular, we must ensure the convergence of the integrals for both large and small q and Ω. After appropriate rescaling of the integration variables, the DIA equations then read

$$\frac{1}{A_1\tilde{\nu}g(s)}=-is+\frac{\nu_0}{\tilde{\nu}}k^{2-z}+\lambda_0^2 k^{d+2-\Delta-z}A_1A_2\times\int_{\mathbf{Q}}\int_t b(\hat{\mathbf{k}},\mathbf{Q})P^{-\Delta}u\left[\frac{s-Q^z t}{P^z}\right]g(t)\ , \tag{4.7}$$

$$\frac{A_2u(s)}{\tilde{\nu}|A_1|^2|g(s)|^2}=\frac{D_0}{\tilde{\nu}}k^{\Delta-2z+4-d-y}+\lambda_0^2A_2^2k^{d+2-\Delta-z}\times\int_{\mathbf{Q}}\int_t a(\hat{\mathbf{k}},\mathbf{Q})P^{-\Delta}Q^{z-\Delta}u\left[\frac{s-Q^z t}{P^z}\right]u(t)\ , \tag{4.8}$$

where $\mathbf{Q}=\mathbf{q}/k$, $\hat{\mathbf{k}}=\mathbf{k}/k$, $\mathbf{P}=\hat{\mathbf{k}}-\mathbf{Q}$, $s=\omega/\tilde{\nu}k^z$, and $t=\Omega/\tilde{\nu}q^z$. The scaling hypothesis is consistent only if the leading behaviors on both sides depend only on the variable s. Since we already know that the nonlinear terms dominate for $y>0$, we conclude that there must be no residual k dependence in their prefactors. By construction, the integrals themselves, as long as they converge, depend only on s. Both (4.7) and (4.8) then yield the hyperscaling relation $\Delta+z=d+2$, as alluded to in (1.19). In order to obtain a second relation among the exponents, we assert that, since the power-law driving controls the spectrum, the driving term in (4.8) must be of the same order as the nonlinear term. This implies that

$$\Delta-2z=d-4+y\ , \tag{4.9}$$

which, when combined with (1.19), immediately yields (1.18) for Δ and z. It is then clear that, since $z<2$, the viscous term in (4.7) is a lower-order *correction* to scaling, vanishing as $k\to 0$. Full, exact scaling over the entire range of variables occurs only in the formal infinite Reynolds number limit $\nu_0\to 0$. We shall see below that this is a perfectly well defined limit for all $y>0$ and we therefore take $\nu_0\equiv 0$ henceforth. In real systems the viscosity dominates for k larger than a dissipation scale Λ and provides a cutoff on the energy spectrum [2]. By examining the corrections to scaling due to the $(\nu_0/\tilde{\nu})k^{2-z}$ term one may estimate Λ, along with the corresponding *dissipation frequency* ω_Λ. This will be discussed in Sec. V B in the light of various experimental and numerical results.

With $\nu_0 \equiv 0$, we may now choose, for convenient normalization purposes, $A_1 = 1/\tilde{\nu} = (\lambda_0^2 D_0)^{-1/3}$ and $A_2 = (D_0/\lambda_0^4)^{1/3}$. The equations for $g(s)$ and $u(s)$ then take the universal forms (dependent only on y and d)

$$\frac{1}{g(s)} = -is + \int_Q \int_t b(\hat{\mathbf{k}},\mathbf{Q}) P^{-\Delta} u\left[\frac{s-Q^z t}{P^z}\right] g(t) , \tag{4.10}$$

$$\frac{u(s)}{|g(s)|^2} = 1 + \int_Q \int_t a(\hat{\mathbf{k}},\mathbf{Q}) P^{-\Delta} Q^{z-\Delta} u\left[\frac{s-Q^z t}{P^z}\right] u(t) , \tag{4.11}$$

with Δ and z given by (1.18). Solving these equations for the two unknown functions $g(s)$ and $u(s)$ is nontrivial, entailing some rather complicated numerics, and we will not address this problem here. For small y many of the details may be worked out using the renormalization group recursion-relation–iteration technique [5,7].

Let us now investigate the convergence properties of (4.10) and (4.11). For what range of y are these equations well defined? The integral over t is perfectly finite since $g(s) \approx -1/is$ for large s [due to the unit discontinuity, in the time domain, of $\hat{G}(\mathbf{k},t)$ at $t=0$] while $u(s)$ is integrable [since the frequency integral $k^{d-1}\int_\omega \hat{U}(\mathbf{k},\omega) = \tilde{\nu} k^{-\zeta} \int_s u(s)$ is proportional to the energy spectrum]. The products in (4.10) and (4.11) are therefore integrable over the scaled variable t. Also, since $\Delta = d + y/3 > d$, the integral over Q converges at infinity for all $y > 0$. The only possible divergence therefore occurs in the infrared: $Q \to 0$ or $P \to 0$. Let us first examine (4.10). Since $z = 2 - y/3 < 2 < d$, it is easy to see that region $Q \to 0$ is convergent. The limit $P \to 0$ is more interesting. In this limit the argument $r \equiv (s - Q^z t)/P^z$ of u varies extremely rapidly with t. Since u is integrable, $u(r)$ acts like a δ function and the essential contribution to the t integration comes from the region $t \approx s$. The contribution to (4.10) from the region $P < \delta \ll 1$ is then

$$\begin{aligned} I_\delta(s) &= \int_{P<\delta} \int_t b(\hat{\mathbf{k}},\mathbf{Q}) P^{-\Delta} u\left[\frac{s-Q^z t}{P^z}\right] g(t) \\ &\approx g(s) u_\infty \int_{P<\delta} b(\hat{\mathbf{k}},\mathbf{Q}) P^{z-\Delta} , \end{aligned} \tag{4.12}$$

where $u_\infty = \int_t u(t)$. From (3.21) and (3.22) it is easy to demonstrate the following asymptotic behaviors for a and b:

$$b(\hat{\mathbf{k}},\mathbf{Q}) = \begin{cases} 1 - (\hat{\mathbf{k}}\cdot\hat{\mathbf{P}})^2 + O(\hat{\mathbf{k}}\cdot\mathbf{P}, P^2), & P \to 0 \\ O(Q), & Q \to 0 \end{cases} \tag{4.13}$$

$$a(\hat{\mathbf{k}},\mathbf{Q}) = \begin{cases} \frac{1}{2}[1 - (\hat{\mathbf{k}}\cdot\hat{\mathbf{P}})^2 + O(\hat{\mathbf{k}}\cdot\mathbf{P}, P^2)], & P \to 0 \\ \frac{1}{2}[1 - (\hat{\mathbf{k}}\cdot\hat{\mathbf{Q}})^2 + O(\hat{\mathbf{k}}\cdot\mathbf{Q}, Q^2)], & Q \to 0 , \end{cases} \tag{4.14}$$

where $\hat{\mathbf{P}} = \mathbf{P}/P$. Thus

$$I_\delta(s) \approx u_\infty \frac{d-1}{d} K_d \frac{\delta^{d+z-\Delta}}{d+z-\Delta} g(s) , \tag{4.15}$$

where $K_d = 2/(4\pi)^{(1/2)d}\Gamma(\frac{1}{2}d)$ is $(2\pi)^{-d}$ times the area of the unit sphere in d dimensions. This result is finite so long as $d + z - \Delta > 0$. From (1.17) this requires $2 - 2y/3 > 0$, i.e.,

$$y < 3 . \tag{4.16}$$

For $y \geq 3$ the assumptions underlying the derivation of (4.10) and (4.11) are violated and, as we shall see below, the renormalization group results (1.18) are no longer valid. An identical analysis of (4.11) yields the same kind of divergence at both $Q = 0$ and $P = 0$. These sum to yield (4.15) with $u(s)$ replacing $g(s)$ on the right-hand side. The identical convergence condition (4.16) therefore results.

B. Scaling for $y \geq 3$

For $y \geq 3$ we must regularize the small-k behavior of the response and correlation functions. We do this by regularizing the driving spectrum at small k. Thus, instead of the purely power-law form, consider

$$\begin{aligned} D(k) &= D_0 \eta(k/m_0) k^{4-d-y} , \\ \eta(x) &\to \begin{cases} 1, & x \to \infty \\ 0, & x \to 0 , \end{cases} \end{aligned} \tag{4.17}$$

where m_0 is an infrared cutoff and $\eta(x)$ must vanish sufficiently rapidly with x to ensure convergence of certain integrals (see below). The amplitude D_0, in general, depends on m_0. Correspondingly, we seek scaling solutions to the DIA equations in the form

$$\hat{G}(\mathbf{k},\omega) = \frac{A_1}{k^z} g\left[\frac{\omega}{\tilde{\nu} k^z}; \frac{k}{m_0}\right] , \tag{4.18}$$

$$\hat{U}(\mathbf{k},\omega) = \frac{A_2}{k^\Delta} u\left[\frac{\omega}{\tilde{\nu} k^z}; \frac{k}{m_0}\right] . \tag{4.19}$$

The amplitudes A_1, A_2, and $\tilde{\nu}$ may also depend on m_0. We assume that

$$g(s;x) \to g(s), \quad u(s;x) \to u(s), \quad x \to \infty , \tag{4.20}$$

while for $x \to 0$ both vanish (see below). Substituting (4.17)–(4.20) into the DIA equations (with $\nu_0 \equiv 0$ still) we obtain

$$\frac{1}{A_1 \tilde{\nu} g(s;x)} = -is + A_1 A_2 k^{d+2-\Delta-z} J_b(s;x) , \tag{4.21}$$

$$\begin{aligned} \frac{A_2 u(s;x)}{\tilde{\nu} |A_1|^2 g(s;x)|^2} &= \frac{D_0}{\tilde{\nu}} \eta(x) k^{\Delta-2z+4-d-y} + A_2^2 k^{d+2-\Delta-z} J_a(s;x) , \end{aligned} \tag{4.22}$$

where

$$J_b(s;x) \equiv \int_Q \int_t b(\hat{\mathbf{k}},\mathbf{Q}) P^{-\Delta} u\left[\frac{s-Q^z t}{P^z}; Px\right] g(t;Qx) , \tag{4.23}$$

$$J_a(s;x)\equiv\int_{\mathbf{Q}}\int_t a(\hat{\mathbf{k}},\mathbf{Q})P^{-\Delta}Q^{z-\Delta}\times u\left[\frac{s-Q^z t}{P^z};Px\right]u(t;Qx)\ . \tag{4.24}$$

Consider now the large-x limit (at fixed s) of both sides of (4.21) and (4.22). This limit is trivial to take except in the regions of integration where either Px or Qx is small. For $y>3$ these regions give rise to the divergent contributions to J_a and J_b when $x\to\infty$. Let us write

$$\begin{aligned}J_b(s;x)&=g(s;x)J_{\text{sing}}(x)+\Delta J_b(s;x)\ ,\\ J_a(s;x)&=u(s;x)J_{\text{sing}}(x)+\Delta J_a(s;x)\ ,\end{aligned} \tag{4.25}$$

where

$$J_{\text{sing}}(x)=\int_{\mathbf{P}}\int_t[1-(\hat{\mathbf{k}}\cdot\hat{\mathbf{P}})^2]P^{-\Delta}u\left[\frac{t}{P^z};Px\right]\ . \tag{4.26}$$

Equation (4.26) is obtained from $J_b(s;x)$ by setting $P=0$ in all nonsingular terms and from $J_a(s;x)$ by summing the two identical contributions obtained by setting, respectively, $P=0$ and $Q=0$ in all nonsingular terms. It should be recalled that the neighborhood of $Q=0$ in $J_b(s;x)$ is nonsingular because b vanishes there [see (4.13)]. Defining

$$u_0=K_d\frac{d-1}{d}\int_{-\infty}^{\infty}\frac{dt}{2\pi}\int_0^{\infty}dw\,w^{d-1+z-\Delta}u(t;w) \tag{4.27}$$

we have

$$J_{\text{sing}}(x)=u_0x^{\Delta-z-d}\ . \tag{4.28}$$

The regularizations (4.17)–(4.19) are now assumed to ensure convergence of (4.27) in the neighborhood of $w=0$. Convergence when $w\to\infty$ is ensured since $u(t;w)\approx u(t)$ is independent of w in this region and because $\Delta-z>d$ for $y>3$. Note that the equal time, equal point correlation function is given by

$$U(\mathbf{x}=\mathbf{0},t=0)=A_2\tilde{\nu}\frac{d}{d-1}m_0^{d+z-\Delta}u_0\equiv\frac{d}{d-1}v_0^2\ , \tag{4.29}$$

so that u_0 and $J_{\text{sing}}(x)$ are rescaled measures of the total kinetic energy density $\varepsilon_0=(d/2)\rho_0v_0^2$, which diverges as $m_0\to0$. The divergences therefore occur because most of the energy lies near the driving range $k\sim m_0$, not in the inertial range $k\gg m_0$. Note that for $\zeta<1$ ($y<3$) the kinetic energy density diverges in the ultraviolet. A finite viscosity is required for convergence. Interestingly enough, no divergences in the DIA equations result: the large energy in the small scales does not feed back significantly on the larger scales.

Having extracted the leading behavior of J_a and J_b, it is now easy to see that ΔJ_a and ΔJ_b are finite when $x\to\infty$ as long as $d<\Delta-z<d+2$. In this limit we obtain

$$\lim_{x\to\infty}\Delta J_b(s;x)\equiv\Delta J_b(s)=\int_{\mathbf{Q}}\int_t u\left[\frac{s-Q^z t}{P^z}\right]P^{-\Delta}\{b(\hat{\mathbf{k}},\mathbf{Q})g(t)-[1-(\hat{\mathbf{k}}\cdot\hat{\mathbf{P}})^2]g(s)\}\ , \tag{4.30}$$

$$\lim_{x\to\infty}\Delta J_a(s;x)\equiv\Delta J_a(s)=\int_{\mathbf{Q}}\int_t\left[a(\hat{\mathbf{k}},\mathbf{Q})u\left[\frac{s-Q^z t}{P^z}\right]P^{-\Delta}Q^{z-\Delta}u(t)-\tfrac{1}{2}[1-(\hat{\mathbf{k}}\cdot\hat{\mathbf{Q}})^2]Q^{z-\Delta}u(s)u(t)-\tfrac{1}{2}[1-(\hat{\mathbf{k}}\cdot\hat{\mathbf{P}})^2]P^{z-\Delta}u(s)u(t)\right]\ . \tag{4.31}$$

The DIA equations now read

$$\frac{1}{A_1\tilde{\nu}g(s;x)}=-is+\lambda_0A_1A_2m_0^{d+2-\Delta-z}x^{d+2-\Delta-z}\times[g(s;x)u_0x^{\Delta-z-d}+\Delta J_b(s;x)] \tag{4.32}$$

$$\begin{aligned}\frac{A_2u(s;x)}{\tilde{\nu}|A_1|^2|g(s;x)|^2}&=\frac{D_0}{\tilde{\nu}}m_0^{\Delta-2z}x^{\Delta-2z+4-d-y}\eta(x)\\&\quad+\lambda_0A_2^2m_0^{d+2-\Delta-z}x^{d+2-\Delta-z}\times[u(s;x)u_0x^{\Delta-z-d}+\Delta J_a(s;x)]\ .\end{aligned} \tag{4.33}$$

We may now consider the large-x limit. The behavior on the right-hand sides of (4.32) and (4.33) is dominated by the singular parts and to leading order we have

$$\frac{1}{A_1\tilde{\nu}g(s)}=-is+\lambda_0^2A_1A_2m_0^{d+2-\Delta-z}x^{2-2z}u_0g(s)\ , \tag{4.34}$$

$$\frac{A_2u(s)}{\tilde{\nu}|A_1|^2|g(s)|^2}=\frac{D_0}{\tilde{\nu}}m_0^{\Delta-2z}x^{\Delta-2z+4-d-y}\eta(x)+\lambda_0^2A_2^2m_0^{d+2-\Delta-z}x^{2-2z}u_0u(s)\ . \tag{4.35}$$

For consistency, the amplitudes and exponents must be chosen in such a way that all m_0 and x dependence drops out. From (4.34) this implies, immediately,

$$z=1 \ . \tag{4.36}$$

Taking $A_1\tilde{\nu}=1$ (A_1 is therefore real) and $\lambda_0^2 u_0 A_1 A_2 m_0^{d+2-\Delta-z}=1$, along with (4.29) this leads to the simple relations

$$\frac{1}{g(s)}=-is+g(s), \quad \tilde{\nu}=\frac{1}{A_1}=\lambda_0 v_0 \tag{4.37}$$

with the solution

$$g(s)=i\left[\frac{s}{2}-\left[\frac{s^2}{4}-1\right]^{1/2}\right], \tag{4.38}$$

where the negative square root is chosen so that $g(s)\approx -1/is$ for large s and has positive real part $\sqrt{1-s^2/4}$ for $|s|\le 2$ [13]. We have therefore solved exactly for the response function in the inertial range. Amazingly, it is completely independent of d and y as long as $y>3$, a reflection of the dominating effects of the large-scale flows.

Consider next Eq. (4.35), which now reads

$$u(s)\left[\frac{1}{|g(s)|^2}-1\right]=\tilde{\delta}_0 x^{\Delta+2-d-y}, \tag{4.39}$$

where $\tilde{\delta}_0=A_1 D_0 m_0^{\Delta-2z}/A_2\tilde{\nu}$ is a rescaled driving amplitude. If the left- and right-hand sides of this equation were of the same order, we would conclude that $\Delta=d-2+y$. Normalizing, say, $\tilde{\delta}_0=1$, this yields $u(s)=1/[|g(s)|^{-2}-1]$. However, from (4.38), $|g(s)|^2=1$ for $|s|\le 2$, which would imply that $u(s)\equiv\infty$ in this same range. This is clearly inconsistent with our convergence assumptions. We therefore must conclude that $\Delta+2-d-y<0$, the driving term is a lower-order correction, and

$$u(s)\left[\frac{1}{|g(s)|^2}-1\right]=0 \ . \tag{4.40}$$

From this we can conclude only that $u(s)=0$ whenever $|g(s)|^2\neq 1$, i.e., when $|s|\ge 2$. This scaling function therefore has support only on the finite interval $-2\le s\le 2$, but its behavior on this interval is as yet undetermined.

To proceed further, we must consider finite-x corrections to (4.34) and (4.35). To see the nature of these corrections we use the identifications we have made so far [for clarity of exposition here and below we will continue to write z explicitly; (4.36) will be substituted only at the end] to write (4.32) and (4.33) in the form

$$\frac{1}{g(s;x)}=-is+g(s;x)+x^{d+2-\Delta-z}\frac{1}{u_0}\Delta J_b(s;x) \ , \tag{4.41}$$

$$\frac{u(s;x)}{|g(s;x)|^2}=\tilde{\delta}_0 x^{\Delta-2z+4-d-y}\eta(x)+u(s;x)+x^{d+2-\Delta-z}\frac{1}{u_0}\Delta J_a(s;x) \ . \tag{4.42}$$

Since $d+2-\Delta-z<0$ we now treat the ΔJ_a and ΔJ_b terms as perturbations for large x. It is clear that we should seek solutions in the form

$$g(s;x)=g(s)+x^{d+2-\Delta-z}g_1(s)+\cdots \ ,$$
$$u(s;x)=u(s)+x^{d+2-\Delta-z}u_1(s)+\cdots \ . \tag{4.43}$$

Substituting (4.43) into (4.41) and (4.42) and using (4.37) and (4.40), we obtain

$$g_1(s)=-\frac{\frac{1}{u_0}\Delta J_b(s)}{\left[1+\frac{1}{g(s)^2}\right]} \tag{4.44}$$

and

$$-\frac{2u(s)}{|g(s)|^2}\mathrm{Re}\left[\frac{g_1(s)}{g(s)}\right]=\tilde{\delta}_0 x^{\theta}+u_1(s)\left[1-\frac{1}{|g(s)|^2}\right]+\frac{1}{u_0}\Delta J_a(s) \ , \tag{4.45}$$

where $\Delta J_b(s)$ and $\Delta J_a(s)$ were defined in (4.30) and (4.31) and the value of the exponent $\theta=2\Delta-z+2-2d-y$ will be addressed below. This last equation gives different results depending on whether $|s|<2$ or $|s|>2$:

$$-u(s)\mathrm{Re}\left[\frac{g_1(s)}{g(s)}\right]=\tilde{\delta}_0 x^{\theta}+\frac{1}{u_0}\Delta J_a(s), \quad |s|<2 \tag{4.46}$$

$$u_1(s)=\frac{\tilde{\delta}_0 x^{\theta}+\frac{1}{u_0}\Delta J_a(s)}{\left[\frac{1}{|g(s)|^2}-1\right]}, \quad |s|>2 \ . \tag{4.47}$$

The behavior of $u_1(s)$ for $|s|<2$ can be inferred only by considering yet higher-order terms in (4.41)–(4.43), but this is of no interest to us. What is important is that (4.46) yields an equation for $u(s)$. Now, if the driving still controls the scaling (though it is now a lower-order effect than it was for $y<3$), we must choose $\theta=0$, i.e., $\Delta=d+\frac{1}{2}(y-1)$, which yields precisely (1.24). We expect this to be the correct choice for y not too large (see below). However, for sufficiently large y we anticipate that the scaling properties will cease to be sensitive to the driving spectrum. In this case we will have $\theta<0$ and (4.46) should be solved with $\tilde{\delta}_0\equiv 0$. We will discuss this point in detail below. Let us then take $\theta=0$ and leave the value of $\tilde{\delta}_0$ free. We now combine (4.38), (4.44), and (4.46) into a single integral equation for the unknown function $u(s)$,

$$\delta_0=-\frac{u(s)}{[1-(s^2/4)]^{1/2}}\mathrm{Re}[\Delta J_b(s)]-\Delta J_a(s) \ , \tag{4.48}$$

where $\delta_0=u_0\tilde{\delta}_0=D_0 u_0 A_1 m_0^{\Delta-2z}/A_2\tilde{\nu}$. More explicitly,

$$\delta_0=\int_Q\int_{-2}^{2}\frac{dt}{2\pi}b(\hat{\mathbf{k}},\mathbf{Q})u\left[\frac{s-Q^z t}{P^z}\right]P^{-\Delta}\times\left[u(s)\left[\frac{1-(t^2/4)}{1-(s^2/4)}\right]^{1/2}-Q^{z-\Delta}u(t)\right], \tag{4.49}$$

where we have made use of the fact that

$$\frac{u(s)}{[1-(s^2/4)]^{1/2}}\mathrm{Re}[g(s)J_{\mathrm{sing}}(x)]-u(s)J_{\mathrm{sing}}(x)=0\ , \tag{4.50}$$

so that ΔJ_b and ΔJ_a may effectively be replaced by their unsubtracted counterparts in (4.48). We have also used the relation (3.24) and the invariance of the product $u(t)u[(s-Q^z t)/P^z]P^{-\Delta}Q^{z-\Delta}$ under the change of variable $\mathbf{Q}'=\mathbf{P}$ and $t'=(s-Q^z t)/P^z$. Convergence of (4.49) when $P\to 0$ (hence $Q\to 1$) is clear because in this limit only $t\approx s$ contributes and the term in large square brackets then vanishes. Convergence when $Q\to 0$ is once again ensured because $b(\hat{\mathbf{k}},\mathbf{Q})$ vanishes in this limit [see (4.13) and (4.14)].

Equation (4.49) is the main result of this section. Its solution completely determines the inertial range behavior in the spherical limit. This equation, in general, has no obvious analytic solution and therefore must be solved numerically. The numerics in this case, however, are quite tractable since the problem has now been reduced to a single equation for a single function of a single variable on a finite interval. Nominally, the Q integration is over an unbounded domain. However, the variable $r-(s-Q^z t)/P^z$ is restricted to $|r|\le 2$ and an appropriate change of variables may be effected to reduce the full integration in (4.49) to a triple integral over a finite three-dimensional box (the three integration variables represent t,Q, and the angular variable $\mu\equiv\hat{\mathbf{k}}\cdot\hat{\mathbf{Q}}$). This, along with details of the numerical procedure, is outlined in Appendix E. Below we present only the results.

C. The onset of turbulence

1. Short-ranged driving

Before describing details of the numerical solutions, we make some general observations regarding the nature of the solutions to (4.49). First, this equation was derived with the assumption of power-law driving. Our ultimate interest, of course, is in real turbulence generated by short-range driving. We claim that equation (4.49) with $\delta_0\equiv 0$ is appropriate to this situation. To see this, note that if we had followed through the derivation of (4.49) using an explicitly short-ranged form for the driving spectrum

$$D(k)=D_0\tilde{\eta}(k/m_0),\quad \tilde{\eta}(x)\to\begin{cases}0, & x\to\infty\\ 1, & x\to 0\end{cases} \tag{4.51}$$

in place of (4.17), the vanishing of $\tilde{\eta}(x)$ at infinity being, at the very least, more rapid than any power law, we would have obtained Eqs. (4.42) and (4.45)–(4.47) with $\tilde{\delta}_0\equiv 0$. Correspondingly, the variable y never appears, the question of the value of the exponent θ never arises, and the exponent Δ is undetermined. Finally, we would have obtained, as claimed above, (4.48) and (4.49) with $\delta_0=0$. The free exponent Δ would then have had to be *tuned* in order to find the solution $u_c(s)$. This solution clearly must represent the Kolmogorov spectrum for the model. A value y_c may be assigned *a postiori* using (1.24) as a definition. Physically, we expect this solution to be unique, given the constraints that $\zeta>1$ and $u(s)\ge 0$.

Two questions must now be addressed. First, since the value of Δ must be determined before (4.49) with $\delta_0=0$ even has a solution, how do we go about finding this solution? Second, what is the connection, if any, between the *a postiori* inferred exponent y_c and power-law driving?

2. Turbulent solution

To answer the first question, we note that (4.49) with $\delta_0=0$ represents a kind of nonlinear eigenvalue problem, with eigenvalue Δ (or, equivalently, y_c) and eigenfunction $u_c(s)$. To see how to solve such a problem, first consider the following linear matrix inversion problem: $(\mathbf{A}-\lambda\mathbf{I})\mathbf{v}=\mathbf{b}$, where $\mathbf{A}$ is a linear operator, $\mathbf{I}$ is the identity operator, λ is a given real number, $\mathbf{b}$ is a given constant vector, and the vector $\mathbf{v}$ is to be found. If λ is not an eigenvalue of $\mathbf{A}$ then $(\mathbf{A}-\lambda\mathbf{I})$ is invertible and the solution $\mathbf{v}$ always exists. If $\mathbf{b}=\mathbf{0}$ then we have the usual eigenvalue problem and a nonzero solution $\mathbf{v}_c$ exists only if $\lambda=\lambda_c$ is an eigenvalue of $\mathbf{A}$. One way of locating eigenvalues is to fix $\mathbf{b}$ and consider the solution $\mathbf{v}(\lambda)$ as a function of λ. For generic choices of $\mathbf{b}$ [i.e., as long as $\mathbf{b}$ does not lie in the range of $(\mathbf{A}-\lambda_c\mathbf{I})$] this solution will *diverge* as $\lambda\to\lambda_c$. Thus λ_c is a pole of the norm $\|\mathbf{v}(\lambda)\|$ or, equivalently, a zero of $\|\mathbf{v}(\lambda)\|^{-1}$ and $\mathbf{n}(\lambda)\equiv\mathbf{v}(\lambda)/\|\mathbf{v}(\lambda)\|$ will converge to the corresponding normalized eigenvector.

This technique generalizes straightforwardly to the present problem. If $\delta_0=0$ on the left-hand side of (4.49) is replaced by some conveniently chosen fixed function $\delta(s)$, then a solution $u(s|y)$ will exist for generic values of y [and associated values of $\Delta=d+\frac{1}{2}(y-1)$ and $z=1$] and will diverge as $y\to y_c$ and $u_c(s)=\lim_{y\to y_c}u(s|y)/u(0|y)$, normalized so that $u_c(0)=1$, is the scaling function we seek. We will simply take $\delta(s)\equiv\delta_0$ to be a constant, i.e., precisely Eq. (4.49). In terms of finding the turbulent solution, this represents a convenient numerical device. The fact that $u(s|y)$ is then also the physical solution in the presence of power-law driving will allow us to make contact between the two problems.

3. Relation to power-law driving: Stability of the turbulent solution

To answer the second question, we shall now show that y_c is precisely the borderline at which power-law driving becomes irrelevant and that for $y>y_c$ all exponents and scaling functions "stick" at their turbulent values. As we

have seen, if we were to normalize $\delta_0=1$, a signal of the approach to y_c would be a pointwise divergence in the solution $u(s|y)\sim(y_c-y)^{-\phi}$ for some exponent ϕ (we shall see below that $\phi=\frac{1}{2}$). This signals the inappropriateness of the chosen normalization and represents the onset of a kind of nonlinear resonance: one is nearing a "natural spectrum" of the system, in essence, one that is produced without any driving at all. A better normalization, therefore, is $u(s=0|y)\equiv 1$, which may then be used to determine $\delta_0(y)$. One should clearly find $\delta_0(y)\sim(y_c-y)^{2\phi}$, vanishing at y_c. In fact, since we will find $2\phi=1$, solutions to (4.49) will exist for $y>y_c$ with $\delta_0<0$. However, the driving spectrum is, by construction, non-negative, such solutions must be unphysical, and the validity of (4.49) should be reexamined in this range of parameters. We claim, in fact, that for $y>y_c$, Δ sticks at $\Delta_c\equiv\Delta(y_c)$ and the exponent θ in (4.45) becomes *negative*. This implies that the driving term has become *irrelevant* and provides only asymptotically vanishing corrections to scaling in the inertial range.

To see how this comes about, we must consider the *stability* of the $y=y_c$, $\delta_0=0$ solution under the influence of power-law driving. Returning to (4.41)–(4.43) we begin by setting $y=y_c$, $\Delta=\Delta_c$, and $\delta_0=0$. Let $g_{1,c}(s)$, $u_c(s)$, and $u_{1,c}(s)$ be the exact solutions for this case [recall that $g(s)$ is always given by (4.38)]. Now treat the term $\tilde{\delta}_0 x^{\Delta_c-2z+4-d-y}$ as a perturbation. We seek, then, solutions in the more general scaling form

$$u_c=u_c(s;\delta_0 x^{\sigma}),\quad u_c(s;0)\equiv u_c(s)\ , \tag{4.52}$$

with similar forms for $g_{1,c}$ and $u_{1,c}$ [formally, to make the expansion (4.43) well defined, we consider the combination variable $w=\delta_0 x^{\sigma}$ to be arbitrary and finite even as $x\to\infty$]. The crossover exponent σ must be determined from the equations (see below). If $\sigma>0$, then $\tilde{\delta}_0$ is *relevant* and the second argument grows without bound for large x. This signals a crossover to the power-law-driven solution proportional to $x^{\Delta_c-\Delta}u(s|y)$. However, if $\sigma<0$, then $\tilde{\delta}_0$ is irrelevant and $u_c(s)$ is recovered for large x, with small corrections,

$$u_c(s;\delta_0 x^{\sigma})=u_c(s)+\delta_0 x^{\sigma}u_c^{(1)}(s)+\cdots\ . \tag{4.53}$$

Substituting the form (4.52) into (4.41)–(4.43), it is straightforward to see that (4.49) generalizes to

$$\delta_0 x^{y_c-y}=\int_Q\int_{-2}^{2}\frac{dt}{2\pi}b(\hat{\mathbf{k}},\mathbf{Q})u\left[\frac{s-Q^{z_c}t}{P^{z_c}};wP^{\sigma}\right]P^{-\Delta_c}\times\left[u(s;w)\left[\frac{1-(t^2/4)}{1-(s^2/4)}\right]^{1/2}-Q^{z_c-\Delta_c}u(t;wQ^{\sigma})\right]\ , \tag{4.54}$$

where it is now clear that consistency requires $w=\delta_0 x^{y_c-y}$ and hence $\sigma=y_c-y$. We see then that δ_0 is relevant for $y<y_c$, irrelevant for $y<y_c$, and we have finally confirmed claim (b). Moreover, we now have a prediction for the form of the corrections. For example, (4.54) leads to $E(k)\approx Ak^{-\zeta_c}[1+\delta_0 a(y)(k/m_0)^{-(y-y_c)}+\cdots]$, where $a(y)=\int_s u_c^{(1)}(s)$ and $\zeta_c\equiv\zeta(y_c)$. The correction exponent $\zeta_c+(y-y_c)$ is *different* from $\zeta(y)=\Delta(y)-z-d+1=\zeta+\Delta(y)-\Delta(y_c)=\zeta_c+\frac{1}{2}(y-y_c)$, obtained by naively extrapolating the $y>3$ results through y_c. The result is therefore not simply a linear superposition of ζ_c and $\zeta(y)$.

D. Numerical results

Now that we understand the general features exhibited by the scaling solutions, let us turn to the numerical verification of these results. In Fig. 11 we show the solutions to (4.49) in $d=3$ for various values of y in the range $3.1\le y\le 4.3$, with the normalization $u(0)=1$. In Fig. 12 we show the corresponding values of $\delta_0(y)$ (still in $d=3$) that lie on a smooth curve passing through zero at a point indistinguishable from $y_c=4$. This last result turns out to be insensitive to the dimension d. In Fig. 13 we show the dimensionality dependence of $u_c(s)$ for various d in the interval $2.5\le d\le 3.3$. It seems reasonable, then, to postulate that [see (1.24)]

$$y_c=4,\quad \Delta=d+\tfrac{3}{2},\quad \zeta=\tfrac{3}{2}\ \text{(for all } d>2) \tag{4.55}$$

are exact answers in the spherical limit. We do not, at this stage, have an analytic proof of this fact, but in Secs. IV E and IV F below we will provide strong physical and analytic motivation for this result.

It is clear from Fig. 11 that the solutions vary smoothly with y: $u(s)$ converges uniformly to $u_c(s)$ as $y\to y_c$. Since there are no singularities in the integration in (4.49) for any y in the neighborhood of y_c, it is then clear

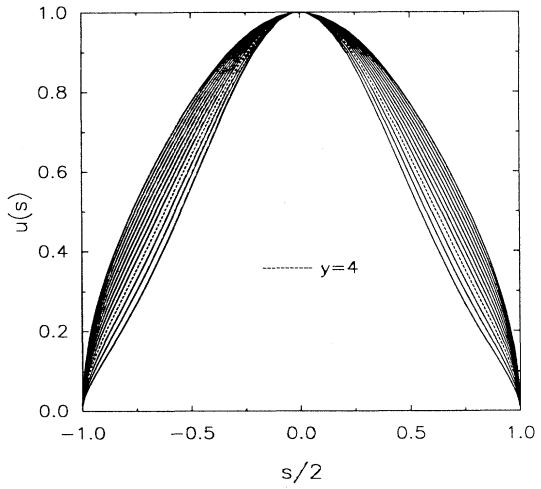

FIG. 11. Numerical results for the spherical limit scaling function $u(s)$ in three dimensions, normalized so that $u(0)=1$, for various values of the driving exponent y. The outermost curve corresponds to $y=3.1$, the innermost to $y=4.3$, and y changes in steps of 0.1 in between. The dashed curve to the critical value $y=4$.

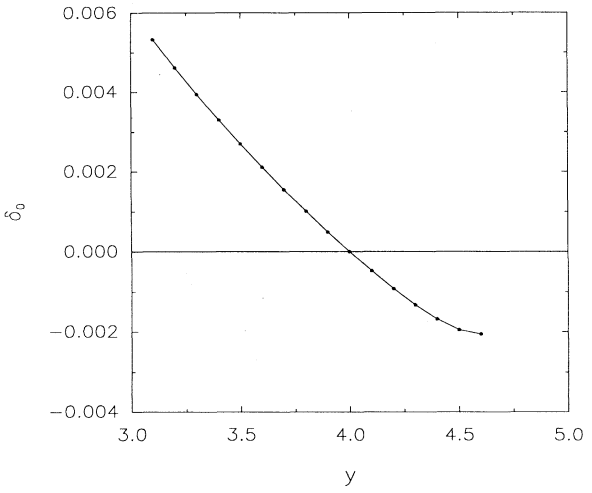

FIG. 12. Normalized driving amplitude δ_0 as a function of driving exponent y in three dimensions. The amplitude vanishes at a point y_c numerically indistinguishable from $y_c=4$.

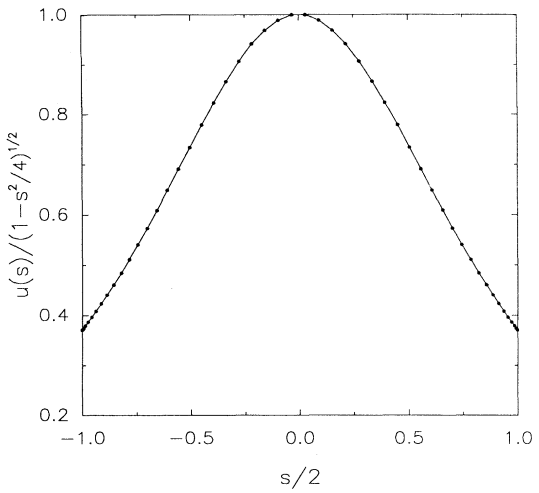

FIG. 14. Turbulent scaling function in three dimensions, with $\sqrt{1-s^2/4}$ divided out. The resulting function is *not* a constant, but is clearly regular at the boundaries $s=\pm 2$.

that $\delta_0(y)$ should vary smoothly and analytically through y_c. Presumably one could establish this fact rigorously if one wished. These observations confirm the exponent value $\phi=\frac{1}{2}$ for the divergence of $u(s|y)$ at fixed $\delta_0=1$.

We note that $u(s)$ always vanishes with a square root singularity at $|s|=2$. In Fig. 14 we plot $u_c(s)/\sqrt{1-s^2/4}$ in $d=3$, showing clearly the finite intercepts at $|s|=2$. This function probably extends analytically through these boundaries. The square root singularity clearly arises from the $\sqrt{1-t^2/4}/\sqrt{1-s^2/4}$ factor in the integrand of (4.49). Kraichnan [13], in his original approximate treatment of the DIA equations, derived a result equivalent to (4.38) and approximated $u_c(s)$ by $\sqrt{1-s^2/4}$. From (4.49) (with $\delta_0=0$) it is clear that this result is correct only if $\Delta=z$ (the quantity in large square brackets then vanishes identically). However, since $z=1$, the requirement $\Delta>d+z$ used in the derivation of (4.49) would then be valid only for $d<0$. It is perfectly straightforward to analytically continue (4.49) to $d<0$ and we have checked numerically that, as expected from (1.24), the Kraichnan solution is indeed correct when $d=-\frac{1}{2}$.

Finally, we note that another exact solution to (4.49) (with $\delta_0=0$) is $u_c(s)=\delta(s)$, with the consistency condition

$$\int_{\mathbf{Q}} b(\hat{\mathbf{k}},\mathbf{Q})P^{z-\Delta}[Q^{-z}-Q^{z-\Delta}]=0 \tag{4.56}$$

(here $z=1$, as usual). This solution is unphysical, as it does not generalize to $\delta_0\neq 0$, and corresponds to a purely *static* ($\omega=0$) inertial range. Amusingly enough, however, it corresponds precisely to the solution of the simplified, frequency-independent model DIA equations discussed in Appendix D. From this Appendix one sees that $\Delta=d+\frac{3}{2}$ solves this equation as well.

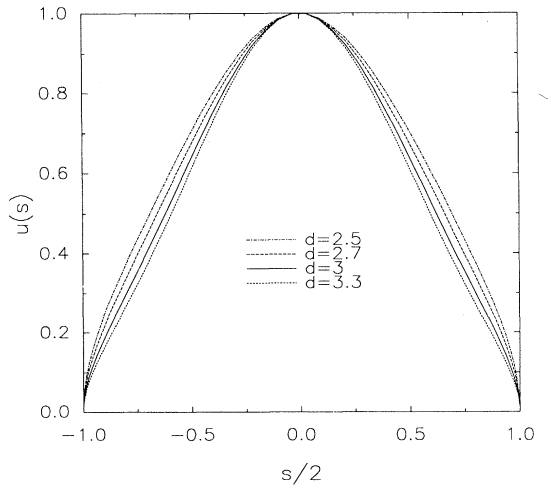

FIG. 13. Dimensionality dependence of the turbulent scaling function $u(s)$ (driving exponent $y=y_c=4$) in the spherical limit.

E. Conformal transformations

In Appendix D we introduce a useful conformal transformation [32], which essentially converts $Q\to 1/Q$, that allows us to solve the simplified DIA equations analytically. The essential requirement is the covariance property $b(\hat{\mathbf{k}},\mathbf{Q})\to Q^{-2}b(\hat{\mathbf{k}},\mathbf{Q})$ under this transformation. Let us perform this same transformation (at fixed t) on the second term in the full equation (4.49) for $u(s)$. One obtains (for $\delta_0=0$)

$$0=\int_Q\int_{-2}^{2}\frac{dt}{2\pi}b(\hat{\mathbf{k}},\mathbf{Q})P^{-\Delta}\times\left[u\left[\frac{s-Q^z t}{P^z}\right]u(s)\left[\frac{1-(t^2/4)}{1-(s^2/4)}\right]^{1/2}-Q^{2d+2-2\Delta+z}u\left[\frac{Q^z s-t}{P^z}\right]u(t)\right]. \quad (4.57)$$

Unfortunately, this is not very useful because the transformation does not leave the argument $r=(s-Q^z t)/P^z$ invariant. *If it had,* one could have immediately concluded that $2d+2-2\Delta+z=0$, i.e.,

$$\Delta=d+1+\frac{z}{2}=d+\frac{3}{2}, \quad (4.58)$$

and $u_c(s)=\sqrt{1-s^2/4}$. We have already seen from our numerics that $u(s)$ is not of this simple form, so it is certainly consistent that r is not invariant. We note, in spite of this, that (4.58) is (indistinguishable from) the correct answer. One can motivate this result a little further. Multiply (4.57) by $\sqrt{1-s^2/4}$ and integrate over s to obtain

$$0=\int_Q\int_{-2}^{2}\frac{ds}{2\pi}\int_{-2}^{2}\frac{dt}{2\pi}b(\hat{\mathbf{k}},\mathbf{Q})P^{-\Delta}\left[u\left[\frac{s-Q^z t}{P^z}\right]u(s)[1-(t^2/4)]^{1/2}-Q^{2d+2-2\Delta+z}u\left[\frac{Q^z s-t}{P^z}\right]u(t)[1-(s^2/4)]^{1/2}\right], \quad (4.59)$$

which, by symmetry under interchange of s and t, vanishes identically for *any* choice of $u(s)$ as long as (4.58) is satisfied. There are presumably solutions to (4.59) for arbitrary values of Δ, so one cannot know, without solving (4.49) fully, that (4.58) is truly the correct choice. The result is nevertheless quite compelling. Equation (4.59) actually has a physical interpretation: it is a statement that energy is conserved in the inertial range cascade process. With (4.58), the physical interpretation becomes even more compelling: the energy cascade proves to be *local.* It was precisely the *assumption* of locality that led Kraichnan [13] to the $\zeta=\frac{3}{2}$ result (see Sec. IV F below).

It is precisely this conformal argument that was applied to a *subtracted* version of the DIA equations [obtained from (4.32) and (4.33) simply by *dropping* the singular terms] by Kuznetsov and L'vov [32]. In this case *both* scaling functions are nontrivial and satisfy (with $\delta_0=0$)

$$\frac{1}{g(s)}=-is+\Delta J_b(s), \quad (4.60)$$

$$\frac{u(s)}{|g(s)|^2}=\Delta J_a(s), \quad (4.61)$$

along with $A_1=1/\tilde{\nu}$, $A_2=1/\lambda_0^2 A_1$, and $\Delta+z=d+2$ [compare (1.19)]. These are identical to (4.10) and (4.11), but with the singular parts of the integrals removed and the 1 dropped from (4.11). The analog of (4.57) is now obtained by noting that Eqs. (4.60) and (4.61) may be combined to yield

$$u(s)\mathrm{Re}\Delta J_b(s)=\Delta J_a(s)\mathrm{Re}g(s), \quad (4.62)$$

which gives (4.49) with $\sqrt{1-s^2/4}$ replaced by $\mathrm{Re}g(s)$, exponents obeying (1.19), and $\delta_0=0$. The conformal transformation then yields (4.57) with these same replacements. Multiplying through by $\mathrm{Re}g(s)$ and integrating over s yields the obvious analog of (4.59), which is again symmetric in s and t and vanishes identically if the first equality in (4.58) holds. With (1.19), this yields the Kolmogorov values $z=\frac{2}{3}$ and $\zeta=\frac{5}{3}$. Based on this argument, the authors of [32] concluded that the Kolmogorov results had been established for these equations. These results are probably correct (locality is then, again, implied), but [aside from the fact that we believe (4.60) and (4.61) to be an inappropriate set of equations to begin with] the argument has precisely the same fallacies as before. A proof would require full solutions to (4.60) and (4.61). These would be very difficult to obtain since both $g(s)$ and $u(s)$ are now nontrivial and nonvanishing for all s. We emphasize, then, that the exactness of the Kraichnan DIA result $\zeta=\frac{3}{2}$ has precisely the same degree of analytic backing as does $\zeta=\frac{5}{3}$ for the corresponding subtracted equations. The numerical backing, at this stage, is nonexistent for the latter, while our own numerics confirm the $\frac{3}{2}$ result beyond a reasonable doubt.

F. Locality, sweeping, and universal amplitudes

In this subsection we finally make precise the various notions of energy flux and sweeping alluded to in Sec. I, using the DIA equations as an explicit example. In so doing we will identify various universal amplitudes that generalize, for example, the Kolmogorov constant C_K in (1.8) to the case when $\zeta\neq\frac{5}{3}$. Our solutions to the DIA equations allow us to calculate these constants exactly in the spherical limit. Our analysis follows closely that of Kraichnan [13].

To begin, let us understand energy conservation in more detail. By multiplying $\hat{U}(\mathbf{k},\omega)$ by the real part of (3.17), subtracting from it $\hat{G}'(\mathbf{k},\omega)=\mathrm{Re}\hat{G}(\mathbf{k},\omega)$ multiplied by (3.18), and then integrating over ω, we obtain

$$\nu_0 k^2\varepsilon(\mathbf{k})=\tfrac{1}{2}\int_{\mathbf{q}}S(k|pq)+\int_\omega\hat{G}'(\mathbf{k},\omega)D(\mathbf{k},\omega), \quad (4.63)$$

where $\mathbf{p}=\mathbf{k}-\mathbf{q}$, $\varepsilon(\mathbf{k})=\int_\omega \hat{U}(\mathbf{k},\omega)$ is the Fourier space energy density per isospin component, divided by $\frac{1}{2}(d-1)(2\pi)^{-d}\rho_0$ (this normalization will be used below, unless otherwise specified), and

$$S(k|pq)=2a(\mathbf{k},\mathbf{q})\theta(k,p,q)-b(\mathbf{k},\mathbf{q})\theta(p,k,q) -b(\mathbf{k},\mathbf{p})\theta(q,k,p)\ , \tag{4.64}$$

with

$$\theta(k,p,q)=\lambda_0^2 k^2\int_\omega\int_\Omega \hat{G}'(\mathbf{k},\omega)\hat{U}(\mathbf{p},\omega-\Omega)\hat{U}(\mathbf{q},\Omega)\ . \tag{4.65}$$

The left-hand side of (4.63) is the viscous dissipation rate and the second term on the right-hand side is the energy input rate from the driving force. The function $S(k|pq)$ represents the net input of energy to mode $\mathbf{k}$ via the nonlinear interaction with modes $\mathbf{p}$ and $\mathbf{q}$. Under the assumption that an inertial range with a constant energy flux exists (which will be verified for the DIA equations below), then in this range the dissipation and driving may be neglected [formally, we take $\nu_0=0$ and $\hat{D}(\mathbf{k},\omega)\equiv 0$]. In this case

$$0=\int_{\mathbf{q}} S(k|pq) \tag{4.66}$$

for $\mathbf{k}$ in the inertial range, which represents (4.59) in unscaled form and states that in the stationary turbulent state no net transfer of energy to mode $\mathbf{k}$ occurs [this is really just the Fourier space form of $\nabla\cdot\mathbf{j}_\varepsilon=0$; see (2.32) and below]. Using S we may introduce precisely the notion of energy flux. Let $\Pi(k)$ be the average rate of transfer of energy from modes $\mathbf{p}$ and $\mathbf{q}$, with $p,q<k$ to any mode $\mathbf{k}'=\mathbf{p}+\mathbf{q}$ with $k'>k$, minus the average transfer rate from modes with $p,q>k$ to any mode $\mathbf{k}'=\mathbf{p}+\mathbf{q}$ with $k'<k$. Thus

$$\Pi(k)=\tfrac{1}{2}\int_{\mathbf{k}'}^{(k'>k)}\int_{\mathbf{q}}^{(p,q<k)} S(k'|pq) -\tfrac{1}{2}\int_{\mathbf{k}'}^{(0\le k'<k)}\int_{\mathbf{q}}^{(p,q>k)} S(k'|pq)\ . \tag{4.67}$$

By straightforward manipulations, one can show that

$$-\frac{\partial\Pi(k)}{\partial k}=\frac{1}{2}K_d k^{d-1}\int_{\mathbf{q}} S(k|pq)\ . \tag{4.68}$$

If (4.66) is valid, then in the inertial range $\partial\Pi/\partial k$ vanishes and we then have

$$\Pi(k)=\bar{\varepsilon}\ , \tag{4.69}$$

i.e., a constant energy flux. Let us define the total rate of energy input by the driving force

$$\bar{\varepsilon}_{\text{in}}=\int_{\mathbf{k}}\int_\omega \hat{D}(\mathbf{k},\omega)\hat{G}'(\mathbf{k},\omega) =D_0 m_0^d\int_{\mathbf{x}}\int_s \tilde{\eta}(x)g(s;x)\equiv D_0 g_0 m_0^d\ , \tag{4.70}$$

where g_0 is a nonuniversal constant of order unity and we have assumed the short-ranged form (4.51) for $D(k)$. We may turn the last equality on the right-hand side around to express the driving spectrum in the physically more transparent form $D(k)=(\bar{\varepsilon}_{\text{in}}/g_0 m_0^d)\tilde{\eta}(k/m_0)$, which serves to elucidate how its amplitude must scale with energy input rate and the width m_0. Energy conservation implies that $\bar{\varepsilon}_{\text{in}}$ must also equal the total rate of energy dissipation by the viscosity

$$\bar{\varepsilon}_{\text{in}}=\bar{\varepsilon}_{\text{out}}\equiv\int_{\mathbf{k}}\nu_0 k^2\varepsilon(\mathbf{k})\ . \tag{4.71}$$

This follows from (4.63) by integrating over all $\mathbf{k}$ and noting that (4.64) implies that $\int_{\mathbf{k}}\int_{\mathbf{q}} S(k|pq)=0$. On the other hand, if the driving and dissipation ranges are well separated in k space, one may substitute (4.68) into (4.63) and integrate over the volume of a sphere whose radius k lies in the inertial range. One finds then that $\bar{\varepsilon}_{\text{in}}=\Pi(k)+\bar{\varepsilon}_<(k)$, where $\bar{\varepsilon}_<(k)=\int_{q<k}\nu_0 q^2\varepsilon(\mathbf{q})$ is the total dissipation rate inside this sphere and we have used the fact that $\Pi(0)=0$. If dissipation is negligible in the inertial and driving ranges, then (4.69) is valid and it follows immediately that the energy flux must equal the energy input rate $\bar{\varepsilon}=\bar{\varepsilon}_{\text{in}}$. Conversely, if the energy flux is not constant, any loss of flux must be accompanied by significant dissipation in the inertial range.

In general (i.e., for finite N) $S(k|pq)$ may be defined in terms of the triple velocity correlator [13]

$$S(k|pq)=\text{Im}\sum_{l,m,n} A_N^{lmn}\frac{2\lambda_0}{(d-1)N} \times\int_\omega\int_\Omega\langle\hat{\mathbf{v}}_l(-\mathbf{k},-\omega)\cdot\hat{\mathbf{v}}_n(\mathbf{q},\Omega) \times\mathbf{k}\cdot\hat{\mathbf{v}}_m(\mathbf{p},\omega-\Omega)\rangle\ , \tag{4.72}$$

which cannot, in general, be reduced simply to a product of pair correlators. However, the definition (4.67) and the relation (4.68) remain valid. An inertial range with a constant energy flux would still be characterized by (4.66), with (4.69) following as before. As shown in Appendix B these results are the k-space equivalents of the real-space von Kármán–Howarth result. The fact that we will establish (4.69) explicitly for the DIA equations represents a direct proof of the validity of the von Kármán–Howarth result in the spherical limit.

Even when valid, Eq. (4.69) in no way implies that this flux is truly local: p and q may be very far from k'. The notion of locality in turbulence is broader and is made precise in the following way: consider two wave numbers k and k' with $k\ll k'$. What is the total rate of energy transfer from modes p,q, at least one of which is smaller than k, to any mode $k''>k'$? This is given by

$$\Pi(k|k')=\tfrac{1}{2}\int_{\mathbf{k}''}^{(k''>k')}\int_{\mathbf{q}}^{(p\text{ or }q<k)} S(k''|pq)\ . \tag{4.73}$$

Notice that this is similar to the first term in (4.67), except that, aside from the fact that $k<k'$, one has relaxed the requirement that both p and q are smaller than k. This is important when k/k' is small because if both p and q are small it is impossible to have $|\mathbf{p}+\mathbf{q}|>k'$. Thus if energy is to be transferred a large distance in k space, it can do so only through the interaction of one small wave vector with two large ones. If the cascade is local, $\Pi(k|k')$ will vanish as $k/k'\to 0$ (see below).

We may evaluate (4.67) and (4.72) in the spherical limit. Consider substituting the scaling forms (1.16) and (1.17) into the expression for S. If one scales out k from the integral in (4.66), one naively concludes that it should

vary as $A_2^2\tilde{\nu}s_d k^{d+z+2-2\Delta}$. It is only by examining the remaining dimensionless coefficient s_d that one finds that it vanishes by virtue of (4.59). Similar scaling of (4.67) leads one to expect that it should vary as $A_2^2\tilde{\nu}e_d k^{2d+z+2-2\Delta}$. However, consistency with (4.68) then implies that the coefficient e_d is proportional to s_d and must therefore vanish as well. This seems to contradict (4.69). There are three possible resolutions to this paradox: (a) our notion of an inertial range in the zero viscosity limit is incorrect and there are no solutions in which (4.66) is obeyed, (b) the integral in (4.67) contains infrared divergences and the naive k dependence is replaced by a constant term $e_d \propto m_0^{d+z+2-2\Delta}$, or (c) the exponent relation (4.58) is valid $2d+z+2-2\Delta=0$ and the naive k dependence indeed yields a constant, with

$$e_d=\tfrac{1}{2}\int_{K'}^{(K'>1)}\int_{Q}^{(P,Q<1)} s(K'|PQ) - \tfrac{1}{2}\int_{K'}^{(0\le K'<1)}\int_{Q}^{(P,Q>1)} s(K'|PQ) \tag{4.74}$$

a dimensionless universal number [here $s(K'|PQ)=k^{2\Delta-z-2}S(k'|pq)/A_2^2\tilde{\nu}$, suitably rewritten using the scaling forms (1.16) and (1.17)]. This does not contradict the proportionality of e_d and s_d because in actuality, $s_d \propto (2d+z+2-2\Delta)e_d$, so that e_d need vanish only if the prefactor does not. Cases (a) and (b) violate locality: a strong dependence on the viscosity, as is assumed, for example, in the Kolmogorov-Oboukhov-Yaglom theory [see [2] and the discussion below (1.9)], implies that there is no sharp distinction between the inertial and dissipation ranges. Similarly, an infrared divergence implies that the driving range strongly perturbs the inertial range cascade process. Note that the fact that $A_2^2\tilde{\nu}$ depends upon m_0 is a separate issue; this latter coefficient is a property only of the two-point correlation functions and sets the overall amplitude of the energy flux (see below), while e_d is a property of a three-point correlation function and characterizes the interactions between different length scales. Only case (c) yields locality: thus, as alluded to earlier, scaling is consistent with locality only if $\zeta=\frac{3}{2}$. Our numerics overwhelmingly support the exponent relation (4.58) and hence case (c). The compelling nature of the physics of case (c) is, more than anything else, what leads us to believe that $\zeta=\frac{3}{2}$ must be an exact result.

Since our results are consistent with locality, we may numerically evaluate e_d in the spherical limit. We find

$$\bar{\epsilon}=e_d A_2^2\tilde{\nu}, \quad e_{d=3}\simeq\frac{3.86}{(2\pi)^6}\simeq 6.28\times 10^{-5}\ . \tag{4.75}$$

Similarly, we may study $\Pi(k|k')$. After some rather tedious algebra we find [13]

$$\Pi(k|k')\approx p_d A_2^2\tilde{\nu}(k/k')^{3-\zeta}\ , \qquad p_{d=3}\simeq\frac{13.9}{(2\pi)^6}\simeq 2.26\times 10^{-4}\ , \tag{4.76}$$

which indeed vanishes as $k/k'\to 0$. The universal number p_d is given by the expression

$$p_d=\frac{1}{2^{d+3}\pi^2}\frac{d-1}{(\Delta-d)(3-\zeta)}\frac{1}{\Gamma(\frac{1}{2}d)\Gamma(\frac{1}{2}d+2)} \times\int_{-2}^{2}u(s)ds \times\int_{-2}^{2}\frac{(\Delta-1)(4-\Delta)s^2+4(\Delta-1)(\Delta-2)}{\sqrt{4-s^2}} \times u(s)ds\ . \tag{4.77}$$

Pulling out the six factors of 2π that appear in the definitions of the integrals in (4.67) and (4.73) gives a better gauge of the magnitude of the universal coefficients. We conclude, then, that most of the energy flux in (4.67) comes from modes not too far from k. Since (4.76) is only power law, this notion of locality is not particularly sharp.

Now, the fact that the energy spectrum depends on the infrared cutoff m_0 means that the energy containing range $k\sim m_0$ has a strong effect on the inertial range $k\gg m_0$. Why does this not contradict locality? As hinted above, the answer is that though the energy transfer is local, the total rate, or overall magnitude, can be suppressed or enhanced by the large-scale motions (presumably through large scale shear, vortex stretching, etc.). Thus locality implies a well-defined Fourier space "pipeline" of energy, but the large-scale motions may control the overall diameter of the pipe. This can be seen explicitly in the derivation of (4.73): the infrared divergences at small p and q cancel in S, so the energy transfer rate from this region is negligible, even though the energy content is large.

G. Universal scaling

Let us now try to put together what we have learned from our analysis of the solutions to the DIA equations in a way that might plausibly generalize to finite N [33]. Recall from Sec. I that, in the Kolmogorov theory, the coefficient C_K in (1.8) is meant to be universal. An important question is whether a similar universal amplitude can be exhibited if $\zeta\neq\frac{5}{3}$. It should be emphasized that writing the energy in the general form (1.9) is not sufficient to make the coefficient C_K' universal. The problem is that m_0 is only one somewhat arbitrarily chosen measure of the shape of the driving spectrum and a different choice will clearly change the value of C_K'. In order to obtain a universal amplitude, it is necessary to uniquely specify the appropriate physical length l_p that should be used to universally nondimensionalize k. This length will be determined in the DIA below. All other lengths, such as $l_0=1/m_0$, will scale linearly with l_p, but with a nonuniversal coefficient that depends on the details of the driving spectrum. Note that, in principle, the same considerations apply to the coefficient $\bar{\epsilon}^{2/3}$ in the original Kolmogorov result (1.8). One could equally well have chosen, for example, the energy input rate $\bar{\epsilon}_{\rm in}$ or the dissipation rate $\bar{\epsilon}_{\rm out}$ in place of the flux $\bar{\epsilon}$ here. It is only energy conservation that dictates that all measures of the energy transfer must be the same. No such conservation law uniquely specifies l_p. Given $\bar{\epsilon}$, we may equivalently define physical velocity scale v_p related to l_p via

$$\bar{\epsilon}=\frac{\lambda_0^3 v_p^3}{l_p} . \tag{4.78}$$

The quantity v_p will be linearly, but again nonuniversally, related to any chosen typical large-scale velocity, say, v_0, analogous to the typical large-scale length l_0. Given v_p and l_p we propose to rewrite the scaling relations (1.16) and (1.17) in the form

$$\hat{U}(\mathbf{k},\omega)=\frac{\lambda_0 v_p l_p^{d+1}}{(kl_p)^{\Delta}} u\left[\frac{\omega}{\omega_p (kl_p)^z}\right] , \tag{4.79}$$

$$\hat{G}(\mathbf{k},\omega)=\frac{1}{\omega_p (kl_p)^z} g\left[\frac{\omega}{\omega_p (kl_p)^z}\right] , \tag{4.80}$$

where the physical frequency is defined in the obvious way by $\omega_p=\lambda_0 v_p/l_p$. The function $g(s_p)\approx -1/is_p$ for large s_p and we remove any residual ambiguity by normalizing $u(0)=1$. We distinguish the scaling variable $s_p\equiv\omega/\omega_p(kl_0)^z$ from the variable s used earlier in this section since they may differ by a scale factor (see below). Comparing with (1.16) and (1.17), we therefore have $A_2=\lambda_0 v_p l_p^{d+1-\Delta}$ and $1/A_1=\tilde{\nu}=\lambda_0 v_p l_p^{z-1}$. These forms are now proposed to be completely universal. Operationally this means that given any set of inertial range numerical or experimental data, we may extract from it the two nonuniversal quantities l_p and v_p [through, say, a measurement of $\bar{\epsilon}$ and of $\hat{U}(\mathbf{k},0)$ at a single reference value of $\mathbf{k}$ in the inertial range] and then use these two quantities to scale the data as specified above. The result will be a single set of universal curves common to *all* data sets. The inertial range is therefore characterized, in general, by *two* nonuniversal parameters, in terms of which all other parameters may be expressed.

An immediate consequence of this is obtained by calculating the energy spectrum (per isospin component) (1.7)

$$E(k)=\rho_0 c_d \bar{\epsilon}^{2/3} l_p^{5/3} (kl_p)^{-\zeta} , \tag{4.81}$$

$$c_d\equiv B_d\int\frac{ds_p}{2\pi}u(s_p) , \tag{4.82}$$

where $\zeta=\Delta-z-d+1$ as before and the coefficient B_d was defined below (1.7). The coefficient c_d is the universal amplitude we seek, appropriately generalizing the Kolmogorov constant.

In the spherical limit we may identify l_p and v_p from the results we have already obtained. From (4.75) and (4.37) we have

$$A_2=\left[\frac{\bar{\epsilon}}{e_d\lambda_0 v_0}\right]^{1/2} . \tag{4.83}$$

Using $\Delta=d+\frac{3}{2}$ and $z=1$ we immediately obtain the results

$$v_p=e_d v_0 , \tag{4.84}$$

$$l_p=\frac{e_d^3\lambda_0^3 v_0^3}{\bar{\epsilon}}=e_d^2\lambda_0^4 u_0^2 l_0 . \tag{4.85}$$

We see then that, up to a universal coefficient, v_p is just the total root mean square velocity. The second equality in (4.85) exhibits the nonuniversal proportionality constant u_0^2 [defined in (4.27)] that connects l_p and $l_0=1/m_0$. Notice that since v_p and v_0 differ by a factor e_d, we have $s\equiv\omega/\lambda_0 v_0 k=e_d s_p$. The universal constant c_d is therefore given by

$$\begin{aligned} &c_d=c_d'/e_d,\quad c_d'\equiv B_d\int_{-2}^{2}\frac{ds}{2\pi}u(s) , \\ &c_{d=3}'\simeq\frac{4.89}{(2\pi)^3}\simeq 1.97\times 10^{-2} , \\ &c_{d=3}\simeq 1.27\times(2\pi)^3\simeq 314 . \end{aligned} \tag{4.86}$$

The combination $c_{d=3}' e_{d=3}^{-1/2}\simeq 2.46$ [obtained in place of c_d if one uses v_0 in place of v_p in the definition of l_p in (4.81)] has been quoted previously in the literature [16] as being in the neighborhood of 2.

What changes in these results might we expect for general N? We will argue in Sec. V that $z=1$ is an exact result, though the exponent Δ is still undetermined. The two scaling functions will, of course, vary with N. In particular, $u(s)$ should not, in general, be confined to a finite interval. Regarding the physical parameters l_p and v_p, since (4.78) is always assumed to hold (i.e., the energy flux is always assumed to be one of the physical scale factors in the inertial range) only one of them, say, v_p, needs to be determined. The fact that v_p is universally related to v_0 is a nontrivial result in the spherical limit. One might conjecture that this remains true for general N, i.e., that $\rho_0 v_p^2$ is always proportional to the total kinetic energy density. A note of caution, however, is in order. As discussed in Sec. V C, the DIA equations have certain unphysical features with regard to the dependence of the energy transfer on v_0, which could somehow feed into the energy flux $\bar{\epsilon}$ and lead to a violation of this assumption: new physics could bring in a new measure v_p of the outer velocity scale, linearly but nonuniversally related to v_0. It would nevertheless be interesting to check this relation numerically and experimentally. A theoretical first step would entail checking it for the model II equations (3.35)–(3.39).

H. Model II

In this final subsection we describe a partial analysis of the extended model, sufficient to verify that the DIA values for the exponents remain unchanged. Obtaining full solutions to model II is left for future work.

Despite the apparent complexity of the equations, the behavior in the inertial range is quite simple and is dominated by infrared divergences in the regions $\mathbf{q}'\to\mathbf{0}$ and $\mathbf{p}'\to\mathbf{0}$ in (3.35)–(3.39). These divergences arise, when $\Delta-z\geq d$, not only from the DIA correlation function $\hat{U}$ but also from the γ's themselves. When $\Delta-d<z$ we shall see that there are no divergences, implying the result obtained generally in Appendix A, namely, that the exponent values (1.15) and (1.18) are valid for $y<3$. For $y>3$ the integrals are dominated by the infrared divergences and just as in the analysis leading to the exact solution (4.38) for $g(s)$, enormous simplifications occur.

To begin, let us first understand the dependence of the γ's on the indices α,β,γ. The key observation is that only the completely *transverse* parts of the γ's enter any physical quantity. For any function $h_{\alpha\beta\gamma}(\mathbf{k},\mathbf{q})$, the transverse part is defined by

$$h^t_{\alpha\beta\gamma}(\mathbf{k},\mathbf{q})=\sum_{\alpha',\beta',\gamma'}\hat{\tau}_{\alpha'\alpha}(\mathbf{k})\hat{\tau}_{\beta'\beta}(\mathbf{q})\hat{\tau}_{\gamma'\gamma}(\mathbf{p})h_{\alpha'\beta'\gamma'}(\mathbf{k},\mathbf{q}) \ . \quad (4.87)$$

We should therefore project all equations in this way before solving them. A general isotropic three-index tensor can be built out of Kronecker δ's functions and components of the two independent vectors, say, $\mathbf{q}$ and $\mathbf{p}$. There are 14 possible combinations. By performing the projections above, it is easy to see that $h^t_{\alpha\beta\gamma}$ can have at most four independent components, which may be expressed in the form

$$h^t_{\alpha\beta\gamma}(\mathbf{k},\mathbf{q})=h_1(\mathbf{k},\mathbf{q})\phi_{\alpha\beta\gamma}(\mathbf{k},\mathbf{q})+h_2(\mathbf{k},\mathbf{p})\phi_{\alpha\gamma\beta}(\mathbf{k},\mathbf{p}) +h_3(\mathbf{k},\mathbf{q})\zeta_{\alpha\beta\gamma}(\mathbf{k},\mathbf{q})+h_4(\mathbf{k},\mathbf{q})\theta_{\alpha\beta\gamma}(\mathbf{k},\mathbf{q}) \ , \quad (4.88)$$

where the index dependence is given by

$$\phi_{\alpha\beta\gamma}(\mathbf{k},\mathbf{q})=\sum_{\alpha',\beta'}\hat{\tau}_{\alpha\alpha'}(\mathbf{k})\hat{\tau}_{\alpha'\gamma}(\mathbf{p})\hat{\tau}_{\beta\beta'}(\mathbf{q})p_{\beta'} \ ,$$

$$\zeta_{\alpha\beta\gamma}(\mathbf{k},\mathbf{q})=\sum_{\alpha',\beta'}\hat{\tau}_{\alpha\alpha'}(\mathbf{k})q_{\alpha'}\hat{\tau}_{\beta\beta'}(\mathbf{q})\hat{\tau}_{\beta'\gamma}(\mathbf{p}) \ , \quad (4.89)$$

$$\theta_{\alpha\beta\gamma}(\mathbf{k},\mathbf{q})=\sum_{\alpha',\beta',\gamma'}\hat{\tau}_{\alpha\alpha'}(\mathbf{k})q_{\alpha'}\hat{\tau}_{\beta\beta'}(\mathbf{q})k_{\beta'}\hat{\tau}_{\gamma\gamma'}(\mathbf{p})k_{\gamma'} \ .$$

It is easy to check that each term is transverse and independent of all the others. Note that $\zeta_{\alpha\gamma\beta}(\mathbf{k},\mathbf{p})=-\zeta_{\alpha\beta\gamma}(\mathbf{k},\mathbf{q})$ and $\theta_{\alpha\gamma\beta}(\mathbf{k},\mathbf{p})=-\theta_{\alpha\beta\gamma}(\mathbf{k},\mathbf{q})$. This implies that if one has the further symmetry $h^t_{\alpha\beta\gamma}(\mathbf{k},\mathbf{q})=h^t_{\alpha\gamma\beta}(\mathbf{k},\mathbf{p})$, then we must have $h_1(\mathbf{k},\mathbf{q})=h_2(\mathbf{k},\mathbf{p})$, $h_3(\mathbf{k},\mathbf{q})=-h_3(\mathbf{k},\mathbf{p})$, and $h_4(\mathbf{k},\mathbf{q})=-h_4(\mathbf{k},\mathbf{p})$.

Let us examine now the various integrals appearing in (3.37)–(3.39). We need to understand what sort of scaling forms the γ's obey. It seems natural that singularities can appear only when one or more of the three momenta $\mathbf{k},\mathbf{q},\mathbf{p}$ approach zero. Scaling will therefore occur away from these points and we may generally expect the scaling form

$$\gamma_a(\mathbf{k},\omega;\mathbf{q},\Omega)=\frac{C_a}{k^{\eta_a}}Y_a\left[\hat{\mathbf{k}}\cdot\hat{\mathbf{q}},\frac{q}{k},\frac{\omega}{\tilde{\nu}k^z},\frac{\Omega}{\tilde{\nu}q^z}\right] \quad (4.90)$$

in the inertial range k,p,q all much larger than m_0. Here the subscript a runs over the five different γ's. Clearly the four arguments may be recombined in different ways to obtain other equivalent scaling forms.

We have already seen that when $y<3$ the DIA correlation function $\hat{U}$ yields no infrared singularities. It is then easy to verify, self-consistently, that the γ's are also nonsingular and that all integrals converge in the scaling limit $m_0\to 0$. Equation (3.37) for $\gamma_{w^{\alpha};v^{\beta}v^{\gamma}}$ is the only one with an inhomogeneous term $P_{\alpha\beta\gamma}(-\mathbf{k})$. This term represents the only nonzero DIA vertex and sets all of the exponents η_a. By simple dimensional analysis we find

$$\eta_{w;vv}=-1, \quad \eta_{w;wv}=\Delta-z-1, \quad \eta_{w;ww}=2\Delta-2z-1 \ . \quad (4.91)$$

In particular, $\eta_{w;vv}=-1$ is exactly the same as its bare value. From Eq. (3.35) for the self-energies, we then find that $\hat{\Sigma}_{vw}$ scales as k^z, $\hat{\Sigma}_{ww}$ scales as $k^{2z-\Delta}$, and hence $\hat{\mathcal{G}}$ and $\hat{\mathcal{U}}$ scale precisely as do their model I DIA counterparts.

Next consider the more relevant case of $y>3$. There are now infrared singularities from the correlation function $\hat{U}$ and, as we shall see, from the γ's themselves. We shall nevertheless demonstrate that $\hat{\mathcal{G}}$ and $\hat{\mathcal{U}}$ still scale in the same way as do $\hat{G}$ and $\hat{U}$, respectively. To see this, we use the same tricks that simplified the DIA equations: the integrals are now dominated by infrared singularities and any nondivergent terms may simply be factored out. To illustrate this, consider just one of the terms on the right-hand side of (3.37), along with the inhomogeneous term:

$$K_{\alpha\beta\gamma}(\mathbf{k},\omega;\mathbf{q},\Omega)\equiv-\frac{i}{2}\lambda_0 P_{\alpha\beta\gamma}(-\mathbf{k})-2\lambda_0^2\sum_{\mu,\nu,\lambda,\sigma}\int_{\mathbf{q}'}\int_{\Omega'}\gamma_{w^{\alpha};v^{\mu}v^{\nu}}(\mathbf{k},\omega;\mathbf{q}',\Omega')$$

$$\times[\hat{U}(\mathbf{q}',\Omega')\hat{G}(\mathbf{q}-\mathbf{q}',\Omega-\Omega')\hat{G}(\mathbf{p}',\omega-\Omega')\hat{\tau}_{\mu\lambda}(\mathbf{q}')P_{\nu\sigma\gamma}(-\mathbf{p}')P_{\sigma\lambda\beta}(\mathbf{q}'-\mathbf{q})$$

$$+\hat{U}(\mathbf{p}',\omega-\Omega')\hat{G}(\mathbf{q}'-\mathbf{q},\Omega'-\Omega)\hat{G}(\mathbf{q}',\Omega')\hat{\tau}_{\nu\lambda}(\mathbf{p}')P_{\mu\sigma\beta}(-\mathbf{q}')P_{\sigma\lambda\gamma}(\mathbf{q}-\mathbf{q}')] \ . \quad (4.92)$$

The transverse part is

$$K^t_{\alpha\beta\gamma}(\mathbf{k},\omega;\mathbf{q},\Omega)=\frac{i}{2}\lambda_0[\phi_{\alpha\beta\gamma}(\mathbf{k},\mathbf{q})+\phi_{\alpha\gamma\beta}(\mathbf{k},\mathbf{p})]-2\lambda_0^2\sum_{\beta',\gamma',\mu,\nu,\sigma}\hat{\tau}_{\beta\beta'}(\mathbf{q})\hat{\tau}_{\gamma\gamma'}(\mathbf{p})\int_{\mathbf{q}'}\int_{\Omega'}\gamma^t_{w^{\alpha};v^{\mu}v^{\nu}}(\mathbf{k},\omega;\mathbf{q}',\Omega')$$

$$\times[\hat{U}(\mathbf{q}',\Omega')\hat{G}(\mathbf{q}-\mathbf{q}',\Omega-\Omega')\hat{G}(\mathbf{p}',\omega-\Omega')P_{\nu\sigma\gamma'}(-\mathbf{p}')P_{\sigma\mu\beta'}(\mathbf{q}'-\mathbf{q})$$

$$+\hat{U}(\mathbf{p}',\omega-\Omega')\hat{G}(\mathbf{q}'-\mathbf{q},\Omega'-\Omega)\hat{G}(\mathbf{q}',\Omega')P_{\mu\sigma\beta'}(-\mathbf{q}')P_{\sigma\nu\gamma'}(\mathbf{q}-\mathbf{q}')] \tag{4.93}$$

where we have used $\sum_{\beta'\gamma'}\hat{\tau}_{\beta\beta'}(\mathbf{q})\hat{\tau}_{\gamma\gamma'}(\mathbf{p})P_{\alpha\beta'\gamma'}(\mathbf{k})=\phi_{\alpha\beta\gamma}(\mathbf{k},\mathbf{q})+\phi_{\alpha\gamma\beta}(\mathbf{k},\mathbf{p})$. Assume now that all three momenta $\mathbf{k},\mathbf{q},\mathbf{p}$ lie in the inertial range. In this case $\mathbf{q}$ and $\mathbf{q}'$ cannot be simultaneously small. In addition, since $z=1$, the combinations $P_{\sigma\mu\beta'}(\mathbf{q}-\mathbf{q}')\hat{G}(\mathbf{q}-\mathbf{q}',\Omega-\Omega')$ and $P_{\sigma\nu\gamma'}(\mathbf{q}-\mathbf{q}')\hat{G}(\mathbf{q}'-\mathbf{q},\Omega'-\Omega)$ do not diverge for small $(\mathbf{q}-\mathbf{q}')$. We assume $\gamma_{w^{\alpha};v^{\mu}v^{\nu}}(\mathbf{k},\omega;\mathbf{q},\Omega)$ to have singularities only when one of the three momenta are small. The divergences in the integration therefore may come only from small $\mathbf{q}'$ and small $\mathbf{p}'$ (since $\mathbf{k}$ is always large). Factoring out all smoothly varying terms we therefore obtain, as $m_0\to 0$,

$$K^t_{\alpha\beta\gamma}(\mathbf{k},\omega;\mathbf{q},\Omega)=\frac{i}{2}\lambda_0[\phi_{\alpha\beta\gamma}(\mathbf{k},\mathbf{q})+\phi_{\alpha\gamma\beta}(\mathbf{k},\mathbf{p})]-2\lambda_0^2\hat{G}(\mathbf{k},\omega)\sum_{\beta',\gamma',\mu,\nu,\sigma}\hat{\tau}_{\beta\beta'}(\mathbf{q})\hat{\tau}_{\gamma\gamma'}(\mathbf{p})$$

$$\times[P_{\nu\sigma\gamma'}(-\mathbf{k})P_{\sigma\mu\beta'}(-\mathbf{q})\hat{G}(\mathbf{q},\Omega)\kappa_{\alpha\mu\nu}(\mathbf{k},\omega)+P_{\mu\sigma\beta'}(-\mathbf{k})P_{\sigma\nu\gamma'}(-\mathbf{p})\hat{G}(\mathbf{p},\omega-\Omega)\kappa_{\alpha\nu\mu}(\mathbf{k},\omega)]\ , \tag{4.94}$$

where

$$\kappa_{\alpha\mu\nu}(\mathbf{k},\omega)\equiv\int_{\mathbf{q}'}\int_{\Omega'}\gamma^t_{w^{\alpha};v^{\mu}v^{\nu}}(\mathbf{k},\omega;\mathbf{q}',\Omega')\hat{U}(\mathbf{q}',\Omega')\ , \tag{4.95}$$

and we have used the symmetry property, (3.37), in the last integral. Since $\kappa_{\alpha\mu\nu}$ is a function only of $\mathbf{k},\omega$ and is transverse to $\mathbf{k}$ in the index α, it must take the form

$$\kappa_{\alpha\mu\nu}(\mathbf{k},\omega)=\kappa_1(\mathbf{k},\omega)\tau_{\alpha\nu}(\mathbf{k})k_\mu+\kappa_2(\mathbf{k},\omega)\tau_{\alpha\mu}(\mathbf{k})k_\nu\ . \tag{4.96}$$

Furthermore, the projection operators $P_{\nu\sigma\gamma'}(-\mathbf{k})$ and $P_{\mu\sigma\beta'}(-\mathbf{k})$ eliminate κ_2 and (4.94) simplifies to

$$K^t_{\alpha\beta\gamma}(\mathbf{k},\omega;\mathbf{q},\Omega)$$
$$=\left\{\frac{i}{2}\lambda_0-2\lambda_0^2\hat{G}(\mathbf{k},\omega)\kappa_1(\mathbf{k},\omega)\right.$$
$$\left.\times[\mathbf{k}\cdot\mathbf{q}\hat{G}(\mathbf{q},\Omega)+\mathbf{k}\cdot\mathbf{p}\hat{G}(\mathbf{p},\omega-\Omega)]\right\}$$
$$\times[\phi_{\alpha\beta\gamma}(\mathbf{k},\mathbf{q})+\phi_{\alpha\gamma\beta}(\mathbf{k},\mathbf{p})]\ , \tag{4.97}$$

with, explicitly,

$$\kappa_1(\mathbf{k},\omega)=\frac{1}{(d-1)k^2}$$
$$\times\int_{\mathbf{q}'}\int_{\Omega'}\sum_{\mu,\nu}k_\mu\gamma^t_{w^{\nu};v^{\mu}v^{\nu}}(\mathbf{k},\omega;\mathbf{q}',\Omega')\hat{U}(\mathbf{q}',\Omega')\ . \tag{4.98}$$

The remaining terms in (3.37) simplify in a similar manner. It should be recalled that the angular dependence of γ^t is given by a linear combination of the form (4.88). The result (4.98) then implies that γ_3 and γ_4 (i.e., the coefficients of $\theta_{\alpha\beta\gamma}$ and $\zeta_{\alpha\beta\gamma}$) both vanish in the inertial range (though they could be important in the driving range), while

$$\gamma_1(\mathbf{k},\omega;\mathbf{q},\Omega)=\gamma_2(\mathbf{k},\omega;\mathbf{p},\omega-\Omega)=\gamma_1(\mathbf{k},\omega;\mathbf{p},\omega-\Omega)$$
$$=\frac{i}{2}\lambda_0-2\lambda_0^2\hat{G}(\mathbf{k},\omega)\kappa_1(\mathbf{k},\omega)[\mathbf{k}\cdot\mathbf{q}\hat{G}(\mathbf{q},\Omega)+\mathbf{k}\cdot\mathbf{p}\hat{G}(\mathbf{p},\omega-\Omega)]+\cdots\ , \tag{4.99}$$

where the ellipsis refers to further terms arising from those neglected in (3.37).

In order to complete the solution we would have to obtain a closed equation for κ_1. Unfortunately, this is very difficult, as it requires extending the solution (4.99) into the driving region $\mathbf{q}\to 0$ and $\mathbf{p}\to 0$. The integral (4.98) is dominated by the infrared divergences in the region of small $\mathbf{q}'$, not the inertial range. Unfortunately, Eq. (4.99)

tells us nothing about this region. However, this result nevertheless allows us to understand the scaling behavior. To get a feel for this, suppose that (4.99) were exact even in the driving range and suppose that we neglect entirely corrections from the further terms we have neglected in (3.37). We would then have

$$\kappa_1(\mathbf{k},\omega)=\int_{\mathbf{q}'}\int_{\Omega'}\gamma_1(\mathbf{k},\omega;\mathbf{q}',\Omega')\hat{U}(\mathbf{q}',\Omega')[1-(\hat{\mathbf{k}}\cdot\hat{\mathbf{q}}')^2]\ . \tag{4.100}$$

Multiplying (4.99) by $\hat{U}(\mathbf{q},\Omega)[1-(\hat{\mathbf{k}}\cdot\hat{\mathbf{q}})^2]$ and integrating over $\mathbf{q}$ and Ω we then obtain the closed equation

$$\kappa_1(\mathbf{k},\omega)=\frac{i}{2}\lambda_0 v_0^2-2\lambda_0^2 v_0^2 k^2\hat{G}(\mathbf{k},\omega)^2\kappa_1(\mathbf{k},\omega)\ , \tag{4.101}$$

with the solution

$$\kappa_1(\mathbf{k},\omega)=\frac{\frac{i}{2}\lambda_0 v_0^2}{1+2\lambda_0^2 v_0^2 k^2\hat{G}(\mathbf{k},\omega)^2}=\frac{\frac{i}{2}\lambda_0 v_0^2}{1+2g(s)^2}\ , \tag{4.102}$$

where v_0 is the driving scale velocity defined in (4.29) and $g(s)$ is the response scaling function (4.38) with $s=\omega/\tilde{\nu}k^z$. In addition, one finds $\kappa_2(\mathbf{k},\omega)=0$. Finally, substituting this into (4.99) yields

$$\gamma_1(\mathbf{k},\omega;\mathbf{q},\Omega)=\frac{i}{2}\lambda_0\left[1-2g(s)\frac{\hat{\mathbf{k}}\cdot\hat{\mathbf{q}}g(t)+\hat{\mathbf{k}}\cdot\hat{\mathbf{p}}g(r)}{1+2g(s)^2}\right]\ , \tag{4.103}$$

where $t=\omega/\tilde{\nu}q^z$ and $r=(\omega-\Omega)/\tilde{\nu}p^z$. Since it contains no new powers of k, the second term in large square brackets represents a *finite,* order-one renormalization of the three-point vertex. The scaling exponents are unchanged. Furthermore, ignoring all but the first term on the right-hand sides of Eqs. (3.35), we obtain in the present approximation

$$\begin{aligned}\hat{\Sigma}_{vw}(\mathbf{k},\omega)&=\lambda_0 v_0 k\frac{g(s)}{1+2g(s)^2}\ ,\\ \hat{\Sigma}_{ww}(\mathbf{k},\omega)&=\lambda_0^2 v_0^2 k^2\hat{U}(\mathbf{k},\omega)\frac{1}{1+2g(s)^2}\end{aligned} \tag{4.104}$$

and therefore

$$\begin{aligned}\frac{1}{\hat{g}(s)}&=-is+\frac{g(s)}{1+2g(s)^2}\ ,\\ \hat{u}(s)&=|\hat{g}(s)|^2\frac{u(s)}{1+2g(s)^2}\ ,\end{aligned} \tag{4.105}$$

where $\hat{g}(s)$ and $\hat{u}(s)$ are the scaling functions for $\hat{G}$ and $\hat{U}$, respectively. Once again, there is a finite renormalization of the scaling functions, but no change in the scaling exponents. Notice that $\hat{u}(s)$ obtained here is not real. This is an artifact of the *ad hoc* approximations we have made. In a full calculation this function must, of course, be real and non-negative.

With the above calculation as a guide, it is easy now to argue that the full exact solution must also have the same set of scaling exponents. The point is that even though we do not know its detailed extension into the driving range, Eq. (4.99) suffices to determine the scaling. What is important is that κ_1 scale with m_0 as $\lambda_0 v_0^2$. Corrections to (4.99) in the driving range, though presumably of relative order unity, can do no more than renormalize the s-dependent coefficient of $\lambda_0 v_0^2$ in (4.102), without changing its scaling dependence on m_0.

Further complications will arise from the terms in (3.37) that we have left out. These will yield three further reduced functions, analogous to $\kappa_{\alpha\beta\gamma}(\mathbf{k},\omega)$, for the other γ's. Equations (3.37)–(3.39) will then contain linear combinations of these κ's. A similar *ad hoc* closure calculation like the one above then yields a closed set of four linear equations in the four unknown κ's. In definitions like (4.95), one finds that the subscript v is always integrated against $\hat{U}$, while the subscript w is always integrated against $\hat{G}$. In results like (4.97), this pairing is reversed: the subscript v always scales with $\hat{G}$, while the subscript w always scales with $\hat{U}$. These correspondences are precisely what guarantee that the scaling exponents always work out.

It is not clear at this stage whether or not a more sophisticated analysis will allow one to solve exactly the model II equations without resorting to numerics. The problem is that many quantities, such as γ_3 and γ_4 above, which vanish in the inertial range, will be of relative order unity in the driving range. We have yet to find a simple ansatz that consistently yields forms for these corrections valid over the full range of wave number and frequency.

V. DISCUSSION, CONCLUSIONS, AND OUTLOOK

In this work we have proposed a set of generalized models for turbulence, parametrized by the number of velocity fields N and a corresponding group G of linear transformations. The essential feature of these models is a simplification which occurs when $N\to\infty$: they become exactly soluble. The results of this exact solution are summarized in Sec. I; see especially Sec. I E and Figs. 2 and 3. In this final section we shall examine various features of these exact solutions in light of the present understanding of some properties of real Navier-Stokes turbulence.

As mentioned at the end of Sec. I E, the result $z=1$ for the dynamical exponent and the infrared divergences that lead to it are a reflection of "sweeping effects." In Sec. V A we will try to place our work in the context of the existing literature by discussing in more detail the common notions of sweeping, turnover times, and the associated Taylor hypothesis. Discussion of the latter may be phrased very conveniently in the language of scaling functions. Of special interest to the former is whether or not precise definitions of turnover times exist and then whether or not they can actually be computed. In Sec. V B we provide one possible definition based on the scaling of the dissipation length with Reynolds number and show that it implies a time scale much longer than the sweeping time with an associated "internal" dynamical exponent $z_{\text{int}}<1$. We end by indicating work for the future.

A. Sweeping, Lagrangian coordinates, and the Taylor hypothesis

1. *Scaling and time series in a fluid with a mean flow*

Sweeping lies at the heart of the connection between spatial and temporal spectra. Essentially all experiments to date are single-point measurements and yield only one-dimensional time series data. From these time series, however, one would like to infer, if possible, the spatial energy spectrum. In many experiments, such as those on grid turbulence or turbulent jets, the single point, call it $\mathbf{r}=\mathbf{0}$, is stationary in the laboratory frame, but the fluid has a nonzero mean flow velocity $\bar{\mathbf{v}}=\langle \mathbf{v}(\mathbf{r},t)\rangle$. The turbulent eddies are then swept past the experimental observation point at constant rate. Under these conditions one is clearly exploring some combination of the spatial and temporal fluctuations in the flow. The scaling form (1.17) allows us to consider both and we shall now explore what it implies about the temporal correlations in a moving fluid.

If $U_{\rm lab}(\mathbf{r},t)=[1/(d-1)]\langle \mathbf{v}(\mathbf{r},t)\cdot\mathbf{v}(\mathbf{0},0)\rangle$ is the velocity-velocity correlation function measured in the laboratory frame, then by appropriate averaging of the time series data one can obtain the temporal part of the correlation function $U_{\rm exp}(t)\equiv U_{\rm lab}(\mathbf{0},t)$ and its Fourier transform, the power spectrum. If we denote by $U(\mathbf{r},t)$ the correlation function measured by an observer traveling with the mean flow (i.e., at constant velocity $\bar{\mathbf{v}}$; this is the function that is calculated theoretically), we have the relation

$$U_{\rm lab}(\mathbf{r},t)=U(\mathbf{r}-\bar{\mathbf{v}}t,t)+\frac{1}{d-1}\bar{v}^2 . \tag{5.1}$$

The experimentally measured function $U_{\rm exp}(t)=U(-\bar{\mathbf{v}}t,t)+[1/(d-1)]\bar{v}^2$ then contains both spatial and temporal information. The question we address, then, is what exponent (or combination of exponents) can be inferred from $U_{\rm exp}(t)$.

To this end, let us translate the Fourier space scaling form (1.17) into real space. We obtain, then,

$$U(\mathbf{r},t)\approx A_2\tilde{\nu}(\tilde{\nu}t)^{(\zeta-1)/z}\int_{\vec{\kappa}}\frac{\tilde{u}(\kappa^z)}{\kappa^{\Delta-z}}e^{-i\vec{\kappa}\cdot\vec{\rho}} , \tag{5.2}$$

where $\vec{\rho}=\mathbf{r}/(\tilde{\nu}t)^{1/z}$, $\vec{\kappa}=(\tilde{\nu}t)^{1/z}\mathbf{k}$, $\zeta=\Delta-d-z+1$ (as before), and $\tilde{u}(\tau)=\int(ds/2\pi)e^{-is\tau}u(s)$ is the Fourier transform of the scaling function. If $\Delta-z<d$, i.e., $\zeta<1$ (we shall discuss the physically relevant case $\zeta>1$ below), the last integral converges and we may safely consider the $m_0\to 0$ limit to obtain the real-space scaling form

$$U(\mathbf{r},t)\approx\frac{A_2\tilde{\nu}}{(\tilde{\nu}t)^{(1-\zeta)/z}}\bar{u}[r/(\tilde{\nu}t)^{1/z}],\quad r,t\to\infty , \tag{5.3}$$

where $\bar{u}(\rho)$ is the integral in (5.2). This form breaks down only for very small r and t where dissipation effects enter. We then obtain the relation

$$U_{\rm exp}(t)-\frac{1}{d-1}\bar{v}^2\approx\frac{A_2\tilde{\nu}}{(\tilde{\nu}t)^{(1-\zeta)/z}}\bar{u}(\bar{v}\tilde{\nu}^{-1/z}t^{1-1/z}) . \tag{5.4}$$

In the simplest case $\bar{v}=0$, scaling then predicts the pure power-law behavior $U_{\rm exp}(t)=U(\mathbf{0},t)\approx A_2\tilde{\nu}(\tilde{\nu}t)^{(\zeta-1)/z}\times\bar{u}(0)$. Only a nontrivial combination of ζ and z can therefore be inferred. Now, if $\bar{v}>0$ there are two possibilities. First, if $z<1$ then the argument of $\bar{u}$ in (5.3) decays to zero for large t and the *same* asymptotic power law results. On the other hand, if $z>1$, the argument of $\bar{u}$ diverges for large t. The behavior of $\bar{u}(\rho)$ for large ρ is obtained by demanding that (5.3) yield a t-independent result for equal time correlations $t\to 0$. This requires that $\bar{u}(\rho)\approx\bar{u}_\infty\rho^{\zeta-1}$ as $\rho\to\infty$ and hence

$$U_{\rm exp}(t)-\frac{1}{d-1}\bar{v}^2\approx A_2\tilde{\nu}\bar{u}_\infty(\bar{v}t)^{\zeta-1} \tag{5.5}$$

for large t. The asymptotics now involves ζ alone and is precisely the *equal time* behavior predicted by (5.3), but with the replacement $r=\bar{v}t$. Note that for the borderline case $z=1$, the spatial and temporal power laws are the same, but

$$U_{\rm exp}(t)-\frac{1}{d-1}\bar{v}^2\approx A_2(\tilde{\nu}t)^{\zeta-1}\bar{u}(\bar{v}/\tilde{\nu}) \tag{5.6}$$

has a nontrivial dependence on the mean flow velocity, being independent of $\bar{v}$ as $\bar{v}\to 0$, but proportional to $\bar{v}^{\zeta-1}$ for large $\bar{v}$.

We see then that if $z\geq 1$ then what we shall call the *"weak" Taylor hypothesis* is valid: the temporal statistics of turbulent flow, possessing a mean uniform velocity $\bar{v}>0$ measured at a fixed point in space, will be effectively the same as the spatial statistics of that flow. An experimental time series then can be used to infer directly the Kolmogorov exponent. If, on the other hand, $z<1$, velocity fluctuations are so large that a background uniform flow is completely masked: large eddies evolve at a rate much larger than that at which they are swept by the observation point and (5.4) yields the same asymptotic result, with the exponent depending on both ζ and z, when $\bar{v}>0$ as when $\bar{v}=0$. The scaling ansatz elucidates the assumptions underlying this hypothesis and allows us to make its statement precise.

Unfortunately, the situation $z\geq 1$ and $\zeta<1$ is valid only for power-law-driven turbulence with $y<3$, but apparently invalid for $y\geq 3$: physically, we know that $\zeta>1$ for real turbulence. Recall, also, that breakdown of the y expansion occurs precisely at $\zeta=1$ (as exemplified by the divergences found in the DIA equations when $y\geq 3$). Divergences occur in (5.2) at precisely this same point. To make sense of this equation for $\zeta\geq 1$ one must again consider a small-k cutoff m_0, using the scaling form (4.19) in place of (1.17). The inverse Fourier transform then becomes

$$\begin{aligned}U(\mathbf{r},t)\approx{}& A_2\tilde{\nu}(\tilde{\nu}t)^{(\zeta-1)/z}\\ &\times\int_{\vec{\kappa}}\frac{1}{\kappa^{\Delta-z}}\{e^{-i\vec{\kappa}\cdot\vec{\rho}}\tilde{u}[\kappa^z;\kappa/m_0(\tilde{\nu}t)^{1/z}]\\ &\qquad-\tilde{u}[0;\kappa/m_0(\tilde{\nu}t)^{1/z}]\}\\ &+\frac{A_2\tilde{\nu}}{m_0^{\zeta-1}}\int_{\mathbf{x}}\frac{\tilde{u}(0;x)}{x^{\Delta-z}} ,\end{aligned} \tag{5.7}$$

where $\tilde{u}(\tau;x)=\int(ds/2\pi)e^{-i\tau s}u(s;x)$. The first term converges when $m_0\to 0$ and the last term is just $U(\mathbf{0},0)=[1/(d-1)]\langle \mathbf{v}^2\rangle$. We therefore have

$$U(\mathbf{r},t)-\frac{1}{d-1}\langle \mathbf{v}^2\rangle=-\frac{1}{d-1}\langle[\mathbf{v}(\mathbf{r},t)-\mathbf{v}(\mathbf{0},0)]^2\rangle$$
$$=A_2\tilde{\nu}(\tilde{\nu}t)^{(\zeta-1)/z}\bar{u}[r/(\tilde{\nu}t)^{1/z}]\,, \tag{5.8}$$

where the real-space scaling function is now

$$\tilde{u}(\rho)=\int_{\vec{\kappa}}\frac{1}{\kappa^{\Delta-z}}[e^{-i\vec{\kappa}\cdot\vec{\rho}}\tilde{u}(\kappa^z)-\tilde{u}(0)] \tag{5.9}$$

and $\tilde{u}(\tau)\equiv\lim_{x\to\infty}\tilde{u}(\tau;x)$. Even though $\bar{v}=0$ in this computation, the divergence has given rise to an effective mean flow velocity $\langle \mathbf{v}^2\rangle^{1/2}\equiv v_0\sqrt{d}$ [see (4.29)], diverging as $m_0^{-(\zeta-1)/2}$.

Let us now reexamine the Taylor hypothesis. Proceeding as before, substituting $\mathbf{r}=\bar{\mathbf{v}}t$, Eq. (5.4) now holds with $\bar{v}^2$ replaced by $v_{0,\mathrm{exp}}^2=\bar{v}^2+v_0^2d$ (the mean squared velocity as measured in the laboratory frame) on the left-hand side. If $z>1$ the argument of the scaling function again diverges and we arrive at (5.5) but now with the subtraction $v_{0,\mathrm{exp}}^2$ on the left. This seems an innocuous change, but in fact leads to a rather strange state of affairs because the latter is completely dominated (for small m_0) by the effective mean flow, whereas, paradoxically, the argument of the scaling function depends only on the actual mean flow $\bar{v}$. Intuitively, if $\zeta>1$ most of the energy is in large-scale, low-frequency fluctuations. On experimental time scales a slow fluctuation will be indistinguishable from a fixed mean flow and ought then to somehow renormalize $\bar{v}$ in the scaling function as well. The renormalization group predictions show that this paradox is avoided by having $\zeta=1$ and $z=1$ occur simultaneously, precisely at the borderline $y=3$. The above considerations hint that this decrease in z with increasing y is a different reflection of this same physics.

Apparently, then, the weak Taylor hypothesis has no meaning in the physically relevant case, $\zeta>1$, as long as $\bar{v}\ll v_0$ (note, however, that if $\bar{v}>v_0$, as is probably the case in turbulent jet experiments, the hypothesis presumably still works). What then should replace it? Suppose first that we take seriously the renormalization group predictions for $y>3$, namely, that $z<1$ and $\zeta>1$. The paradox above no longer arises: as before, the appropriately altered equation (5.4) predicts the temporal power law $U_{\mathrm{exp}}(t)\sim t^{(\zeta-1)/z}$ for large t, irrespective of the value of $\bar{v}$. However, one now encounters two serious problems. First, the Kolmogorov exponent can no longer be inferred directly. Despite this, the experimental inference of the Kolmogorov $\frac{5}{3}$ law is *based* on the Taylor hypothesis: the value $\zeta=\frac{5}{3}$ is calculated by assuming that $U_{\mathrm{exp}}(t)\sim t^{\theta}$, with $\theta=\zeta-1$. The experimental value is $\theta\simeq\frac{2}{3}$. However, if $\theta=(\zeta-1)/z$ one infers $\zeta=\theta z+1\simeq\frac{13}{9}$ (using the renormalization group prediction $z=\frac{2}{3}$). This value of ζ differs quite significantly from the Kolmogorov result, which would require, apparently, a measured value of $\theta\simeq 1$. We arrive then at a contradiction: $z=\frac{2}{3}$ and $\zeta=\frac{5}{3}$ cannot be simultaneously consistent with the experimental results, irrespective of whether or not there exists a mean flow.

The second problem is a more serious internal inconsistency. The point is that the cutoff m_0 determines an outer scale $l_0=1/m_0$ and $t_0\equiv l_0/v_0$ defines a characteristic turnover time for the large-scale eddies. Smaller eddies, of size $\lambda<l_0$, then have *two* time scales associated with them: the time scale $t_\lambda=\lambda/v_0$ over which the large-scale flows sweep them past a fixed observer, and some characteristic *intrinsic* turnover time $\tau_\lambda=t_0(\lambda/l_0)^{z_{\mathrm{int}}}$ of the moving eddy. We may suppose that $z_{\mathrm{int}}<1$ is some continuation to $y>3$ of $z(y)$ for $y<3$. However, if $z_{\mathrm{int}}<1$ then $t_\lambda/\tau_\lambda=(\lambda/l_0)^{1-z_{\mathrm{int}}}\ll 1$ is negligible in the inertial range $\lambda\ll l_0$: the turnover time is much *longer* than the sweeping time. The latter therefore dominates the dynamics at a fixed observation point and z_{int} cannot enter the scaling of the two-point functions.

Our results avoid both problems, at least at the level of the DIA equations, by having z stick at the value unity for all $\zeta>1$. The above argument makes clear why this particular DIA result ought to extend to the general case. We state it, then, as a general principle, which we call the *"strong" Taylor hypothesis*: large eddies, of $O(l_0)$ in size, basically constitute a mean background flow for smaller ones, which then *internally* generates the shortest time scale in the problem and therefore, self-consistently, requires $z=1$. It is apparently impossible to have $z<1$ in the presence of an effective mean flow v_0 and the scaling combination must then be r/v_0t [i.e., $\tilde{\nu}\propto v_0$; see (4.80)]. The Taylor hypothesis exists in the strong form, but not in the weak form. This is actually quite satisfying: the velocity v_0 now determines *both* the subtraction on the left-hand side of (5.8) *and* the scaling of time on the right-hand side. For small m_0 any externally applied mean flow $\bar{v}$ has a negligible effect on both since the argument of the scaling function in (5.6) is now $\bar{v}/v_0\ll 1$.

2. *Turnover times and Lagrangian coordinates*

The notion of an intrinsic turnover time (and associated dynamical exponent), supposedly obtained by an observer that *follows* an eddy of size λ in a "freely falling" frame of reference, comoving with the fluctuating mean background flow (with velocity of order v_0), is very common in the literature. The reason such notions dominate the discourse so strongly is that the Kolmogorov cascade is often phrased in terms of the breakup of larger eddies into smaller ones and it is felt that the dynamics of this process is *local* and should therefore be an intrinsic phenomenon, not one dominated by the outer scale l_0. The existence of two (or more) dynamical exponents is an unusual feature from the point of view of dynamical scaling and arises, once again, from the fact that $z\to 1$ as $y\to 3$. In most equilibrium problems (critical dynamics, for example) z is significantly greater than unity and sweeping time scales are much longer than "critical" turnover time scales. In turbulence, however, these two scales change places at $y=3$ and the question is then how

to access the now much longer turnover time scale. Although we have seen that the strong Taylor hypothesis precludes seeing such a time scale in the velocity-velocity correlation function, there are other ways of observing it. One famous way is through Reynolds diffusion, in which the time dependence of the *separation* between two passively advected particles is considered. A single advecting particle in a turbulent flow will undergo ordinary Gaussian diffusion $r \approx (Dt)^{1/z_{GD}}$, characterized therefore by a dynamical exponent $z_{GD}=2$ and with diffusion constant $D \sim v_0^2$ set by the outer velocity scale. In contrast, the divergence of the trajectories of two nearby particles will be non-Gaussian, due precisely to the dynamics of small eddies, and obey a Kolmogorov-type law $\Delta r \sim t^{1/z_{RD}}$ with $z_{RD} \simeq \frac{2}{3}$ [34]. This kind of behavior is seen in numerical simulations, but its experimental verification requires simultaneous spatial and temporal data, something that is just now beginning to become feasible [35].

Since it involves following the trajectories of freely advecting particles, Reynolds diffusion is an intrinsically Lagrangian quantity. *Lagrangian history* methods represent a way of generalizing these ideas further. Here one defines a more general velocity field $\mathbf{u}(\mathbf{x},t_0|t) \equiv \mathbf{v}(\mathbf{r}(\mathbf{x},t_0|t),t)$, which is the velocity of the fluid element at time t that was (or will be) at point $\mathbf{x}$ at time t_0. The "diffeomorphism" $\mathbf{r}(\mathbf{x},t_0|t) \equiv \mathbf{x} - \vec{\xi}(\mathbf{x},t_0|t)$ gives the position of this fluid element at the measuring time t and one clearly must have $\mathbf{u}(\mathbf{x},t_0|t) = (\partial/\partial t)\mathbf{r}(\mathbf{x},t_0|t)$. Considered as a function of t at fixed $\mathbf{x}$ and t_0, this is the usual Lagrangian description of the velocity field with initial condition $\mathbf{u}(\mathbf{x},t_0|t_0)=\mathbf{v}(\mathbf{x},t_0)$. On the other hand, if $t \equiv t_0$ then $\mathbf{r} \equiv \mathbf{x}$ and one obtains the usual Eulerian description. One may write down, in a straightforward way, a formal perturbation theory for $\mathbf{u}(\mathbf{x},t_0|t)$ in powers of the nonlinearity λ_0 [16] and hence derive diagrammatic expansions for correlation functions, such as

$$U(\mathbf{x},t_0|t;\mathbf{y},s_0|s) \equiv \frac{1}{d-1}\langle \mathbf{u}(\mathbf{x},t_0|t)\cdot\mathbf{u}(\mathbf{y},s_0|s)\rangle \ . \qquad (5.10)$$

From this expansion, suitable infinite subclasses of diagrams may be resummed. A generalized set of DIA equations results from the simplest nontrivial subclass. Since these equations reduce to the standard DIA equations when $s_0=s$ and $t_0=t$, they contain precisely the same sweeping effects, along with $z=1$ and $\zeta=\frac{1}{2}$. The equations are enormously more complicated for s_0 and t_0 different from s and t, so it is not clear what the detailed scaling properties are in this case. Kraichnan [16] has shown, however, that with a straightforward redefinition of some of the time coordinates in these integral equations, a new set of *Lagrangian history* DIA (LHDIA) equations may be defined that have nicer Galilean invariance properties (namely, covariance under "random Galilean transformations") and are argued to yield Kolmogorov's $\frac{5}{3}$ law and presumably a new dynamical exponent $z_{LH}=\frac{2}{3}$. The reason for the different results is that certain cancellations now occur in just such a way as to eliminate the infrared divergences encountered in Sec. IV. It would be interesting to see how these equations behave in the presence of power-law driving, in particular, whether or not they encounter ultraviolet divergences for $y<3$ and whether or not they recover properly the renormalization group results in their region of validity. This is an especially important question as the renormalization group results are also a consequence of Galilean invariance. Kraichnan [36] has also shown that the LHDIA equations may be systematically extended to higher order, still maintaining their nice invariance properties.

Realizability now becomes a problem however. As mentioned in Sec. II D, Kraichnan [29] showed some time ago that the DIA equations represent an exact solution in a large-N limit, in his case with random coefficients A_N^{lmn} (the so-called random coupling models). However, he was unable to show the same property for the LHDIA equations [16]. It is possible, then, that these equations *do not* arise from any large-N limit. If this is so, they cannot be the basis for a systematic expansion in powers of $1/N$. However, it is this property that we believe to be fundamental. Without the systematic parameter N the determination of which diagrams contribute at a given order becomes a matter of taste and it is impossible to state whether the alterations that lead from DIA to LHDIA yield a more or a less systematic expansion. With the parameter N it is seen that any alterations to the spherical limit equations *cannot survive* for large N. In our case we would interpret this to mean that the unaltered DIA equations (or their model II counterparts) are fundamental.

3. *Quasi-Lagrangian coordinates and their limitations*

Belinicher and L'vov [3(b)] have recently presented a diagrammatic proof that $z=1$, resumming exactly the most divergent parts of the response function. They have also shown, in general, that the most divergent parts of the correlation function U cancel exactly and, therefore, that ζ and Δ are not so simply determined. Lower-order terms, as we have seen explicitly at the level of the DIA analysis, must be taken into account. Taking a path intermediate between the fully Eulerian and fully Lagrangian approaches, these authors have also proposed a new *quasi-Lagrangian* diagrammatic formalism in which the coordinate transformation $\vec{\xi}(t)$ is taken to be *independent* of $\mathbf{x}$, and is the displacement, at time t, of the fluid element that was at an arbitrarily chosen point $\mathbf{r}_0$ at time t_0: $\vec{\xi}(t)=\xi(\mathbf{r}_0,t_0|t)$, satisfying $d\vec{\xi}/dt=\mathbf{v}(\mathbf{r}_0+\vec{\xi}(t),t)$. This change of variables has no effect on the equal time correlation functions, but is claimed to eliminate sweeping effects from the unequal time ones, at least in the neighborhood of the point $\mathbf{r}_0$. Specifically, if one assumes that the change of variables leads to a *new* dynamical exponent $\frac{1}{3}<z'<1$ and that the hyperscaling relation $\Delta+z'=d+2$ [i.e., Eq. (1.19) with z' replacing z] holds, then each individual diagram converges. In particular, this is true for the Kolmogorov values $z'=\frac{2}{3}$ and $\zeta=\frac{5}{3}$. Unfortunately, though self-consistent, the theory provides no way of confirming these underlying assumptions.

In particular, there is nothing in the theory that rules out residual sweeping effects (i.e., m_0 dependence) in the quasi-Lagrangian correlation functions. The assumption that the hyperscaling relation can still be made to hold seems especially optimistic: in our picture a completely different fixed point controls the behavior for $y>4$, so there is no reason why such a relation ought to be "analytically continued" through $y=3$, all the way beyond $y=4$. The quasi-Lagrangian formulation serves only to provide a sophisticated diagrammatic reformulation of the Kolmogorov argument. It allows one at least to point to specific formal expressions, which, when assumed to behave in certain specified ways, yield the Kolmogorov exponent values. Prior to this, one had to rely on more imprecise notions.

4. *Advantages and limitations of the DIA equations*

The advantage of the large-N expansion is that at least it gives rise to clean, well defined calculations with unambiguous answers and without hidden, unverifiable assumptions. It allows *direct* and perhaps even systematic (see Sec. V C below) calculations of experimentally relevant correlation functions. In addition, even the spherical limit $N\rightarrow\infty$ contains much of the correct physics of the balance between power-law driving and inertial range sweeping effects that is the key to understanding the different regimes of scaling behavior. To be fair, we should point out that the DIA equations are far from perfect. Kraichnan [37] has shown that sweeping effects in the DIA equations, though present, are not included in a completely Galilean invariant manner. He demonstrated that the DIA equations are not invariant under random Galilean transformations and that this leads to a completely unphysical effect of the driving range on the *energy transfer* between inertial range wave vectors and that this is part of what is responsible for the non-Kolmogorov $\frac{3}{2}$ law. Within the large-N approach we may understand this as arising from the interaction between different isospin components of the velocity as they sweep through each other. Eyink [38] has also emphasized this feature as a deep problem with the physics of the DIA and a potential roadblock to making the large-N expansion systematic. In particular, it may be a feature that survives for all $N>1$, disappearing discontinuously only right at $N=1$. Model II may be healthier in this regard [39]. For further discussion, see Sec. V C.

We end this subsection by emphasizing an important point regarding the status of the Kolmogorov $\frac{5}{3}$ law. The Kolmogorov theory is often regarded as a cornerstone upon which more sophisticated theories should be based, much as are mean field theories of critical phenomena [40]. However, unlike mean theories, which are exact descriptions in certain limits (usually the limit of infinite range or large dimension), *there is no known limit* of any realistic model based on the Navier-Stokes equations that exhibits an exact $\frac{5}{3}$ law. As mentioned at the end of Sec. IV E, there are *ad hoc* subtracted versions of the DIA equations that most probably exhibit a $\frac{5}{3}$ law. These can be most easily understood in terms of Kraichnan's [37] "distant interactions excluded" modified Navier-Stokes equations in which interactions between wave numbers that differ in order of magnitude are simply removed from the model. In particular, there is no direct interaction between the inertial and driving ranges. The DIA equations for this model contain precisely the right subtractions to eliminate the infrared divergences in the original DIA. Clearly, however, this model is in the wrong "universality class" since sweeping effects have been removed at the outset and the essential physics of the original Navier-Stokes has been badly violated. The same problem arises in the popular "shell models" of turbulence, in which each decade (shell) in wave-vector space is replaced by a single velocity variable and again only near-neighbor interactions between shells are kept (see [38] and references therein). One is therefore left in the unfortunate position where the most desirable starting point is unrealizable, while the realizable models all have certain undesirable features. Concisely, this is the underlying reason for the lack of fundamental progress in understanding the Kolmogorov cascade. In summary, one would like to put the maximal possible amount of physics into a realizable starting point, but it appears that only the full Navier-Stokes equations themselves contain all desired features in a fully Galilean invariant way.

B. The dissipation scale

In the preceding subsection we have seen that the notion of a turnover time is most naturally discussed from the Lagrangian point of view. Fortunately or unfortunately, the theoretical techniques presented in this paper are intrinsically Eulerian and we must address the question of whether the same information can somehow be extracted from a Eulerian correlation function. Since the two-point correlation functions contain only the sweeping time scale, the problem of extracting turnover times can probably be resolved only by examining the behavior of higher-order correlation functions. As a simple example, which has been used to interpret experimental results, here we will describe a definition in terms of a three-point correlation function. We will show that it leads to an intrinsic dynamical exponent $z_{\rm int}=\zeta-1$. It is an open question whether or not this definition coincides with any of the previous ones.

The idea is that one should examine the *dissipation* process in the presence of viscosity and in particular how viscosity cuts off the inertial range at large wave numbers. Since dissipation depends only on local gradients of the velocity field, it should be more intrinsic to the flow and hence less sensitive to large-scale sweeping effects.

We have seen that the formal limit $\nu_0\rightarrow 0$ does not entail any divergences in the DIA equations, but only defines a viscous cutoff scale $l_\nu=1/\Lambda$ beyond which energy dissipation dominates and the power-law energy spectra become exponentially decaying. Only the physical outer scale (see Sec. IV G), $l_p\sim l_0=1/m_0$ contributes to the renormalization of the Kolmogorov exponent ζ. It seems likely to us that, to the extent that locality remains valid (see Sec. IV F), this will remain true for $N=1$ as well.

It is nevertheless interesting to understand what deter-

mines l_ν. Dimensional analysis leads one to expect, generally, that $l_\nu=(\nu_0^3/\bar{\epsilon})^{1/4}$ [see (1.4)]. The Kolmogorov theory then yields $\Lambda/m_0=l_0/l_\nu\sim l_p/l_\nu=\mathrm{Re}^{3/4}$, where $\mathrm{Re}=\lambda_0 v_p l_p/\nu_0\equiv\nu_{\mathrm{turb}}/\nu_0$ is the Reynolds number and $\nu_{\mathrm{turb}}=\lambda_0 v_p l_p$ is an effective turbulent viscosity. This relation is obtained by assuming that the scale-dependent Reynolds number $R_\lambda\equiv v_\lambda\lambda/\nu_0$ is of order unity at the dissipation scale. Within the Kolmogorov theory, one finds (by the usual, less general, dimensional analysis arguments) $v_\lambda=(\bar{\epsilon}\lambda)^{1/3}$ and from this follow the above results. In any case, we may include the dissipation scale via a new scaling variable k/Λ, so that

$$E(k)\approx Ak^{-\zeta}F(k/\Lambda)\ , \tag{5.11}$$

where $F(x)\to 1$ as $x\to 0$, decreases exponentially as $x\to\infty$ [2,13,41], and, to the extent that the standard viscous term is an accurate description of dissipation at all scales of interest, should be a universal function. Within the Kolmogorov theory we may write

$$\frac{E(k)}{\bar{\epsilon}^{2/3}\Lambda^{-5/3}}\approx C_K\left[\frac{k}{\Lambda}\right]^{-5/3}F\left[\frac{k}{\Lambda}\right]\ . \tag{5.12}$$

Since $\bar{\epsilon}^{2/3}\Lambda^{-5/3}=\bar{\epsilon}^{1/4}\nu_0^{5/4}$, we may check this relation for experimental and numerical data by plotting energy in units of $\bar{\epsilon}^{1/4}\nu_0^{5/4}$ and wave number in units of $\Lambda=\bar{\epsilon}^{1/4}\nu_0^{-3/4}$ for various different values of $\bar{\epsilon}$ and ν_0. If this relation is valid, all data sets should collapse onto the single universal curve $C_K x^{-5/3}F(x)$. The validity of (5.12) was confirmed by early measurements [2], but was called into question by later data [42]. Note that, more generally, in order to go beyond the Kolmogorov theory, one should multiply Eq. (4.81) by a scaling function $F(k/\Lambda)$. Scaling collapse would then be obtained by plotting $E(k)/\bar{\epsilon}^{2/3}l_p^{5/3-\zeta}\Lambda^{-\zeta}$ versus k/Λ. Notice that the outer length scale l_p now enters and it would be interesting to check the experimental data for such dependence.

In order to construct a more general phenomenology for Λ, let us assume that the dynamics of the dissipation process has an associated dissipation *frequency* $\omega_\Lambda=1/\tau_\Lambda$. It has been proposed [43] that the relation between ω_Λ and Λ should reflect an *intrinsic* dynamical exponent z_{int} via $\omega_\Lambda\sim t_0^{-1}(\Lambda/m_0)^{z_{\mathrm{int}}}$, with, as argued above, $z_{\mathrm{int}}<1$. The energy dissipation rate at length scale Λ is proportional to $\nu_0\Lambda^2E(\Lambda)$. Dividing this by the energy content $E(\Lambda)$ at scale Λ, we may then postulate that $\omega_\Lambda\sim\nu_0\Lambda^2$. Thus τ_Λ is proportional to the half-life of an eddy at the boundary between the inertial and dissipation ranges. The hope, then, is that at this crossover scale, dissipation is still sufficiently weak that it can be used as a *probe* of the inertial range dynamics without fundamentally altering them. If this is true, it is reasonable that τ_Λ be of the same order as the intrinsic turnover time at scale Λ in the *absence* of dissipation. This definition yields

$$\frac{\Lambda}{m_0}\sim\mathrm{Re}^{1/(2-z_{\mathrm{int}})} \tag{5.13}$$

and this may be taken as the *definition* of z_{int}. The Kolmogorov theory evidently predicts that $z_{\mathrm{int}}=\frac{2}{3}$, which matches the data rather well [2,42]. However, before taking this as a further vindication of the Kolmogorov theory, one should attempt to relate z_{int} more generally to other known exponents. We shall now argue that $z_{\mathrm{int}}=\zeta-1$ and is therefore really just the Kolmogorov exponent in disguise. Its proximity to $\frac{2}{3}$ is not an independent result, but is already implied by the proximity of ζ to $\frac{5}{3}$.

Let us first compute z_{int} explicitly in the spherical limit. Consider Eq. (4.41), but now generalized to include the ν_0k^2 viscous term, to be treated as a small perturbation:

$$\frac{1}{g(s;x;y_\nu)}=-is+g(s;x;y_\nu)+\frac{\nu_0}{\tilde{\nu}}m_0^{2-z}x^{2-z}+x^{d+2-\Delta-z}\frac{1}{u_0}\Delta J_b(s;x;y_\nu)\ , \tag{5.14}$$

where $y_\nu\propto\nu_0$ is an appropriate viscous scaling variable, to be determined below. In the limit $x\to\infty$ and $\nu_0\to 0$, Eq. (4.38) for $g(s)$ is recovered. Corrections to this are obtained by treating the remaining terms as perturbations and performing an expansion of the form

$$g(s;x;y_\nu)=g(s)+x^{d+2-\Delta-z}g_1(s;y_\nu)+\cdots\ , \tag{5.15}$$

which then yields

$$g_1(s;y_\nu)=\frac{\frac{1}{u_0}\Delta J_b(s;y_\nu)+\frac{\nu_0}{\tilde{\nu}}m_0^{2-z}x^{\Delta-d}}{1+\frac{1}{g(s)^2}}\ , \tag{5.16}$$

and this may be substituted into (4.46) (generalized, in the obvious way, to include ν_0) in order to calculate $u(s;y_\nu)$. This equation is valid as long as the second term in the numerator is, at most, of the same order as the first, i.e., in the formal limit $x\to\infty$ and $m_0\to 0$, but

$$y_\nu\equiv\frac{\nu_0}{\tilde{\nu}}m_0^{2-z}x^{\Delta-d} \tag{5.17}$$

finite. Clearly y_ν is the new scaling variable that we seek. When $y_\nu\to 0$ we recover the unbounded inertial range described by (4.44); when y_ν becomes large dissipation has a strong effect and the inertial range power-law spectra are cut off. Note that the response function $g(s;y_\nu)\approx g(s)$ is insensitive to the dissipation unless $(\nu_0/\tilde{\nu})m_0^{2-z}x^{2-z}=\nu_0k/\lambda_0v_0\ll y_\nu$ is of order unity, i.e., only very deep into the dissipation range. We may define a crossover scale $x_\Lambda\equiv\Lambda/m_0$ separating the two limits via

$$y_\nu=1\Longrightarrow x_\Lambda=\left[\frac{\tilde{\nu}}{\nu_0m_0^{2-z}}\right]^{1/(\Delta-d)}\ . \tag{5.18}$$

From (4.75), (4.37), and the results in Sec. IV G, we have (using now $z=1$)

$$\frac{\tilde{\nu}}{\nu_0m_0^{2-z}}=\frac{\lambda_0v_0}{\nu_0m_0}=\frac{\lambda_0v_0l_0}{\nu_0}\propto\mathrm{Re}\ . \tag{5.19}$$

Thus

$$\frac{\Lambda}{m_0} \propto \mathrm{Re}^{1/(\Delta-d)} = \mathrm{Re}^{2/3} , \tag{5.20}$$

i.e., $z_{\mathrm{int}} = d + 2 - \Delta = \frac{1}{2}$. We see, then, that even in the spherical limit, nontrivial scaling of dissipation with Reynolds number occurs. Note that $\frac{3}{4}$ and $\frac{2}{3}$ do not differ by very much.

Now let us derive a *general* relation between z_{int} and ζ containing both the spherical and Kolmogorov results. The derivation relies crucially on the assumption of locality discussed in Sec. IV F. Consider the energy balance equation (4.63). Far outside the driving range one has

$$\nu_0 k^2 E(k) = -\frac{d-1}{2} \rho_0 \frac{\partial \Pi}{\partial k} , \tag{5.21}$$

where we have used (4.68). In the inertial range both sides of this equation essentially vanish. Let us define the scale Λ as that at which the energy flux $\Pi(k)$ differs significantly from its inertial range value $\bar{\epsilon}$. Consider then

$$\int_{k_0}^{\Lambda} \nu_0 k^2 E(k) dk = \frac{d-1}{2} \rho_0 [\Pi(k_0) - \Pi(\Lambda)] , \tag{5.22}$$

where k_0 lies in the inertial range $m_0 \ll k_0 \ll \Lambda$ and the right-hand side is defined to be of order $\bar{\epsilon}$. We estimate the left-hand side using the inertial range spectrum [see (4.81)]

$$E(k) = C_K' \rho_0 \bar{\epsilon}^{2/3} \left[\frac{v_p^3}{\bar{\epsilon}} \right]^{5/3-\zeta} k^{-\zeta} , \tag{5.23}$$

where $\lambda_0^3 v_p^3 / \bar{\epsilon} = l_p$ is the outer length scale [see (4.78)]. Up to factors of order unity, we may then define Λ via

$$\nu_0 \bar{\epsilon}^{2/3} \left[\frac{v_p^3}{\bar{\epsilon}} \right]^{5/3-\zeta} \Lambda^{3-\zeta} = \bar{\epsilon} , \tag{5.24}$$

which yields

$$\frac{\Lambda}{m_0} \sim \frac{l_p}{l_\nu} = \left[\frac{\bar{\epsilon}^{1/3} l_p^{4/3}}{\nu_0} \right]^{1/(3-\zeta)} = \left[\frac{v_p l_p}{\nu_0} \right]^{1/(3-\zeta)} = \mathrm{Re}^{1/(3-\zeta)} \tag{5.25}$$

and hence

$$z_{\mathrm{int}} = \zeta - 1 , \tag{5.26}$$

as claimed. From this argument one sees that $\omega_\Lambda \sim \Pi'(\Lambda)/E(\Lambda)$ is intrinsic to the energy transfer function and therefore involves correlation functions that are of third order in the velocity field.

The most important observation is, then, that it is possible to define internal dynamical exponents different from z, but that it is important to seek general scaling relations that relate them to previously defined exponents in order to understand their significance. Information about them will generally reside in higher-order correlation functions.

C. Work for the future

The large-N technique has wide applicability, limited only by one's ability to invent suitable generalized equations of motion. One particularly interesting model, for which the formalism presented in this paper goes over almost without change, is the Kardar-Parisi-Zhang (KPZ) equation for interface growth [44]. Here one considers an interface height field $h(\mathbf{r},t)$ obeying the equation

$$\frac{\partial h}{\partial t} = \kappa_0 \nabla^2 h - \tfrac{1}{2} \lambda_0 |\nabla h|^2 + \phi(\mathbf{r},t) , \tag{5.27}$$

where $\phi(\mathbf{r},t)$ describes the stochastic "raining" of particles onto the interface, $\langle \phi(\mathbf{r},t) \rangle = \phi_0$ being the average growth rate, κ_0 is the diffusion constant for adsorbed particles, and the nonlinear term is the simplest one can add that breaks the symmetry in $h \leftrightarrow -h$ (i.e., with or against the direction of growth). Defining $\mathbf{u} = \nabla h$ and $\mathbf{f} = \nabla \phi$, this equation becomes

$$\frac{\partial \mathbf{u}}{\partial t} + \lambda_0 (\mathbf{u} \cdot \nabla) \mathbf{u} = \kappa_0 \nabla^2 \mathbf{u} + \mathbf{f}, \quad \nabla \times \mathbf{u} = \nabla \times \mathbf{f} = \mathbf{0} , \tag{5.28}$$

which is just Burger's equation. It is now obvious how to generalize this equation to N fields. The topological structure of the diagrammatic perturbation theory in λ_0 is identical to that for the incompressible Navier-Stokes equations; in particular all of the considerations in Sec. III leading to the $N \to \infty$ limit can be taken over without change and a pair of coupled nonlinear integral equations for the response and correlation functions can be derived in this limit [45]. Of special interest is the height-height correlation function

$$\langle [h(\mathbf{r}) - h(\mathbf{r}')]^2 \rangle \sim |\mathbf{r} - \mathbf{r}'|^{\omega}, \quad |\mathbf{r} - \mathbf{r}'| \to \infty , \tag{5.29}$$

which measures the surface roughness (the larger the exponent ω, the rougher the surface). The major conceptual difference between incompressible turbulence and the KPZ equation is the form of the driving spectrum. Whereas turbulence corresponds to a spectrum concentrated around zero wave number, the growth model is driven by white noise, i.e., "uncorrelated raindrops." The driving spectrum is therefore constant in momentum space and the dimension of interest is $d = 2$ (the interface being a *surface* in $d = 3$). This corresponds to $y = 2$ and, as for the DIA equations, there are no infrared divergences. Unfortunately, although Burger's equation does have a renormalization group expansion for small $y > 0$ [5(a)], exact results to all orders do not exist. Thus, not only are the exponents unknown in $d = 2$, but the infrared divergences that *simplified* the analysis in Sec. IV are no longer present. One must now solve numerically for *both* scaling functions simultaneously, with scaling variables no longer restricted to a finite interval. Doherty *et al.* [45] have used a simple scaling ansatz based on a fluctuation-dissipation relation (rigorously valid only in $d = 1$) to estimate the exponents as a function of d, obtaining an upper critical dimension $d_u \approx 3.6$ at which $z = 2$. However, the full numerical problem has now been solved by Tu [46], who finds no upper critical dimension.

Other problems of interest include turbulence in nonlinear waves, especially capillary and gravity waves on

fluid surfaces; transmission of waves, especially electromagnetic waves, through disordered media; and coupled map models of spatiotemporal chaos (Sompolinsky, Crisanti, and Sommers [47] have considered large-N limits of such models, but without the extra group symmetry emphasized here; it would be interesting to reconsider their results within our formalism).

In terms of more direct extensions of our results for the Navier-Stokes equations, we have already mentioned the importance of a more detailed study of model II, especially regarding the effects of Galilean invariance. A more interesting, but highly speculative idea would be to investigate an N-component generalization of the Lagrangian history formalism. In principle, this is straightforward to do: one now needs N diffeomorphisms $\mathbf{r}^l(\mathbf{x},t_0|t)$ that define the position at time t of a particle being swept along by velocity field $\mathbf{v}^l$, given that it was at point $\mathbf{x}$ at time t_0. One could then define correlation functions analogous to (5.10). The fundamental question here is whether or not the spherical limit yields an exactly soluble set of LHDIA-type equations and how they compare to those of Kraichnan [16].

There are deeper, more formal questions underlying the one above. One can think of the diffeomorphisms $\mathbf{r}^l(\mathbf{x},t_0|t)$ as providing a family of gauge transformations, parametrized by the reference time t_0, between different but entirely equivalent coordinate systems [48]. One knows from gauge theories in quantum field theory that it is important to be able to do perturbation theory, order by order, in a gauge-invariant fashion: physical quantities must not depend on the choice of gauge. Standard fluid dynamics perturbation theory in λ_0 is *not* gauge invariant and this lack lies at the root of all problems dealing with the relation between Lagrangian and Eulerian viewpoints. Attempts to develop a gauge-invariant perturbation theory have, so far, been unsuccessful. The large-N method, in principle, avoids these problems by yielding an exact solution in a given fixed gauge (i.e., N-fold Eulerian coordinates), but if one could understand what this exact solution looks like in other gauges, one might gain some insight into how to develop a proper gauge-invariant perturbation theory at $N=1$.

Along different lines, the most difficult, and possibly most important, extension of our results would be to compute the first nontrivial correction to the spherical limit in powers of $1/N$. As stated in Sec. III C, the investigations of Amit and Roginsky[26] into the large-N behavior of the Wigner $(3kj)$ coefficients suggest that the next-order terms should be of order $1/N^\alpha$ with $\alpha=\frac{1}{2}$. At this order the $6j$ coefficients and the $9j$ coefficients (see Fig. 7) contribute. The evidence for this is largely numerical and much more work would be needed to establish these results in detail. The $6j$ coefficients yield seven new diagrams that must be added to the DIA equations and the $9j$ coefficients even more. Another strange feature is that the $6j$ coefficients *oscillate in sign* periodically with N with a finite period [24]. Such behavior in the scaling exponents would be rather odd, to say the least.

These difficulties with the $O(3)$ Wigner symbols lead us to believe that a different sequence of groups should be found that allow for a simpler analysis at large N. Most optimistically we would like only the analogs of the $6j$ symbols, i.e., diagrams with only two more vertices, to appear as leading corrections. In any case, once the appropriate diagrams are identified [49], one would seek corrected scaling functions in the form

$$g(s)=g_{\mathrm{DIA}}(s)+\frac{1}{N^\alpha}g_1(s)+\cdots,$$
$$u(s)=u_{\mathrm{DIA}}(s)+\frac{1}{N^\alpha}u_1(s)+\cdots \tag{5.30}$$

and a corrected Kolmogorov exponent in the form

$$\zeta=\frac{3}{2}+\frac{\zeta_1}{N^\alpha}+\cdots \tag{5.31}$$

and extract ζ_1, g_1, and u_1 (probably numerically) from the resulting integral equations. One is guided here by the $1/N$ expansion for the N-vector spin models: the correction ζ_1, for example, will appear as a *logarithmic correction* to the Kolmogorov spectrum

$$E(k)\approx\frac{E_0}{k^{3/2}}\left[1-\frac{\zeta_1}{N^\alpha}\ln(k/m_0)+\cdots\right]. \tag{5.32}$$

The expression in large square brackets is exponentiated to yield (5.31). One therefore needs to extract a $k^{-3/2}\ln(k)$ dependence from the new terms, with the universal coefficient ζ_1/N^α. It is possible, of course, that such logarithmic corrections will not exist at any finite order in $1/N$, in which case we would conclude either that corrections are exponentially small in N or that the large-N expansion is simply not systematic. However, a confirmation of (5.31) would definitively establish our method and, for the first time, provide a systematic means of calculating properties of the turbulent inertial range and truly test the assumptions underlying the Kolmogorov picture.

It should be emphasized that the group theory is required only to produce the set of exponents $\alpha_{2k}^{(i)}$ and corresponding coefficients $J_{2k}^{(i)}(N)$ [see (3.9)]. If one optimistically *assumes* that a sequence of group representations can be found that yield only the tetrahedron graph I_4 [see Fig. 7(b)], as the leading correction, one could then parametrize this correction using a single combined variable $\epsilon\equiv J_4(N)N^{1-\alpha_4}$, without actually needing to know the exact form of the right-hand side. Thus only ϵ will appear in (5.30) and (5.31), e.g., $\zeta=\frac{3}{2}+\epsilon\tilde{\zeta}_1+\cdots$, where $\tilde{\zeta}_1$ is a universal number. It would be very interesting, then, to calculate $\tilde{\zeta}_1$. This calculation would be completely independent of all group theoretical considerations, involving only the next in the usual sequence of self-consistent integral equations for $\hat{G}$ and $\hat{U}$ [20,38]. Further group theoretical investigations could then be carried out separately in parallel.

ACKNOWLEDGMENTS

We have benefited from conversations and communications with M. C. Cross, D. I. Meiron, E. D. Siggia, G. Falkovich, J. Miller, R. H. Kraichnan, D. R. Nelson, D.

S. Fisher, M. E. Fisher, A. Ludwig, M. Nelkin, N. Goldenfeld, P. Dimotakis, and B. Shraiman. We especially thank G. L. Eyink for many stimulating conversations, particularly regarding the problem of Galilean invariance and the proper role of renormalization group theory in turbulence, and P. C. Hohenberg for helping us clarify the proper formulation of universal scaling in turbulence. We thank the Aspen Center for Physics for hospitality during the final stages of this work. The financial support of the ONR, through Grant No. N0001491-J-1600, Dowell Schlumberger (C.-Y.M.), and the Sloan Foundation is also gratefully acknowledged.

APPENDIX A: GALILEAN INVARIANCE, WARD IDENTITIES, AND THE EXTENDED MULTICOMPONENT MODEL

The exactness of the exponent relations (1.15) and (1.19) to all orders in y for the usual Navier-Stokes equations is closely related to Galilean invariance. In this appendix we shall discuss this issue for general N. It will turn out that a similar result can be proven only for the extended model discussed in Sec. II F. Without the additional zero mode, the argument fails.

We begin by generalizing the partition function to include source fields $\mathbf{J}_1^l(\mathbf{r},t)$ and $\mathbf{J}_2^l(\mathbf{r},t)$. Thus define [see (2.20)]

$$Z[\mathbf{J}_1,\mathbf{J}_2]=\int D\mathbf{v}\int D\mathbf{w}\exp\left\{\mathcal{L}[\mathbf{v},\mathbf{w}]+\int dt\int d^dr\sum_l[\mathbf{J}_1^l\cdot\mathbf{v}_l+\mathbf{J}_2^l\cdot\mathbf{w}_l+\text{c.c.}]\right\} \tag{A1}$$

with the associated "free energy"

$$F[\mathbf{J}_1,\mathbf{J}_2]=-\ln Z[\mathbf{J}_1,\mathbf{J}_2]\ , \tag{A2}$$

which generates the connected correlation functions [50]. The vertex generating function $\Gamma[\bar{\mathbf{v}},\bar{\mathbf{w}}]$ is obtained by performing a Legendre transform on F:

$$\Gamma[\bar{\mathbf{v}},\bar{\mathbf{w}}]=F[\mathbf{J}_1,\mathbf{J}_2]+\int dt\int d^dr\sum_l[\mathbf{J}_1^l\cdot\bar{\mathbf{v}}_l+\mathbf{J}_2^l\cdot\bar{\mathbf{w}}_l+\text{c.c.}]\ , \tag{A3}$$

where the equations

$$\bar{\mathbf{v}}^l(\mathbf{r},t)\equiv\langle\mathbf{v}^l(\mathbf{r},t)\rangle=-\frac{\delta F}{\delta\mathbf{J}_{1,l}(\mathbf{r},t)}\ ,\qquad \bar{\mathbf{w}}^l(\mathbf{r},t)\equiv\langle\mathbf{w}^l(\mathbf{r},t)\rangle=-\frac{\delta F}{\delta\mathbf{J}_{2,l}(\mathbf{r},t)} \tag{A4}$$

are to be used to eliminate $\mathbf{J}_1^l$ and $\mathbf{J}_2^l$ in favor of $\bar{\mathbf{v}}^l$ and $\bar{\mathbf{w}}^l$. It is clear that $\bar{\mathbf{v}}^l$ and $\bar{\mathbf{w}}^l$ vanish when $\mathbf{J}_1^l$ and $\mathbf{J}_2^l$ do.

We now consider the effect of a Galilean transformation on the vertex functional. It is clear that $\bar{\mathbf{v}}^l$ and $\bar{\mathbf{w}}^l$ undergo precisely the same Galilean transformations that, respectively, $\mathbf{v}^l$ and $\mathbf{w}^l$ do (see Sec. II F). From (2.67) we see that the Lagrangian transforms via

$$\mathcal{L}[\mathbf{v}',\mathbf{w}']=\mathcal{L}[\mathbf{v},\mathbf{w}]+u_0\delta\mathcal{L}[\mathbf{v},\mathbf{w}]\ , \tag{A5}$$

where

$$\delta\mathcal{L}[\mathbf{v},\mathbf{w}]=\lambda_0\int d^dr\int dt\times\sum_l\left\{\mathbf{w}_l(\mathbf{r},t)\cdot(\hat{\mathbf{u}}\cdot\nabla)\left[\mathbf{v}^l-\frac{1}{\mu}\sum_n\bar{A}_{N,ln}(h)\mathbf{v}_n\right]+\text{c.c.}\right\}\ , \tag{A6}$$

where $\hat{\mathbf{u}}\equiv\mathbf{u}_0/u_0$ is a unit vector. The additive piece $u_0\delta\mathcal{L}$ vanishes identically only when an exact Galilean symmetry exists, i.e., only if (2.70) holds. In this case, taking $\mathbf{J}_1$ and $\mathbf{J}_2$ to transform in the same way that $\mathbf{w}$ and $\bar{\mathbf{w}}$ do, we have the exact relations

$$\mathcal{L}[\mathbf{v}',\mathbf{w}']=\mathcal{L}[\mathbf{v},\mathbf{w}]\ ,\qquad F[\mathbf{J}_1',\mathbf{J}_2']=F[\mathbf{J}_1,\mathbf{J}_2]+\int dt\int d^dr\,\mathbf{J}_1\cdot\mathbf{u}_0\ , \tag{A7}$$

$$\Gamma[\bar{\mathbf{v}}',\bar{\mathbf{w}}']=\Gamma[\bar{\mathbf{v}},\bar{\mathbf{w}}]\ .$$

Assume now that the transforming velocity $\mathbf{u}_0=u_0\hat{\mathbf{u}}$ is infinitesimal. Equation (A7) then yields, to $O(u_0)$,

$$0=\frac{1}{2}\int dt\int d^dr\times\sum_l\left\{\frac{\delta\Gamma}{\delta\bar{\mathbf{v}}^l(\mathbf{r},t)}\cdot\left[\lambda_0 t(\hat{\mathbf{u}}\cdot\nabla)\bar{\mathbf{v}}^l(\mathbf{r},t)-\frac{1}{\mu}h^l\hat{\mathbf{u}}\right]+\frac{\delta\Gamma}{\delta\bar{\mathbf{w}}^l(\mathbf{r},t)}\cdot\lambda_0 t(\mathbf{u}\cdot\nabla)\bar{\mathbf{w}}^l(\mathbf{r},t)+\text{c.c.}\right\}\ . \tag{A8}$$

Integration by parts yields

$$0=\frac{1}{2}\int dt\int d^dr\times\sum_l\left\{\lambda_0 t(\mathbf{u}\cdot\nabla)\frac{\delta\Gamma}{\delta\bar{\mathbf{v}}^l(\mathbf{r},t)}\cdot\bar{\mathbf{v}}^l(\mathbf{r},t)+\frac{1}{\mu}h^l\mathbf{u}\cdot\frac{\delta\Gamma}{\delta\bar{\mathbf{v}}^l(\mathbf{r},t)}+\lambda_0 t(\mathbf{u}\cdot\nabla)\frac{\delta\Gamma}{\delta\bar{\mathbf{w}}^l(\mathbf{r},t)}\cdot\bar{\mathbf{w}}^l(\mathbf{r},t)+\text{c.c.}\right\}\ . \tag{A9}$$

In the case that $\delta\mathcal{L}$ does not vanish identically, (A9) is valid with $\langle\delta\mathcal{L}\rangle_{u_0=0}$ appearing on the left-hand side. From this result one can obtain an infinite sequence of relations between vertex functions of different orders. The special case important to us is derived by functionally differentiating (A9) first with respect to $\bar{v}_\beta^m(\mathbf{r}_1,t_1)$, then with respect to $\bar{w}_{\gamma,n}(\mathbf{r}_2,t_2)$, and finally setting $\bar{\mathbf{v}}=\bar{\mathbf{w}}\equiv 0$:

$$0=\lambda_0(t_2-t_1)(\mathbf{u}\cdot\nabla_2)\frac{\delta^2\Gamma}{\delta\bar{v}^m_\beta(\mathbf{r}_1,t_1)\delta\bar{w}_{\gamma,n}(\mathbf{r}_2,t_2)}+\frac{1}{2}\int dt\int d^dr$$
$$\times\sum_{\alpha,l}\left[\frac{1}{\mu}h^l\hat{u}_\alpha\frac{\delta^3\Gamma}{\delta\bar{v}^l_\alpha(\mathbf{r},t)\delta\bar{v}^m_\beta(\mathbf{r}_1,t_1)\delta\bar{w}_{\gamma,n}(\mathbf{r}_2,t_2)}+\frac{1}{\mu^*}h_l\hat{u}_\alpha\frac{\delta^3\Gamma}{\delta\bar{v}_{\alpha,l}(\mathbf{r},t)\delta\bar{v}^m_\beta(\mathbf{r}_1,t_1)\delta\bar{w}_{\gamma,n}(\mathbf{r}_2,t_2)}\right], \tag{A10}$$

or

$$0=\lambda_0(t_2-t_1)(\mathbf{u}\cdot\nabla)\Gamma^{(2)}_{v^m_\beta w_{\gamma,n}}(\mathbf{r}_2-\mathbf{r}_1,t_2-t_1)+\frac{1}{2}\int dt\int d^dr$$
$$\times\sum_{\alpha,l}\left[\frac{1}{\mu}h^l\hat{u}_\alpha\Gamma^{(3)}_{v^l_\alpha v^m_\beta w_{\gamma,n}}(\mathbf{r}_2-\mathbf{r},t_2-t;\mathbf{r}_1-\mathbf{r},t_1-t)+\frac{1}{\mu^*}h_l\hat{u}_\alpha\Gamma^{(3)}_{v_{\alpha,l}v^m_\beta w_{\gamma,n}}(\mathbf{r}_2-\mathbf{r},t_2-t;\mathbf{r}_1-\mathbf{r},t_1-t)\right]. \tag{A11}$$

Fourier transforming this result, using the fact that $\hat{\Gamma}^{(2)}_{v^m_\beta w_{\gamma,n}}(\mathbf{k},\omega)=\hat{\tau}_{\beta\gamma}(\mathbf{k})\hat{G}_m(\mathbf{k},\omega)^{-1}\delta^n_m$ and that the direction of $\hat{\mathbf{u}}$ is arbitrary, we obtain

$$0=\frac{1}{2}\lambda_0P_{\alpha\beta\gamma}(\mathbf{k})\frac{\partial}{\partial\omega}\hat{G}_m(\mathbf{k},\omega)^{-1}\delta^n_m$$
$$+\frac{1}{2}\sum_l\left[\frac{1}{\mu}h^l\tilde{\Gamma}^{(3)}_{v^l_\alpha v^m_\beta w_{\gamma,n}}(\mathbf{k},\omega;-\mathbf{k},-\omega)\right.$$
$$\left.+\frac{1}{\mu^*}h_l\tilde{\Gamma}^{(3)}_{v_{\alpha,l}v^m_\beta w_{\gamma,n}}(\mathbf{k},\omega;-\mathbf{k},-\omega)\right], \tag{A12}$$

where we have symmetrized the indices β and γ: $\tilde{\Gamma}^{(3)}_{\alpha\beta\gamma}\equiv\frac{1}{2}[\Gamma^{(3)}_{\alpha\beta\gamma}+\Gamma^{(3)}_{\alpha\gamma\beta}]$. Specializing to the extended model where $G_m=\mathcal{G}\delta_{m0}+G(1-\delta_{m0})$, μ is real, and $h^l=\delta_{l,0}$, we obtain finally

$$0=\frac{1}{2}\lambda_0P_{\alpha\beta\gamma}(\mathbf{k})\frac{\partial}{\partial\omega}\hat{G}(\mathbf{k},\omega)^{-1}$$
$$+\frac{1}{\mu}\tilde{\Gamma}^{(3)}_{v^0_\alpha v^m_\beta w_{\gamma,m}}(\mathbf{k},\omega;-\mathbf{k},-\omega)\quad(m\neq0),$$
$$0=\frac{1}{2}\lambda_0P_{\alpha\beta\gamma}(\mathbf{k})\frac{\partial}{\partial\omega}\hat{\mathcal{G}}(\mathbf{k},\omega)^{-1} \tag{A13}$$
$$+\frac{1}{\mu}\tilde{\Gamma}^{(3)}_{v^0_\alpha v^0_\beta w_{\gamma,0}}(\mathbf{k},\omega;-\mathbf{k},-\omega)\quad(m=0).$$

Equation (A13) is the Ward identity we seek. Following the arguments given by DeDominicis and Martin [5(b)], this identity implies that $\tilde{\Gamma}^{(3)}$'s with at least one vanishing isospin index do not have ultraviolet divergences. By arguments similar to those of DeDominicis and Martin [5(b)], this implies that (1.15) and (1.19) hold for the *zero-mode* correlation functions $\hat{\mathcal{G}}$ and $\hat{\mathcal{U}}$.

The remaining modes, with correlation functions G and U, *do not necessarily* obey (1.15) and (1.19) except when $N\to\infty$. Only diagrams beyond the lowest-order bubbles have sufficient structure to violate (A13) when all indices are nonzero. To see this, it is useful to translate (A13) into diagrammatic language. Consider first the space-time parts of the diagrams. The ω derivative acting on a graph may be defined in such a way that it produces a sum of terms in which G_0 is replaced by $\partial G_0/\partial\omega=iG_0^2$ along a unique sequence of G_0 bonds [the "bare backbone" of the graph [3(b)] connecting the two external legs. This is precisely equivalent to summing over all diagrams obtained by attaching a third external leg with zero frequency and zero momentum to the middle of each of these bonds. However, $\tilde{\Gamma}^{(3)}$ is obtained by summing over all diagrams obtained by attaching such a leg to the middle of *every* bond in the graph (U_0 bonds are then replaced by $\partial U_0/\partial\omega=iU_0[G_0-G_0^*]$). The two turn out to be equal because a sequence of integrations by parts on the *internal* frequencies allows one to transfer all derivatives in the latter onto the bare backbone. This property is not obvious and would probably not have been discovered without the shortcut derivation obtained via Galilean invariance. However, we have neglected to discuss the effect of this newly attached leg on the isospin symmetry factors. If the attached leg has nonzero isospin index l, the bond, which is really just g^{mn}_N, is replaced by $\sum_{m'n'}\bar{A}^{lm'n'}_N\delta^m_{m'}\delta^n_{n'}=\bar{A}^{lmn}_N$, whereas if $l=0$, $\bar{g}^{mn}_N$ is replaced by $\bar{g}^{m'n'}_N\delta^m_{m'}\delta^n_{n'}=\bar{g}^{mn}_N$, i.e., is *unchanged*. Therefore, in the former case the symmetry factor for the diagram depends in a nontrivial way upon which bond the third leg is attached to (except in the case of the bubble graphs, in which all bonds are essentially equivalent) and the integration by parts process mentioned above *fails*: the required delicate cancellations no longer occur. However, in the latter case, the symmetry factors are all unchanged and the relations (A13) between $(\partial/\partial\omega)G^{-1}$, $(\partial/\partial\omega)\mathcal{G}^{-1}$, and $\tilde{\Gamma}^{(3)m}_{0m}$ are recovered.

APPENDIX B: THE VON KÁRMÁN–HOWARTH RESULT

In this appendix we discuss one of the few exact results that exist in the turbulence literature. This result due to von Kármán and Howarth [1(b)], originally derived for freely decaying turbulence, but valid also for stochastically driven turbulence, states that for a fluid in a homogeneous, isotropic turbulent state the third-order radial velocity correlator has the form

$$\langle\{[\mathbf{v}(\mathbf{r})-\mathbf{v}(\mathbf{0})]\cdot\hat{\mathbf{r}}\}^3\rangle=-\tfrac{4}{5}\bar{\epsilon}r,\quad l_\nu\ll r\ll l_0, \tag{B1}$$

where $\hat{\mathbf{r}}=\mathbf{r}/r$, $\bar{\epsilon}$ is the energy dissipation rate (see below), and l_0 and l_ν were defined in Sec. I A. The average is now obtained by integrating over all positions of the ori-

gin **0** at the given fixed time t (which we usually suppress from our notation). In order to motivate, once again, our claim that Eq. (2.1) represents an appropriate generalization of the Navier-Stokes equations, we will now derive the analogous result appropriate to general N.

In momentum space, incompressibility implies that all correlation functions involve the transverse projection operator $\hat{\tau}_{\alpha\beta}(\mathbf{k})$. In real space this implies certain differential relations among the correlators for different components of the velocity field. For example, if we define

$$B^{lm}_{\alpha\beta}(r)=\langle [v^l_\alpha(\mathbf{r})-v^l_\alpha(\mathbf{0})][v^m_\beta(\mathbf{r})-v^m_\beta(\mathbf{0})]\rangle \ , \tag{B2}$$

where we have now included the isospin index on $\mathbf{v}$, then [1(b)]

$$B^{lm}_{tt}=\frac{1}{2r^{d-2}}\frac{d}{dr}(r^{d-1}B^{lm}_{rr}), \quad B^{lm}_{rt}=B^{lm}_{rt}=0 \ . \tag{B3}$$

We have used the notation $B^{lm}_{rr}=\sum_{\alpha,\beta}\hat{r}_\alpha B^{lm}_{\alpha\beta}\hat{r}_\beta$, $B^{lm}_{tt}=\sum_{\alpha,\beta}\hat{t}_\alpha B^{lm}_{\alpha\beta}\hat{t}_\beta$, etc., where $\hat{\mathbf{t}}$ is any unit vector transverse to $\hat{\mathbf{r}}$: $\hat{\mathbf{r}}\cdot\hat{\mathbf{t}}=0$. Similarly, if define the third moments

$$B^{lmn}_{\alpha\beta\gamma}(r)=\langle [v^l_\alpha(\mathbf{r})-v^l_\alpha(\mathbf{0})][v^m_\beta(\mathbf{r})-v^m_\beta(\mathbf{0})] \times[v^n_\gamma(\mathbf{r})-v^n_\gamma(\mathbf{0})]\rangle \ , \tag{B4}$$

then

$$B^{lmn}_{rtt}=\frac{1}{3(d-1)r^{d-3}}\frac{d}{dr}(r^{d-2}B^{lmn}_{rrr}) \ , \qquad B^{lmn}_{rrt}=B^{lmn}_{ttt}=0 \ . \tag{B5}$$

These are trivial generalizations of the relations that hold when $N=1$.

Using the generalized Navier-Stokes equations (2.1), we may derive a relation between the second and third moments. Consider then

$$\begin{aligned}\frac{\partial}{\partial t}\sum_l\langle v^l_\alpha(\mathbf{r})v_{\beta,l}(\mathbf{r}')\rangle=&-\lambda_0\sum_{l,m,n}\sum_\gamma A^{lmn}_N\frac{\partial}{\partial r_\gamma}\langle v_{\gamma,m}(\mathbf{r})v_{\alpha,n}(\mathbf{r})v_{\beta,l}(\mathbf{r}')\rangle\\ &-\lambda_0\sum_{l,m,n}\sum_\gamma A_{N,lmn}\frac{\partial}{\partial r'_\gamma}\langle v^l_\alpha(\mathbf{r})v^m_\gamma(\mathbf{r}')v^n_\beta(\mathbf{r}')\rangle-\frac{1}{\rho_0}\sum_l\frac{\partial}{\partial r_\alpha}\langle p^l(\mathbf{r})v_{\beta,l}(\mathbf{r}')\rangle\\ &-\frac{1}{\rho_0}\sum_l\frac{\partial}{\partial r'_\alpha}\langle v'_\alpha(\mathbf{r})p_l(\mathbf{r}')\rangle+\nu_0\sum_l\nabla^2\langle v^l_\alpha(\mathbf{r})v_{\beta,l}(\mathbf{r}')\rangle+\nu_0\sum_l\nabla'^2\langle v^l_\alpha(\mathbf{r})v_{\beta,l}(\mathbf{r}')\rangle \ .\end{aligned} \tag{B6}$$

Isotropy implies that $\langle p^l(\mathbf{r})v_{\beta,m}(\mathbf{r}')\rangle=0$ [1(b)]. Translation invariance and isotropy imply that both sides of (B6) are functions only of $|\mathbf{r}-\mathbf{r}'|$. Therefore, if we define

$$\begin{aligned}b^{lm}_{\alpha\beta}(r)&=\langle v^l_\alpha(\mathbf{r})v^m_\beta(\mathbf{0})\rangle \ ,\\ b^{lm,n}_{\alpha\beta,\gamma}(r)&=\langle v^l_\alpha(\mathbf{r})v^m_\beta(\mathbf{r})v^n_\gamma(\mathbf{0})\rangle\\ &=-\langle v^l_\alpha(\mathbf{0})v^m_\beta(\mathbf{0})v^n_\gamma(\mathbf{r})\rangle \ ,\end{aligned} \tag{B7}$$

then

$$\frac{\partial}{\partial t}\sum_l b^l_{\alpha,l\beta}=\lambda_0\sum_{l,m,n}\sum_\gamma\frac{\partial}{\partial r_\gamma}[A^{lmn}_N b_{\alpha n,\gamma m;\beta l}+A_{N,lmn}b^{mn,l}_{\gamma\beta,\alpha}] +2\nu_0\nabla^2\sum_l b^l_{\alpha,l\beta} \ . \tag{B8}$$

One can relate $b^{lm,n}_{\alpha\beta,\gamma}$ to B^{lmn}_{rrr} via [1(b)]

$$\begin{aligned}b^{lm,n}_{\alpha\beta,\gamma}=&-\frac{1}{6(d-1)}B^{lmn}_{rrr}\delta_{\alpha\beta}\hat{r}_\gamma\\ &+\frac{1}{12(d-1)}\left[r\frac{\partial}{\partial r}B^{lmn}_{rrr}+(d-1)B^{lmn}_{rrr}\right]\\ &\times(\delta_{\beta\gamma}\hat{r}_\alpha+\delta_{\alpha\gamma}\hat{r}_\beta)\\ &-\frac{1}{6(d-1)}\left[r\frac{\partial}{\partial r}B^{lmn}_{rrr}-B^{lmn}_{rrr}\right]\hat{r}_\alpha\hat{r}_\beta\hat{r}_\gamma \ .\end{aligned} \tag{B9}$$

Using this, (B8) may be reduced to

$$\begin{aligned}-\frac{2}{d}\bar{\epsilon}-\frac{1}{2}\frac{\partial}{\partial t}\sum_l B^l_{r,lr}&=\lambda_0\frac{1}{6r^{d+1}}\frac{\partial}{\partial r}\left[r^{d+1}\sum_{l,m,n}A_{N,lmn}B^{lmn}_{rrr}\right]\\ &-\frac{\nu_0}{r^{d+1}}\frac{\partial}{\partial r}\left[r^{d+1}\sum_l\frac{\partial}{\partial r}B^l_{r,lr}\right] \ ,\end{aligned} \tag{B10}$$

where $\rho_0\bar{\epsilon}=-(\partial/\partial t)\langle\varepsilon\rangle$ is the energy dissipation rate (see Eq. (2.32) for the definition of ε; note that the $\bar{\epsilon}$ used here is $[(d-1)/2]N$ times the flux $\bar{\epsilon}$ used in Secs. IV and V). In deriving this equation we have used the identity [1(b)] $\sum_l b^l_{\alpha,l\beta}=(2/\rho_0 d)\langle\varepsilon\rangle\delta_{\alpha\beta}-\frac{1}{2}\sum_l B^l_{\alpha,l\beta}$. Equation (B10) is the result we seek. Specializing now to the inertial range, we assume, first, that $\sum_l B^l_{r,lr}(r)$ varies only on the scale of the turnover time of the largest structures of size l_0 and is therefore a much slower function of time than is $\langle\varepsilon\rangle$. This is a locality assumption, i.e., an assumption that the large scales do not significantly affect the detailed correlations in the inertial range. We also assume, as usual, that the viscosity ν_0 may be neglected. We therefore have

$$-\frac{2}{d}\bar{\epsilon}=\frac{\lambda_0}{6r^{d+1}}\frac{\partial}{\partial r}\left[r^{d+1}\sum_{l,m,n}A_{N,lmn}B^{lmn}_{rrr}\right] \ , \tag{B11}$$

$$l_\nu\ll r\ll l_0 \ ,$$

which may be integrated [noting that $B^{lmn}_{rrr}(0)=0$] to yield

$$\lambda_0 \sum_{l,m,n} A_{N,lmn} \langle \hat{\mathbf{r}}\cdot[\mathbf{v}^l(\mathbf{r})-\mathbf{v}^l(\mathbf{0})]\hat{\mathbf{r}}\cdot[\mathbf{v}^m(\mathbf{r})-\mathbf{v}^m(\mathbf{0})] \times \hat{\mathbf{r}}\cdot[\mathbf{v}^n(\mathbf{r})-\mathbf{v}^n(\mathbf{0})]\rangle = -\frac{12}{d(d+2)}\bar{\epsilon} r \ . \quad \text{(B12)}$$

This is the appropriate generalization of (B1).

We have done this calculation under the assumption that the turbulence is freely decaying. This same result actually holds for steady state driven turbulence as well. The point is that even though the left-hand side of (B6) now vanishes, there is now an extra term on the right coming from the driving force, which then contributes a term corresponding to the large-scale energy input rate to the right-hand side of (B10). Locality ensures that this energy input rate is precisely the same as the dissipation rate appearing in (B10) and hence that (B12) is still correct as written.

It is worth discussing the relationship between the von Kármán–Howarth result and the definition of the energy flux used in Sec. IV F [see especially Eq. (4.63) and below]. The Fourier transform of (4.63) [with (4.72)] is precisely (B8). In real space, Eq. (B11) is just a more compact rewrite of (B8). In momentum space, the direct use of (B8) is more convenient. Under the assumption, embodied in (4.66), of an inertial range with a constant energy flux, the energy balance equation (4.63) implies that the right-hand side of (4.68) is negative, with total integrated area $-\bar{\epsilon}$, in the driving range $k \lesssim m_0$; is positive, with total integrated area $\bar{\epsilon}$, is the dissipation range $k \gtrsim \Lambda$; and is zero in the inertial range $m_0 \ll k \ll \Lambda$. The inverse Fourier transform of this right-hand side, which is proportional to the first term on the right-hand side of (B8), therefore vanishes for $r \gg 1/m_0$ and for $r \ll 1/\Lambda$ and yields precisely $-\bar{\epsilon}$ for $1/\Lambda \ll r \ll 1/m_0$. This result is precisely equivalent to (B11) and the von Kármán–Howarth result is then exactly the same as the statement of constant energy flux (4.69). In Sec. IV we prove directly the existence of a constant energy flux and therefore the validity of the von Kármán–Howarth result in the spherical limit.

Note that, as yet, no group-theoretic properties of A^{lmn}_N have been used. The von Kármán–Howarth result is therefore a rather weak constraint on the theory. Using the group-theoretic properties of A^{lmn}_N we may simplify the result considerably since the isospin index dependence of B^{lmn}_{rrr} is then known. For the simpler class of models, without the zero mode, one has $B^{lmn}_{rrr} \equiv B_{rrr} A^{lmn}_N$ and $B^{l}_{\alpha,m\beta} = B_{\alpha\beta}\delta^l_m$ and hence (B10) reads

$$-\frac{d-1}{d}\bar{\epsilon} - \frac{1}{2}\frac{\partial}{\partial t}B_{rr} = \lambda_0 \frac{1}{6r^{d+1}}\frac{\partial}{\partial r}(r^{d+1}B_{rrr}) - \frac{\nu_0}{r^{d+1}}\frac{\partial}{\partial r}\left[r^{d+1}\sum_l \frac{\partial}{\partial r}B_{rr}\right] , \quad \text{(B13)}$$

where we have chosen the normalization (3.8) and used $\bar{\epsilon} = [(d-1)/2]N\bar{\epsilon}$. Equation (B12) then reads

$$\lambda_0 B_{rrr} = -\frac{6(d-1)}{d(d+2)}\bar{\epsilon} r, \quad l_\nu \ll r \ll l_0 \ . \quad \text{(B14)}$$

Both equations are independent of N. It is straightforward to verify, using the results of Sec. IV F, that the solutions to the DIA equations explicitly satisfy (B14).

For the extended model we may derive two equations, one for the zero mode and one for all the rest. Using (3.28) we have (recall that $\mu = 1/\sqrt{N+1}$)

$$\begin{aligned} B^{lmn}_{rrr} &\equiv B^{>}_{rrr} A^{lmn}_N + \mu B^{0,>}_{rrr}(\delta_{l0}g^{mn}_N + \delta_{m0}g^{ln}_N + \delta_{n0}g^{mn}_N) \\ &\quad + \mu B^0_{rrr}\delta_{l0}\delta_{m0}\delta_{n0} \ , \\ B^{l}_{r,mr} &\equiv B^{>}_{rr}\delta^l_m + B^0_{rr}\delta_{l0}\delta_{m0} \ . \end{aligned} \quad \text{(B15)}$$

If we begin with (B6), but keep *only* the $l=0$ term in the sum over l, we obtain

$$-\frac{d-1}{d}\bar{\epsilon}^0 - \frac{1}{2}\frac{\partial}{\partial t}B^0_{rr} = \frac{\lambda_0}{6r^{d+1}}\frac{\partial}{\partial r}\left[r^{d+1}\left[\frac{N}{N+1}B^{0,>}_{rrr} + \frac{1}{N+1}B^0_{rrr}\right]\right] - \frac{\nu_0}{r^{d+1}}\frac{\partial}{\partial r}\left[r^{d+1}\frac{\partial}{\partial r}B^0_{rr}\right] , \quad \text{(B16)}$$

where $\bar{\epsilon}^0 = [1/(d-1)]\langle \mathbf{v}^0\cdot\mathbf{v}_0\rangle$. Equation (B14) then becomes

$$\lambda_0\left[\frac{N}{N+1}B^{0,>}_{rrr} + \frac{1}{N+1}B^0_{rrr}\right] = -\frac{6(d-1)}{d(d+2)}\bar{\epsilon}^0 r \ . \quad \text{(B17)}$$

Similarly, if the $l=0$ term is *dropped* from the sum over l, we obtain

$$-\frac{d-1}{d}\bar{\epsilon}^{>} - \frac{1}{2}\frac{\partial}{\partial t}B^{>}_{rr} = \frac{\lambda_0}{6r^{d+1}}\frac{\partial}{\partial r}\left[r^{d+1}\left[B^{>}_{rrr} + \frac{2}{N+1}B^{0,>}_{rrr}\right]\right] - \frac{\nu_0}{r^{d+1}}\frac{\partial}{\partial r}\left[r^{d+1}\frac{\partial}{\partial r}B^{>}_{rrr}\right] , \quad \text{(B18)}$$

where $\bar{\epsilon}^{>}[=1/(d-1)N]\sum_l \langle \mathbf{v}^l\cdot\mathbf{v}_l\rangle$. Equation (B14) therefore becomes

$$\lambda_0\left[B^{>}_{rrr} + \frac{2}{N+1}B^{0,>}_{rrr}\right] = -\frac{6(d-1)}{d(d+2)}\bar{\epsilon}^{>} r \ . \quad \text{(B19)}$$

APPENDIX C: CUBIC INVARIANTS FOR SU(M)

In this appendix we discuss trace invariants associated with SU(M). This group has $N=M^2-1$ generators and the main problem in dealing with them is finding the most convenient choice of basis. We shall examine the 't Hooft basis [51]. Let $M=2L+1$ be odd and define a two-dimensional grid of integers $\mathbf{n}=(n_1,n_2)$, with $-L \le n_1, n_2 \le L$. Then there exists a set of N $M\times M$ unitary matrices J_n labeled by $\mathbf{n}$, which satisfy

$$J_{\mathbf{n}'}J_{\mathbf{n}''}=e^{(2\pi i/M)\mathbf{n}'\times\mathbf{n}''}J_{\mathbf{n}'+\mathbf{n}''}\ , \tag{C1}$$

$$J_{\mathbf{n}}^{\dagger}=J_{-\mathbf{n}}=J_{\mathbf{n}}^{-1}\ , \tag{C2}$$

$$\frac{1}{M}\mathrm{tr}(J_{\mathbf{n}'}^{\dagger}J_{\mathbf{n}''})=\delta_{\mathbf{n}',\mathbf{n}''}\ , \tag{C3}$$

where $\mathbf{n}'\times\mathbf{n}''\equiv n_1'n_2''-n_2'n_1''$ and, for any integer vector $\mathbf{p}=(p_1,p_2)$, we use the periodicity convention

$$J_{\mathbf{n}+M\mathbf{p}}=J_{\mathbf{n}}\ . \tag{C4}$$

This allows one to make sense of (C1) when $\mathbf{n}'+\mathbf{n}''$ lies outside the allowed values of $\mathbf{n}$. Note that we define $J_0=\mathbf{I}$ to be the identity matrix, but it is not counted as one of the generators. The explicit matrix forms of the generators may be found in [51], but will not be required here. For later convenience we define the periodic δ function

$$\tilde{\delta}(\mathbf{n})=\begin{cases}1 & \text{if } \mathbf{n}=M\mathbf{p} \text{ for some } \mathbf{p}\\ 0 & \text{otherwise}\ .\end{cases} \tag{C5}$$

Since these matrices are unitary, not Hermitian, the group elements are generated by (2.35) with complex coefficients $a_{\mathbf{n}}(g)$ satisfying $a_{-\mathbf{n}}=a_{\mathbf{n}}^{*}$. The structure constants are now most conveniently defined via

$$[J_l,J_{\mathbf{m}}]=i\sum_{\mathbf{n}}f^{l\mathbf{m}\mathbf{n}}J_{\mathbf{n}}^{\dagger}\ , \tag{C6}$$

whence

$$\begin{aligned}f^{l\mathbf{m}\mathbf{n}}&=\frac{1}{iM}\mathrm{tr}([J_l,J_{\mathbf{m}}]J_{\mathbf{n}})\\&=2\sin\left[\frac{2\pi}{M}l\times\mathbf{m}\right]\tilde{\delta}(l+\mathbf{m}+\mathbf{n})\ .\end{aligned} \tag{C7}$$

These are completely antisymmetric. Of main interest to us, however, are the completely *symmetric* coefficients obtained from the anticommutation relations

$$\{J_l,J_{\mathbf{m}}\}=i\sum_{\mathbf{n}}g^{l\mathbf{m}\mathbf{n}}J_{\mathbf{n}}^{\dagger}\ , \tag{C8}$$

whence

$$\begin{aligned}g^{l\mathbf{m}\mathbf{n}}&=\frac{1}{M}\mathrm{tr}(\{J_l,J_{\mathbf{m}}\}J_{\mathbf{n}})\\&=2\cos\left[\frac{2\pi}{M}l\times\mathbf{m}\right]\tilde{\delta}(l+\mathbf{m}+\mathbf{n})\ .\end{aligned} \tag{C9}$$

It is these latter that we shall use in our generalized Navier-Stokes equations. We therefore define

$$A_N^{l\mathbf{m}\mathbf{n}}=f(N)g^{l\mathbf{m}\mathbf{n}} \tag{C10}$$

with the normalization $f(N)$ chosen so that

$$I_2=\sum_{l,\mathbf{m},\mathbf{n}}{}'(A_N^{l\mathbf{m}\mathbf{n}})^2=N\ , \tag{C11}$$

where the prime on the sum means that $\mathbf{0}$ is excluded. In order to do this sum we will need the result

$$\sum_l{}'e^{i(2\pi/M)l\times\mathbf{m}}=\sum_l{}'e^{i(2\pi/M)l\cdot\mathbf{m}}=(N+1)\tilde{\delta}(\mathbf{m})-1\ , \tag{C12}$$

which follows from the usual formulae for discrete Fourier series. We find then

$$\begin{aligned}\sum_{l,\mathbf{m},\mathbf{n}}{}'(g^{l\mathbf{m}\mathbf{n}})^2&=\sum_{l,\mathbf{m}}{}'[e^{i(2\pi/M)l\times\mathbf{m}}+e^{-i(2\pi/M)l\times\mathbf{m}}]^2\\&=\sum_{\mathbf{m}}{}'[2N+2(N+1)\tilde{\delta}(2\mathbf{m})-2]\\&=2N(N-1)\end{aligned} \tag{C13}$$

and we therefore choose

$$f(N)=\frac{1}{\sqrt{2(N-1)}}\ . \tag{C14}$$

The most important consequence of (C13) is that the constant, zero-phase terms in the expansion of the product dominate for large N. This conclusion, as we shall demonstrate, applies to all 2PI diagrams. Unfortunately, as we shall also demonstrate, this means that all 2PI diagrams contribute *equally* at large N and therefore the choice (C10) is not a useful basis for a large-N expansion.

To see the existence of zero-phase terms in any given diagram, assign arrows to the lines in such a way that all vertices are of the form shown in Fig. 15(a) or 15(b), i.e., at each vertex, either two indices combine into one or one

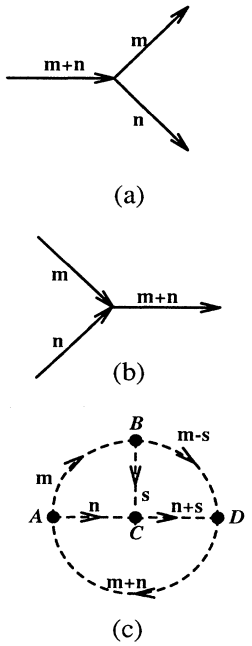

FIG. 15. Isospin diagrams for SU(M). The two possible configurations of arrows are shown in (a) and (b). (c) Example of the construction of a zero-phase term for the tetrahedron graph.

index splits into two. In expanding the product of cosines associated with the diagram, a phase factor $e^{i(2\pi/M)\mathbf{m}\times\mathbf{n}}$ or $e^{i(2\pi/M)\mathbf{n}\times\mathbf{m}}$ (where $\mathbf{m}$ and $\mathbf{n}$ are the pair of ingoing or outgoing indices) is contributed by each vertex. A zero-phase term is constructed by noticing that "current conservation" ensures that if two indices $\mathbf{m}$ and $\mathbf{n}$ depart from some vertex, they must recombine at some other vertex. One then need only choose the phase factor $e^{i(2\pi/M)\mathbf{m}\times\mathbf{n}}$ at the first vertex and that which yields a factor $e^{-i(2\pi/M)\mathbf{m}\times\mathbf{n}}$ at the second. This by itself does not cancel all of the $\mathbf{m}$ and $\mathbf{n}$ dependence: each may still appear separately inside various phase factors; however, if one carries out this pairing procedure for all vertices, it is not hard to convince oneself that full cancellation is ensured. We have not attempted to construct a formal proof of this fact, but we have verified it for the first few 2PI graphs.

As an example, consider the tetrahedron graph Fig. 15(c), which is given by

$$I_4=16f(N)^4\sum_{l,\mathbf{m},\mathbf{n}}{}'\cos\left[\frac{2\pi}{M}\mathbf{m}\times\mathbf{n}\right]\cos\left[\frac{2\pi}{M}(\mathbf{m}-l)\times l\right]\times\cos\left[\frac{2\pi}{M}\mathbf{n}\times l\right]\cos\left[\frac{2\pi}{M}(\mathbf{n}+l)\times(\mathbf{m}-l)\right]. \tag{C15}$$

It is easy to check that

$$e^{i(2\pi/M)\mathbf{m}\times\mathbf{n}}e^{i(2\pi/M)(\mathbf{m}-l)\times l}e^{i(2\pi/M)\mathbf{n}\times l}\times e^{i(2\pi/M)(\mathbf{n}+l)\times(\mathbf{m}-l)}=1 \tag{C16}$$

and one finds

$$I_4=\frac{N(N^2-2N+5)}{2(N-1)^2}\approx\frac{N}{2},\quad N\to\infty, \tag{C17}$$

with the zero-phase term contributing the leading large-N behavior.

For a 2PI graph with $2k$ vertices there are $k+1$ free dummy indices and the sum yields a factor N^{2k+1}. The zero-phase terms therefore contribute

$$I_{2k}^{(i)}\approx f(N)^{2k}2N^{k+1}\approx\frac{N}{2^{k-1}}. \tag{C18}$$

All 2PI graphs are then of order N and by the results of Sec. III contribute when $N\to\infty$ since all exponents $\alpha_{2k}^{(i)}$ then vanish. From (3.7), the large-N symmetry factor is then

$$D=\delta_l^{l'}2^{\left(-\sum_{k=1}^{\infty}\sum_{i=1}^{n_k}(k-1)m_{2k}^{(i)}\right)},\quad N\to\infty, \tag{C19}$$

compared to $D=\delta_l^{l'}$ for $N=1$.

APPENDIX D: SIMPLIFIED DIA EQUATIONS

In order to improve one's intuition about the asymptotic scaling analyses performed in Sec. IV, it is extremely useful to consider a simplified set of DIA equations (SDIA; historically, the contents of this appendix predated the contents of Sec. IV) in which the frequency dependence is simply suppressed. Thus consider the coupled pair of equations

$$\frac{1}{\hat{G}(\mathbf{k})}=\nu_0k^2+\lambda_0^2k^2\int_{\mathbf{q}}b(\mathbf{k},\mathbf{q})\hat{U}(\mathbf{k}-\mathbf{q})\hat{G}(\mathbf{q}), \tag{D1}$$

$$\hat{U}(\mathbf{k})=|\hat{G}(\mathbf{k})|^2\left[D(\mathbf{k})+\lambda_0^2k^2\int_{\mathbf{q}}a(\mathbf{k},\mathbf{q})\hat{U}(\mathbf{k}-\mathbf{q})\hat{U}(\mathbf{q})\right]. \tag{D2}$$

These equations actually originate from a well defined model: consider the "hydrostatic" Navier-Stokes equations

$$\lambda_0(\mathbf{v}\cdot\nabla)\mathbf{v}=-\frac{1}{\rho_0}\nabla p+\nu_0\nabla^2\mathbf{v}+\mathbf{f},\quad\nabla\cdot\mathbf{v}=0, \tag{D3}$$

where the static incompressible field $\mathbf{v}(\mathbf{r})$ is to be determined for a given quenched random force $\mathbf{f}(\mathbf{r})$ with Fourier transformed covariance $\langle\hat{f}_\alpha(\mathbf{k})\hat{f}_\beta(\mathbf{k}')\rangle=D(\mathbf{k})\hat{\tau}_{\alpha\beta}(\mathbf{k})\delta(\mathbf{k}+\mathbf{k}')$. Perturbation theory in λ_0 is formally identical to that for the time dependent problem, with $\hat{G}^0(\mathbf{k})=1/\nu_0k^2$ at zeroth order and with identical vertex. The generalization to $N>1$ is also obvious and the $N\to\infty$ limit yields the corresponding bubble diagrams, which can be resummed to yield (D1) and (D2).

The advantage one has gained by this simplification is that one seeks solutions in the form of pure power laws

$$\hat{G}(\mathbf{k})\approx\frac{h_1}{k^z},\quad\hat{U}(\mathbf{k})\approx\frac{h_2}{k^{\Delta-z}},\quad k\to0 \tag{D4}$$

(the choice of parametrization of the second exponent is for later convenience). We take the driving spectrum to be of the form

$$D(k)=D_0k^{6-d-\bar{y}} \tag{D5}$$

for reasons that will become clear below. Substituting these forms into the SDIA equations, and changing variables to $\mathbf{Q}=\mathbf{q}/k$, we obtain

$$1=h_1\nu_0k^{2-z}+\lambda_0^2h_1^2h_2k^{d+2-\Delta-z}\int_{\mathbf{Q}}b(\hat{\mathbf{k}},\mathbf{Q})P^{z-\Delta}Q^{-z}, \tag{D6}$$

$$1=D_0h_1^2h_2^{-1}k^{\Delta-3z+6-d-y}+\lambda_0^2h_1^2h_2k^{d+2-\Delta-z}\int_{\mathbf{Q}}a(\hat{\mathbf{k}},\mathbf{Q})P^{z-\Delta}Q^{z-\Delta}. \tag{D7}$$

The integrals converge as long as $d<\Delta<d+z$. For $\Delta<d$ the unscaled integrals in (D1) remain finite as $k\to0$ and renormalized "linear hydrostatics" results with $z=2$ and $\hat{G}(\mathbf{k})\approx1/\nu_Rk^2$. For $\Delta>d$ the nonlinear term dominates the scaling and consistency requires

$$\Delta+z=d+2 \tag{D8}$$

[compare (1.19): this motivates the definition of Δ in (D4)]. Matching the driving term as well then yields

$$6-d-\bar{y}=3z-\Delta \tag{D9}$$

so that

$$z=2-\frac{\tilde{y}}{4},\quad \Delta=d+\frac{\tilde{y}}{4}\ , \tag{D10}$$

which should be compared with (1.18). Since $\tilde{y}=0$ coincides with $\Delta=d$ it is clear that this determines the borderline between linear and nonlinear behavior [hence the parametrization in (D5)]. For $\tilde{y}>0$ one has $z<2$ and the viscous term is irrelevant. For simplicity we therefore take $\nu_0\equiv 0$ from now on. The solutions (D10) may also be derived to all orders in $\tilde{y}$ using renormalization group methods on the original model (D3). These solutions therefore play exactly the same role as do (1.18) in the full dynamical problem.

The energy spectrum may be defined via

$$E(k)=\frac{d-1}{2}K_d\rho_0 k^{d-1}\hat{U}(\mathbf{k})\ , \tag{D11}$$

which yields $\zeta=\Delta-z-d+1$, precisely as in (1.20). From (D10) one has then

$$\zeta=\frac{\tilde{y}}{2}-1\ , \tag{D12}$$

which should be compared with (1.24).

In order to fix the amplitudes h_1 and h_2, let us define

$$\Gamma_b(\Delta-z,z;d)\equiv\int_Q b(\hat{\mathbf{k}},\mathbf{Q})P^{z-\Delta}Q^{-z}\ , \tag{D13}$$

$$\Gamma_a(\Delta-z,\Delta-z;d)\equiv\int_Q a(\hat{\mathbf{k}},\mathbf{Q})P^{z-\Delta}Q^{z-\Delta}\ . \tag{D14}$$

We then choose $\lambda_0^2 h_1^2 h_2\Gamma_b=1$ and $\lambda_0^2 h_1^2 h_2\Gamma_a+D_0 h_1^2 h_2^{-1}=1$, i.e.,

$$h_1=\left[\frac{\Gamma_b-\Gamma_a}{\lambda_0^2 D_0\Gamma_b^2}\right]^{1/4},\quad h_2=\left[\frac{D_0\lambda_0^{-2}}{\Gamma_b-\Gamma_a}\right]^{1/2}. \tag{D15}$$

Explicit forms for Γ_a and Γ_b will be given below.

Equations (D10) and (D15) represent complete analytic solutions, as long as $\Delta-z<d$. The borderline $\Delta-z=d$ is reached when $\tilde{y}=4$. This should be compared to $y=3$ for the dynamical problem. In both cases the borderline corresponds to $\zeta=1$, where the energy spectrum goes from being ultraviolet to infrared divergent. For $\tilde{y}>4$ one must regularize the infrared behavior. We therefore replace (D5) by

$$D(k)=D_0\eta(k/m_0)k^{6-d-\tilde{y}}\ , \tag{D16}$$

where $\eta(x)\to 1$ for $x\to\infty$ and vanishes rapidly for $x\to 0$. Correspondingly, we seek more general solutions

$$\hat{G}(\mathbf{k})=\frac{h_1}{k^z}g(k/m_0)\ ,\qquad \hat{U}(\mathbf{k})=\frac{h_2}{k^{\Delta-z}}u(k/m_0)\ , \tag{D17}$$

where $g(x)$ and $u(x)$ approach unity for large x. Substituting these forms into the SDIA equations (with $\nu_0=0$), we find

$$\frac{1}{g(x)}=\lambda_0^2 h_1^2 h_2(m_0x)^{d+2-\Delta-z}J_b(x)\ ,$$
$$\frac{u(x)}{|g(x)|^2}=h_1^2 h_2^{-1}D_0(m_0x)^{\Delta-3z+6-d-y}\eta(x)+\lambda_0^2 h_1^2 h_2(m_0x)^{d+2-\Delta-z}J_a(x)\ . \tag{D18}$$

We may now isolate the singular parts of the integrals

$$J_b(x)\equiv\int_Q b(\hat{\mathbf{k}},\mathbf{Q})P^{z-\Delta}Q^{-z}u(xP)g(xQ)=g(x)J_{\text{sing}}(x)+\Delta J_b(x)\ ,$$
$$J_a(x)\equiv\int_Q a(\hat{\mathbf{k}},\mathbf{Q})P^{z-\Delta}Q^{z-\Delta}u(xP)u(xQ)=u(x)J_{\text{sing}}(x)+\Delta J_a(x)\ , \tag{D19}$$

where [compare (4.25) and (4.26)]

$$J_{\text{sing}}(x)=\int_Q[1-(\hat{\mathbf{k}}\cdot\hat{\mathbf{Q}})^2]Q^{z-\Delta}u(xQ)=\tilde{u}_0 x^{\Delta-d-z} \tag{D20}$$

and

$$\tilde{u}_0=\frac{d-1}{d}K_d\int_0^\infty dw\frac{u(w)}{w^{\Delta-z-d+1}} \tag{D21}$$

is assumed to be finite. The finite parts

$$\Delta J_b(x)=\int_Q\{b(\hat{\mathbf{k}},\mathbf{Q})Q^{-z}g(xQ)-[1-(\hat{\mathbf{k}}\cdot\hat{\mathbf{P}})^2]g(x)\}P^{z-\Delta}u(xP)\ ,$$
$$\Delta J_a(x)=\int_Q\{a(\hat{\mathbf{k}},\mathbf{Q})Q^{z-\Delta}P^{z-\Delta}u(xQ)u(xP)-\tfrac{1}{2}[1-(\hat{\mathbf{k}}\cdot\hat{\mathbf{Q}})^2]Q^{z-\Delta}u(xQ)u(x)-\tfrac{1}{2}[1-(\hat{\mathbf{k}}\cdot\hat{\mathbf{P}})^2]P^{z-\Delta}u(xP)u(x)\} \tag{D22}$$

are nonsingular when $x\to\infty$:

$$\lim_{x\to\infty}\Delta J_b(x)\equiv\Gamma_b(\Delta-z,z;d)=\int_Q\{b(\hat{\mathbf{k}},\mathbf{Q})Q^{-z}-[1-(\hat{\mathbf{k}}\cdot\hat{\mathbf{P}})^2]\}P^{z-\Delta}\ ,$$
$$\lim_{x\to\infty}\Delta J_a(x)\equiv\Gamma_a(\Delta-z,\Delta-z;d)=\int_Q\{a(\hat{\mathbf{k}},\mathbf{Q})Q^{z-\Delta}P^{z-\Delta}-\tfrac{1}{2}[1-(\hat{\mathbf{k}}\cdot\hat{\mathbf{Q}})^2]Q^{z-\Delta}-\tfrac{1}{2}[1-(\hat{\mathbf{k}}\cdot\hat{\mathbf{P}})^2]P^{z-\Delta}\} \tag{D23}$$

[compare (4.30) and (4.31)] where we have extended the definitions of Γ_a and Γ_b in (D14) into the region $\Delta-z>d$. Matching up the leading behavior for large x, the first equation in (D18) yields

$$z=1,\quad h_1^2 h_2\tilde{u}_0\lambda_0^2 m_0^{d+2-\Delta-z}=1\ . \tag{D24}$$

If, in the second equation, the driving term was also of leading order, we would conclude that $\Delta=d-3+y$ and $h_1^2 h_2^{-1}D_0+h_1^2 h_2\tilde{u}_0\lambda_0^2=1$. However, the latter equality can be satisfied only if the first term vanishes. We therefore conclude, as below (4.39), that the driving must be of lower order $\Delta<d-3+y$ and the second equation yields

(D24) as well. Thus Δ is as yet undetermined.

To proceed further, we treat the ΔJ_a and ΔJ_b terms as perturbations and expand

$$g(x)\approx 1+g_1 x^{d+2-\Delta-z}+\cdots ,$$
$$u(x)\approx 1+u_1 x^{d+2-\Delta-z}+\cdots \tag{D25}$$

for large x [compare (4.43)]. Matching up the next-to-leading-order terms, one then finds

$$g_1=-\frac{1}{2}h_1^2 h_2^{-1} m_0^{\Delta-3z+6-d-\tilde{y}} D_0 x^{\theta_0}-\frac{1}{2\tilde{u}_0}\Gamma_b(\Delta-z,z;d)$$
$$=\frac{1}{2\tilde{u}_0}\Gamma_a(\Delta-z,\Delta-z;d) , \tag{D26}$$

with u_1 determined only at yet higher order [compare the discussion below (4.47)]. The exponent $\theta_0\equiv 2\Delta-2z+4-2d-\tilde{y}$ must vanish if the driving is to still control the scaling. Thus [compare (1.24)]

$$\Delta=d+z-2+\tfrac{1}{2}\tilde{y}=d-1+\tfrac{1}{2}\tilde{y} . \tag{D27}$$

We then define $d_0=h_1^2 h_2^{-1} D_0 m_0^{\Delta-3z+6-d-\tilde{y}}$ and obtain

$$d_0=\Gamma_a(\Delta-z,\Delta-z;d)-\Gamma_b(\Delta-z,z;d) , \tag{D28}$$

which should be compared with (4.48). More explicitly, using $a(\hat{\mathbf{k}},\mathbf{Q})=\frac{1}{2}[b(\hat{\mathbf{k}},\mathbf{Q})+b(\hat{\mathbf{k}},\mathbf{P})]$,

$$d_0=\int_{\mathbf{Q}} b(\hat{\mathbf{k}},\mathbf{Q})P^{z-\Delta}[Q^{z-\Delta}-Q^{-z}] , \tag{D29}$$

which should be compared with (4.49) [and was alluded to in (4.56)]. Note that there are no free parameters in this equation: $d_0=d_0(\tilde{y})$ is determined completely by $\tilde{y}$ through (D24) and (D27). Precisely as for the dynamical problem (see Sec. IV C), there is a special value $\tilde{y}=\tilde{y}_c$, hence $\Delta_c=\Delta(\tilde{y}_c)$, for which $d_0(\tilde{y})$ *vanishes*, i.e.,

$$\Gamma_a(\Delta_c-1,\Delta_c-1;d)=\Gamma_b(\Delta_c-1,1;d) . \tag{D30}$$

This is the same equation we would have obtained if we had replaced the driving spectrum (D16) by the explicitly short-ranged form

$$D(k)=D_0\tilde{\eta}(k/m_0) , \tag{D31}$$

where $\tilde{\eta}(x)$ is rapidly decreasing at large x. Equation (D26) would then have resulted with no driving term at all. We conclude, therefore, that the vanishing of $d_0(\tilde{y})$ coincides with true short-ranged hydrostatic turbulence.

To find $\tilde{y}_c$ we must solve (D30). We first outline a brute force method for doing this. We begin with the result

$$C(\alpha,\beta;d)\equiv\int_{\mathbf{Q}} P^{-\alpha}Q^{-\beta}$$
$$=\frac{1}{2}K_d\frac{\Gamma\left[\frac{d}{2}\right]\Gamma\left[\frac{\alpha+\beta-d}{2}\right]\Gamma\left[\frac{d-\beta}{2}\right]\Gamma\left[\frac{d-\alpha}{2}\right]}{\Gamma\left[\frac{\alpha}{2}\right]\Gamma\left[\frac{\beta}{2}\right]\Gamma\left[d-\frac{\alpha+\beta}{2}\right]}, \quad \alpha,\beta<d,\ \alpha+\beta>d , \tag{D32}$$

which may be derived by standard methods [50]. By breaking up $b(\hat{\mathbf{k}},\mathbf{Q})$ into a sum of terms of the form $P^{-\alpha}Q^{-\beta}$ [using, for example, $\mathbf{P}\cdot\mathbf{Q}=\frac{1}{2}(1-P^2-Q^2)$] we find

$$\Gamma_b(\alpha,\beta;d)=-\frac{d-1}{8}C(\alpha+2,\beta;d)+\frac{d-1}{4}C(\alpha+2,\beta-2;d)-\frac{d-1}{8}C(\alpha+2,\beta-4;d)-\frac{d+1}{8}C(\alpha-2,\beta;d)$$
$$+\frac{1}{8}C(\alpha,\beta+2;d)+\frac{1}{8}C(\alpha,\beta-4;d)-\frac{1}{8}C(\alpha-6,\beta+2;d)+\frac{2d-3}{8}C(\alpha,\beta-2;d)+\frac{3}{8}C(\alpha-4,\beta+2;d)$$
$$+\frac{2d-3}{8}C(\alpha,\beta;d)-\frac{3}{8}C(\alpha-2,\beta+2;d)+\frac{3}{8}C(\alpha-2,\beta;d)-\frac{3}{8}C(\alpha-2,\beta-2;d) . \tag{D33}$$

Many of the arguments here lie outside the convergent range given in (D32). However, it is easy to show that (D32) remains correct as long as we take the *finite part* of the integral (i.e., that obtained after all appropriate ultraviolet and infrared subtractions have been made). Since we have ensured that Γ_b is finite [see (D23)], all subtractions required to make the right-hand side of (D33) are automatically accounted for. Using (D33) and (D32) we may numerically compute $d_0(\tilde{y})$ from (D24) and (D27). We find that $d_0(\tilde{y})$ vanishes at a point indistinguishable from $\tilde{y}_c=5$ in all dimensions of interest. This yields $\Delta_c=d+\frac{3}{2}$ and $\zeta_c=\frac{3}{2}$ [compare (4.55)]. One can verify this solution analytically using the properties of the Γ function. The fundamental identity needed is

$$C(\alpha,\beta;d)=C(\alpha,2d-\alpha-\beta;d) \quad \text{for all } \alpha,\beta \tag{D34}$$

and can be used to verify (D30) term by term in the expansion (D33).

A much more elegant way of proceeding is to perform a "conformal transformation" on (D27) [32]. Thus, if we

define $\mu=\hat{\mathbf{k}}\cdot\hat{\mathbf{Q}}$, then

$$b(\hat{\mathbf{k}},\mathbf{Q})\equiv b(Q,\mu) = \frac{Q(1-\mu^2)[(d-1+4\mu^2)Q-2\mu(1+Q^2)]}{(d-1)(1-2Q\mu+Q^2)} \tag{D35}$$

and from this it is easy to check that

$$b\left[\frac{1}{Q},\mu\right]=\frac{1}{Q^2}b(Q,\mu)\ . \tag{D36}$$

Therefore,

$$\Gamma_b(\alpha,\beta;d)=K_{d-1}\int_0^\infty dQ\,Q^{d-1-\alpha}\int_{-1}^1 d\mu(1-\mu^2)^{(d-3)/2}\frac{b(Q,\mu)}{(1-\mu Q+Q^2)^{\beta/2}}$$
$$=K_{d-1}\int_0^\infty d\bar{Q}\,\bar{Q}^{\alpha+\beta-3-d}\int_{-1}^1 d\mu(1-\mu^2)^{(d-3)/2}\frac{b(\bar{Q},\mu)}{(1-\mu\bar{Q}+\bar{Q}^2)^{\beta/2}}\ , \tag{D37}$$

where $\bar{Q}=1/Q$. This immediately implies

$$\Gamma_b(\alpha,\beta;d)=\Gamma_b(\alpha,2d+2-\alpha-\beta;d)\ , \tag{D38}$$

which can also be demonstrated for all values of α and β as long as the finite part of the integral in (D37) is used. Performing this transformation only on the second term in square brackets in (D29) we find

$$d_0=\int_Q b(\hat{\mathbf{k}},\mathbf{Q})P^{z-\Delta}[Q^{z-\Delta}-Q^{\Delta-2d-2}]\ , \tag{D39}$$

whose integrand vanishes identically if $\Delta-z=2d+2-\Delta$, i.e.,

$$\Delta_c=d+1+\frac{z_c}{2}=d+\frac{3}{2},\quad \zeta_c=\frac{3}{2}\ , \tag{D40}$$

as before [compare (4.58)]. Note that (D29) vanishes identically for $\Delta=2z=2$, but the requirement $\Delta>d$ makes this a solution possible only if $d<2$. This solution coincides with (D40) when $d=\frac{1}{2}$.

In order to confirm that the exponents stick to the values (D40) when $\tilde{y}>\tilde{y}_c$, one performs precisely the same analysis as in Sec. IV C. Thus one tests the stability of the $\tilde{y}=\tilde{y}_c$ solutions against power-law driving. A scaling analysis demonstrates that, indeed, the driving is relevant for $\tilde{y}<\tilde{y}_c$ and irrelevant for $\tilde{y}>\tilde{y}_c$. See Sec. IV C for details. To summarize, the exponents are

$$z=\begin{cases}2-\dfrac{\tilde{y}}{4}, & 4\geq\tilde{y}\geq 0\\ 1, & \tilde{y}\geq 4\ ,\end{cases} \tag{D41}$$

$$\Delta=\begin{cases}d+\dfrac{\tilde{y}}{4}, & 4\geq\tilde{y}\geq 0\\ d-1+\dfrac{\tilde{y}}{2}, & 5\geq\tilde{y}\geq 4\\ d+\dfrac{3}{2}, & \tilde{y}\geq 5\ ,\end{cases} \tag{D42}$$

$$\zeta=\begin{cases}\dfrac{\tilde{y}}{2}-1, & 5\geq\tilde{y}\geq 0\\ \dfrac{3}{2}, & \tilde{y}\geq 5\ .\end{cases} \tag{D43}$$

Note that, as in (4.60) and (4.61), we could also consider subtracted versions of the SDIA equations. One would then find that (D29) still holds for $\tilde{y}>4$, but with exponents now given by (D10). The same conformal transformation now produces, from the first equality in (D40), $\tilde{y}_c=\frac{16}{3}$, $z_c=\frac{2}{3}$, $\Delta_c=d+\frac{4}{3}$, and $\zeta_c=\frac{5}{3}$. These are the analogs of the Kolmogorov values. Though details differ between (D41)–(D43) and Fig. 2, the close analogy between the two is clear.

APPENDIX E: DETAILS OF NUMERICAL WORK

In this appendix we outline the numerical methods used to determine $u(s)$ and y_c in Sec. IV. We start from (4.48), which we write in the form

$$-u(s)\mathrm{Re}\Delta J_b(s)-[1-(s^2/4)]^{1/2}\Delta J_b(s) -[1-(s^2/4)]^{1/2}\delta_0=0\ , \tag{E1}$$

where

$$-\mathrm{Re}\Delta J_b(s)=\int_Q\int_t u\left[\frac{s-Qt}{P}\right]P^{-\Delta}\{b(\hat{\mathbf{k}},\mathbf{Q})[1-(t^2/4)]^{1/2}-[1-(\hat{\mathbf{k}}\cdot\hat{\mathbf{P}})^2][1-(s^2/4)]^{1/2}\}\ , \tag{E2}$$

$$\Delta J_a(s)=\int_Q\int_t u\left[\frac{s-Qt}{P}\right]P^{-\Delta}\{b(\hat{\mathbf{k}},\mathbf{Q})Q^{1-\Delta}u(t)-[1-(\hat{\mathbf{k}}\cdot\hat{\mathbf{P}})^2]u(s)\}\ , \tag{E3}$$

and we reemphasize that the integrals are over the domain $|t| \leq 2$ and $|(s-Qt)/P| \leq 2$. For convenience we scale out the factor of 2 and define $s'=s/2$, $t'=t/2$, and $\tilde{u}(s)=u(2s)$. We define also the angular variable $\mu=\hat{\mathbf{k}}\cdot\hat{\mathbf{Q}}$, and it is easy to show that $P=\sqrt{1-2\mu Q+Q^2}$ and $\hat{\mathbf{k}}\cdot\hat{\mathbf{P}}=(1-\mu Q)/P$. Then, for example, we may write

$$\int_Q \int_{-2}^{2} \frac{dt}{2\pi} b(\hat{\mathbf{k}},\mathbf{Q})[1-(t^2/4)]^{1/2} P^{-\Delta} u\left[\frac{s-Qt}{P}\right]$$

$$=2A_{d-1}\int_{-1}^{1} dt' \int_0^{\infty} dQ \int_{-1}^{1} d\mu (1-\mu^2)^{(d-3)/2} Q^{d-1} b(Q,\mu) \frac{\sqrt{1-t'^2}}{(1-2\mu Q+Q^2)^{\Delta/2}} \tilde{u}\left[\frac{s'-Qt'}{\sqrt{1-2\mu Q+Q^2}}\right]$$

$$\equiv 2A_{d-1} I(s') , \tag{E4}$$

where $A_{d-1}=K_d/2\pi$ and $b(Q,\mu)$ is displayed in (D35). We may convert the unbounded integral over Q into one over a finite interval by performing a conformal transformation $Q \to 1/Q$ on the domain $1 \leq Q < \infty$. We find then that

$$I(s')=\int_{-1}^{1} dt' \int_0^1 dQ \int_{-1}^{1} d\mu \sqrt{1-t'^2}\mathcal{K}_d(Q,\mu)\left[\tilde{u}\left[\frac{s'-Qt'}{\sqrt{1-2\mu Q+Q^2}}\right]Q^{d-1}+\tilde{u}\left[\frac{t'-Qs'}{\sqrt{1-2\mu Q+Q^2}}\right]Q^{\Delta-d-3}\right] \tag{E5}$$

where

$$\mathcal{K}_d(Q,\mu)=(1-\mu^2)^{(d-3)/2}\frac{b(Q,\mu)}{(1-2\mu Q+Q^2)^{\Delta/2}} \tag{E6}$$

and we have used (D36). The singular point is at $\mu=1$, $Q=1$, but will occur subtracted in our final expressions. We may rewrite all remaining integrals in the same way and (E1) finally becomes

$$\tilde{u}(s')B(s')-\sqrt{1-s'^2}A(s')-\sqrt{1-s'^2}\delta_0'=0 , \tag{E7}$$

where $\delta_0'=\delta_0/2A_{d-1}$ and we have defined

$$A(s')=\int_{-1}^{1} dt' \int_0^1 dQ \int_{-1}^{1} d\mu \left\{\tilde{u}\left[\frac{s'-Qt'}{\sqrt{1-2\mu Q+Q^2}}\right][\mathcal{K}_d(Q,\mu)\tilde{u}(t')Q^{d-\Delta}-\mathcal{K}_d^{\text{sing}}(Q,\mu)\tilde{u}(s')Q^{d-1}]\right.$$
$$\left.+\tilde{u}\left[\frac{t'-Qs'}{\sqrt{1-2\mu Q+Q^2}}\right][\mathcal{K}_d(Q,\mu)\tilde{u}(t')Q^{2\Delta-d-4}-\mathcal{K}_d^{\text{sing}}(Q,\mu)\tilde{u}(s')Q^{\Delta-d-3}]\right\} , \tag{E8}$$

$$B(s')=\int_{-1}^{1} dt' \int_0^1 dQ \int_{-1}^{1} d\mu \left\{\tilde{u}\left[\frac{s'-Qt'}{\sqrt{1-2\mu Q+Q^2}}\right][\mathcal{K}_d(Q,\mu)\sqrt{1-t'^2}Q^{d-1}-\mathcal{K}_d^{\text{sing}}(Q,\mu)\sqrt{1-s'^2}Q^{d-1}]\right.$$
$$\left.+\tilde{u}\left[\frac{t'-Qs'}{\sqrt{1-2\mu Q+Q^2}}\right][\mathcal{K}_d(Q,\mu)\sqrt{1-t'^2}Q^{\Delta-d-3}-\mathcal{K}_d^{\text{sing}}(Q,\mu)\sqrt{1-s'^2}Q^{\Delta-d-3}]\right\} , \tag{E9}$$

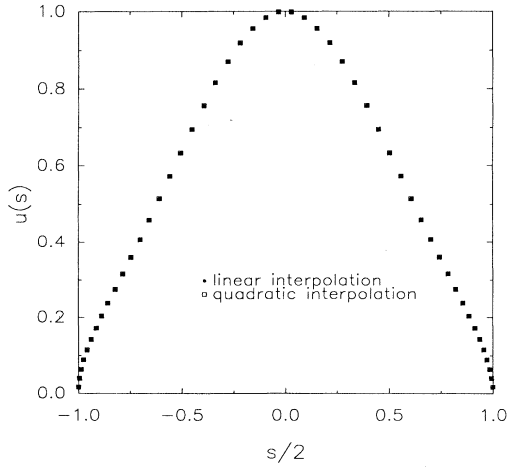

FIG. 16. Comparison of linear and quadratic interpolation in the numerical solution for the scaling function $u(s)$.

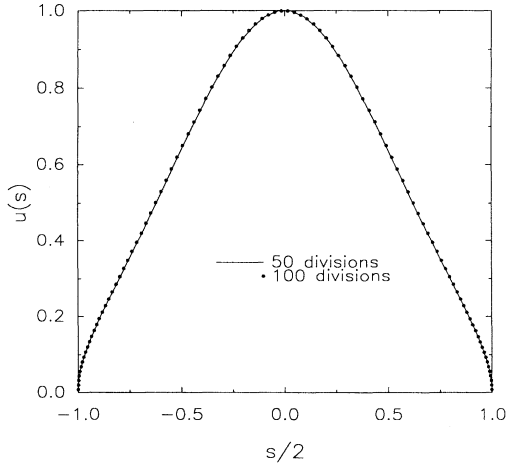

FIG. 17. Comparison of 50 and 100 divisions in the numerical solution for the scaling function $u(s)$.

where

$$\mathcal{K}_d^{\text{sing}}(Q,\mu)=(1-\mu^2)^{(d-3)/2}\frac{Q^2(1-\mu^2)}{(1-2\mu Q+Q^2)^{(\Delta+2)/2}} \tag{E10}$$

is the singular part of $\mathcal{K}_d(Q,\mu)$. The integration is done by Gaussian quadrature using Gauss-Legendre weights and points. Thus

$$\int_{-1}^{1}dt'\int_{0}^{1}dQ\int_{-1}^{1}d\mu\,F(s',t',Q,\mu) \approx \sum_{i=1}^{n}\sum_{j=n_1}^{n}\sum_{k=1}^{n}w(i)w(j)w(k) \times F[x(l),x(i),x(j),x(k)]\,, \tag{E11}$$

where $w(i)$ are weights and $x(i)$ are the Gauss-Legendre points in the interval $(-1,1)$. We have performed computations using $n=50$, $n_1=26$ and $n=100$, $n_1=51$. The discretization (E11) converts the nonlinear integral equation (E1) into a system of n nonlinear equations in n unknowns, which may then be fed into any standard subroutine designed for such a problem. When finding a root, our error bars are always at most $O(10^{-12})$ for each individual equation.

We have used a linear interpolation scheme to infer $u(s)$ at intermediate points [the combination $r'=(s'-Qt')/P$ does not, in general, lie in the set of Gauss-Legendre points]. For comparison, we ran the computation at $\Delta=d+\frac{3}{2}$ and $d=3$ using a quadratic interpolation scheme. As can be seen in Fig. 16, the difference is very tiny. Increasing n from 50 to 100 also has very little effect (see Fig. 17).

As described in Sec. IV C, in order to obtain smooth, finite solutions through $y=y_c$, it is best to fix the value of $\tilde{u}(s')$ at some particular s' [we choose $\tilde{u}(0)=0$] and scale δ_0' accordingly. In our numerics, this normalization is used as an extra equation and the rest of the function is then determined uniquely.

[1] (a) A.N. Kolmogorov, C. R. Acad. Sci. U.S.S.R. **30**, 301 (1941); **32**, 16 (1941); see also (b) L. D. Landau and E. M. Lifshitz, *Fluid Mechanics*, 2nd ed. (Pergamon, New York, 1987), especially Sec. 33.

[2] See, e.g., A. Monin and A. M. Yaglom, *Statistical Fluid Mechanics* (MIT Press, Cambridge, MA, 1975), Vol. 2.

[3] See, e.g., (a) T. S. Lundgren, Phys. Fluids **25**, 2193 (1982); (b) V. I. Belinicher and V. S. L'vov, Zh. Eksp. Teor. Fiz. **93**, 533 (1987) [Sov. Phys. JETP **66**, 303 (1987)]; (c) V. S. L'vov, Phys. Rep. **207**, 1 (1991); (d) V. Yakhot and V. E. Zakharov, Physica D **64**, 379 (1993).

[4] Such coincidences are not so uncommon in the theory of critical phenomena. Consider, for example, the proximity of the critical correlation decay exponent η to the mean field value $\eta=0$. Also, the specific heat exponent α for the superfluid transition in ^{4}He is very nearly zero and the susceptibility exponent γ for the three-dimensional Ising model is very close to $\frac{5}{4}$. One knows in all of these cases that the exponents are not simple rational numbers and there is no easy way of obtaining their exact values.

[5] (a) D. Forster, D. R. Nelson, and M. J. Stephen, Phys. Rev. A **16**, 732 (1977); (b) C. DeDominicis and P. C. Martin, *ibid.* **19**, 419 (1979).

[6] See, e.g., P. Manneville, *Dissipative Structures and Weak Turbulence* (Academic, New York, 1990). Questions like these have also been investigated in nonequilibrium surface growth problems. Here the deterministic (but chaotic) Kuramoto-Sivashinsky equation has been compared to the stochastically driven Kardar-Parisi-Zhang equation. The two models have been argued to be in the same universality class. For recent reatments, see C. Jayaprakash, F. Hayot, and R. Pandit, Phys. Rev. Lett. **71**, 12 (1993), and references therein.

[7] See, e.g., V. Yakhot and S. A. Orszag, J. Sci. Comput. **1**, 3 (1986).

[8] This analogy, as far as we know, originates from an oral presentation by P. C. Hohenberg and was brought to our attention by M. C. Cross (private communication). P. C. Hohenberg (private communication) also credits D. S. Fisher. M. Nelkin (private communication) has suggested that, due to the incompressibility condition, a spin model with dipolar interactions might yield an even closer analogy. A more recent discussion of the relation between renormalization group theories of turbulence and of critical phenomena is given in Ref. [15].

[9] M. E. Fisher, S.-K. Ma, and B. G. Nickel, Phys. Rev. Lett. **29**, 917 (1972).

[10] See, e.g., K. G. Wilson and J. Kogut, Phys. Rep. C **12**, 75 (1974).

[11] J. Sak, Phys. Rev. B **8**, 281 (1973); **15**, 4344 (1977).

[12] R. Abe, Prog. Theor. Phys. **49**, 113 (1973); S.-K. Ma, Phys. Rev. A **7**, 2172 (1973).

[13] R. H. Kraichnan, J. Fluid Mech. **5**, 497 (1959).

[14] For a recent review, see V. Privman, P. C. Hohenberg, and A. Aharony, in *Phase Transitions and Critical Phenomena*, edited by C. Domb and J. L. Lebowitz (Academic, New York, 1994), Vol. 14.

[15] For a recent discussion of infrared versus ultraviolet behavior in turbulence, see G. Eyink and N. Goldenfeld, Phys. Rev. E **50**, 4679 (1994).

[16] R. H. Kraichnan, Phys. Fluids **8**, 575 (1965).

[17] C.-Y. Mou and P. B. Weichman, Phys. Rev. Lett. **70**, 1101 (1993).

[18] D. R. Nelson and E. Domany, Phys. Rev. B **13**, 236 (1976).

[19] We could further compactify the notation, with a general relativistic flavor, using upper and lower indices on $\mathbf{D}_N$ and *defining* $D^{l}_{N,l'}(g)=D^{l'}_{N,l}(g^{-1})$, but we wish to spare the reader the added confusion.

[20] P. C. Martin, E. D. Siggia, and H. Rose, Phys. Rev. A **8**, 423 (1973).

[21] H. W. Wyld, Ann. Phys. (N.Y.) **14**, 143 (1961).

[22] See, e.g., J. Zinn-Justin, *Quantum Field Theory and Critical Phenomena* (Clarendon, Oxford, 1989), Chap. 16.

[23] See, e.g., G. Baym, *Lectures on Quantum Mechanics* (Benjamin/Cummings, Reading, MA, 1969), Chap. 17.

[24] For a thorough discussion of the symmetry and orthogonality properties of the $3j$ (and higher-order) symbols see L. D. Landau and E. M. Lifshitz, *Quantum Mechanics,*

3rd ed. (Pergamon, New York, 1977), Chaps. 4, 8, and 14.
[25] See, e.g., H. Georgi, *Lie Algebras in Particle Physics* (Benjamin/Cummings, Reading, MA, 1982).
[26] D. J. Amit and D. V. I. Roginsky, J. Phys. A **12**, 689 (1979).
[27] See, e.g., M. Tinkham, *Group Theory and Quantum Mechanics* (McGraw-Hill, New York, 1964).
[28] This is actually not quite accurate: The Wigner $3kj$ symbols for $k \geq 3$ comprise, by convention, only the *three-particle* irreducible graphs. Thus, for example, only the second graph in Fig. 7(c) is a $9j$ symbol. The first reduces, by rule (d), to I_4^2/I_2. By this convention, there are only two $12j$ symbols, though there are far more than two 2PI graphs with eight vertices.
[29] R. H. Kraichnan, J. Math. Phys. **2**, 124 (1961).
[30] See R. H. Kraichnan and S. Chen, Physica D **37**, 160 (1989) for a review.
[31] This is apparently well known by those who know it well [E. D. Siggia (private communication)], but we are aware of only partial esults in this direction: see J. Bhattacharjee, J. Phys. A **21**, L551 (1988). Note that this should lead one to question the significance of any apparent agreement between experimentally measured quantities and their calculated values based on extrapolations of the one-loop y expansion [7]. Note also that one should be very careful to distinguish the formal renormalization group description of the turbulent state [see, e.g., G. L. Eyink, Phys. Lett. A **172**, 355 (1993)], which is believed to be exact, from the various *approximate implementations* of the renormalization group, like the y expansion, which contain further uncontrolled assumptions [see G. L. Eyink, Phys. Fluids A **6**, 3063 (1994) for a detailed discussion of this point].
[32] E. A. Kuznetsov and V. S. L'vov, Physica D **2**, 203 (1981).
[33] We are indebted to P. C. Hohenberg for clarifying discussions on this issue.
[34] We thank Boris Shraiman for discussions on this point.
[35] Paul Dimotakis (private communication).
[36] R. H. Kraichnan, J. Fluid Mech. **83**, 349 (1977).
[37] R. H. Kraichnan, Phys. Fluids **7**, 1723 (1964).
[38] G. L. Eyink, Phys. Rev. E **49**, 3990 (1994).
[39] The extended model will likely also have this feature at finite N, but the hope is that the problem will disappear "continuously" as $N \rightarrow 0$. This kind of behavior is seen in n-vector models of magnetism where, for any $n \neq 1$, one has low-energy "spin wave" excitations that completely alter the character of the magnetized state from that of the Ising model. However, explicit calculations [see, e.g., P. B. Weichman and K. Kim, Phys. Rev. B **42**, 10 505 (1990)] show that the amplitude for such excitations vanishes continuously as $n \rightarrow 1$ and that they pose no problem for the large-n expansion or for the calculation of exponents.
[40] See, for example, G. L. Eyink, Phys. Lett. A (Ref. [31]), where various "anomalous" exponents are defined relative to those of Kolmogorov.
[41] S. Chen, G. Doolen, J. R. Herring, R. H. Kraichnan, S. A. Orszag, and Z. S. She, Phys. Rev. Lett. **70**, 3051 (1993).
[42] See, e.g., C. W. Van Atta and W. Y. Chen, J. Fluid Mech. **44**, 145 (1970); F. Anselmet, F. Gagne, and E. J. Hopfinger, *ibid.* **140**, 63 (1984).
[43] D. R. Nelson (private communication).
[44] M. Kardar, G. Parisi, and Y. Zhang, Phys. Rev. Lett. **56**, 889 (1986).
[45] Inspired by our work, this has also been done independently by J. P. Doherty, M. A. Moore, J. M. Kim, and A. J. Bray, Phys. Rev. Lett. **72**, 2041 (1994). The resulting equations are known as the "mode-coupling equations": see H. Van Beijren, R. Kutner, and H. Spohn, *ibid.* **54**, 2026 (1985).
[46] Y. Tu, Phys. Rev. Lett. **73**, 3109 (1994).
[47] H. Sompolinsky, A. Crisanti, and H. J. Sommers, Phys. Rev. Lett. **61**, 259 (1988).
[48] Jonathan Miller (private communication).
[49] Some of these corrections have been written down formally in Ref. [38].
[50] D. J. Amit, *Field Theory, the Renormalization Group, and Critical Phenomena* (World Scientific, Singapore, 1984).
[51] G. 't Hooft, Nucl. Phys. B **138**, 1 (1978); D. B. Fairlie and Z. K. Zachos, Phys. Lett. B **224**, 101 (1989).

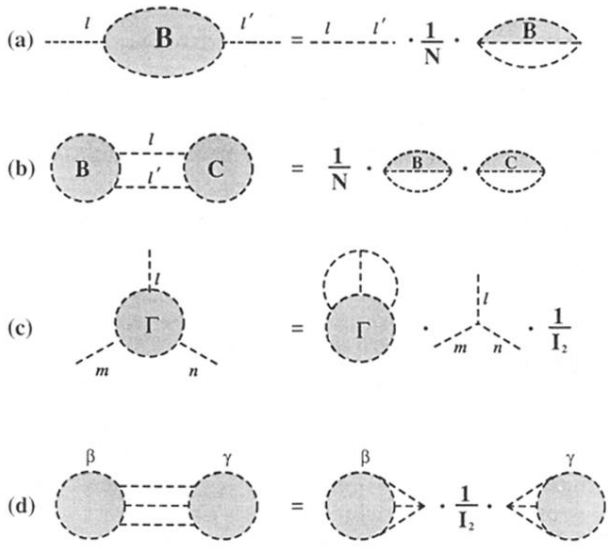

FIG. 6. Reduction rules (a)–(d) for the isospin shadow diagrams. See the text for details.